**University of Alberta**

# Analysis of the Genetic Basis of Axenfeld Rieger Malformations

by

**Douglas B. Gould** ©

A thesis submitted to the Faculty of Graduate Studies and Research in partial fulfilment of the requirements for the degree of

**Doctor of Philosophy**

In

**Medical Sciences – Medical Genetics**

Edmonton, Alberta

Fall 2001

National Library of Canada
Acquisitions and Bibliographic Services
395 Wellington Street
Ottawa ON K1A 0N4
Canada

Bibliothèque nationale du Canada
Acquisitions et services bibliographiques
395, rue Wellington
Ottawa ON K1A 0N4
Canada

*Your file Votre référence*

*Our file Notre référence*

The author has granted a non-exclusive licence allowing the National Library of Canada to reproduce, loan, distribute or sell copies of this thesis in microform, paper or electronic formats.

L'auteur a accordé une licence non exclusive permettant à la Bibliothèque nationale du Canada de reproduire, prêter, distribuer ou vendre des copies de cette thèse sous la forme de microfiche/film, de reproduction sur papier ou sur format électronique.

The author retains ownership of the copyright in this thesis. Neither the thesis nor substantial extracts from it may be printed or otherwise reproduced without the author's permission.

L'auteur conserve la propriété du droit d'auteur qui protège cette thèse. Ni la thèse ni des extraits substantiels de celle-ci ne doivent être imprimés ou autrement reproduits sans son autorisation.

0-612-69833-5

Canada

**University of Alberta**

**Library Release Form**

**Name of Author: Douglas Bradley Gould**

**Title of Thesis: Analysis of the Genetic Basis of Axenfeld Rieger Malformations**

**Degree: Doctor of Philosophy**

**Year this Degree Granted: 2001**

Permission is hereby granted to the University of Alberta Library to reproduce single copies of this thesis and to lend or sell copies for private, scholarly, or scientific research purposes only.

The author reserves all other publication and other rights in association with the copyright in the thesis, and except as hereinbefore provided, neither the thesis nor any substantial portion thereof may be printed or otherwise reproduced in any material form whatever without the author's prior written permission.

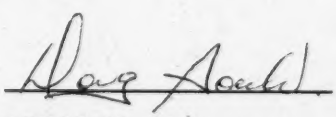

10841-83 Avenue
Edmonton, Alberta
T6E 2E6

April 28, 2001

**University of Alberta**

**Faculty of Graduate Studies and Research**

The undersigned certify that they have read, and recommend to the Faculty of Graduate Studies and Research for acceptance, a thesis entitled **Analysis of the Genetic Basis of Axenfeld Rieger Malformations** submitted by Douglas B. Gould in partial fulfillment of the requirements for the degree of Doctor of Philosophy in Medical Sciences-Medical Genetics.

Julia E. Richards
Dr. Julia Richards

John B. Bell
Dr. John Bell

Heather M. Dermid
Dr. Heather McDermid

Ian MacDonald
Dr. Ian MacDonald

April 26, 2001

Michael Walter
Dr. Michael Walter

To Marlene Gould.

Mom, I dedicate this thesis, with love, to your memory.

**ABSTRACT**

My research has been to identify regions of the human genome and then genes within these regions, which are involved in Axenfeld-Rieger eye malformations. I have, in parallel with Dr. Alan Mears, mapped a novel locus for autosomal dominant iridogoniodysgenesis anomaly (IGDA) with secondary glaucoma to human chromosome 6p25. I then mapped two additional families with Axenfeld Rieger anomaly (ARA) and Axenfeld Rieger syndrome (ARS) to the same chromosomal location at 6p25.

To further restrict the critical interval of the locus at 6p25, I conducted molecular analysis of patients with deletions of the short arm of chromosome 6. I have provided evidence that a second locus for eye anterior segment analysis exists at 6p25. I have also provided preliminary evidence for the existence of an autosomal dominant, progressive, hearing loss locus at 6p25.

Finally, I have conducted mutational analysis on two candidate genes for AR malformations. The first, *FOXF2*, maps within the critical interval at 6p25 and therefore is a positional candidate gene for AR malformations that map to 6p25. *FOXF2* is

also a functional candidate gene because mutations in a paralogous gene, *FOXC1*, have been shown to cause AR malformations. Mutational analysis of *FOXF2* in families with AR malformations that map to 6p25 did not reveal any disease causing alterations but three sequence polymorphisms were identified.

I also cloned and characterized a novel human gene, *BARX1*, and examined it as a functional candidate gene in patients with sporadic eye anterior segment malformations. The expression of *BARX1* in iris and craniofacial mesenchyme is consistent with *BARX1* being involved in AR malformations. Mutational analysis of 55 patients with eye anterior segment malformations did not reveal any disease causing mutations, however six sequence polymorphisms were observed.

**Acknowledgements**

I would like to take this rare opportunity to acknowledge those people who have made this possible.

First and foremost, I thank my family. My parents for giving me first the freedom to choose any path I desired and secondly for making it possible to follow that path. My brother and sister, Dale and Denise, for providing exactly the support one expects from family. Thank you.

I thank Corrine for everything she is to me. Through it all, she has always been there. Unconditionally. Thank you.

I thank Terry for being the kind of friend that adds meaning to life. Thank you.

I thank Don and Barb for teaching me how to be a better person. They are strong role models and two better people you will not find. Thank you.

I thank Ramsey for the conversation, the perspectives and the insights. Every second was time well spent. Thank you.

I thank Dave for being here even when you are not. Thank you.

I thank Owen for reminding me how to approach life and for helping me approach it the same way. Thank you.

To Mike, Candice, Paul, Monica, Peter, Janice, Ronn, Mick, Kelly, Curtis, Curtis, Darren, Chris, Charlie, Brad and all my friends in Consort, Coronation, Edmonton, Calgary and elsewhere, Thank you.

To Dr. Michael Walter whose knowledge, guidance, support, leadership and friendship are all responsible for any success I have had. Thank you.

To Dr. Ian MacDonald for setting a high standard and inspiring everyone he meets without knowing it. Thank you.

To James for the late night conversations, Farideh for the daily assistance, Fred for the coffee, Kathy for the cake, Mike for the parties, Vince for the stories, Kerry, Jody and Sherry for the help and of course Dean for the crib. Thank you all.

# Table of Contents

## Chapter One: Intorduction


Introduction.....Page 1

A) Ocular Histology .....Page 3

B) Ocular Embryology.....Page 23

C) The Genetics of Ocular Development.....Page 39

i) Genes in *Drosophila*.....Page 42

ii) Genes in Mammals.....Page 46

D) Glaucoma.....Page 49

i) Aqueous Humor Dynamics.....Page 50

ii) Classification of Glaucomas.....Page 52

E) The Genetics of Glaucoma.....Page 54

i) Primary Open Angle Glaucoma.....Page 55

ii) Primary Congenital Glaucoma.....Page 60

iii) Secondary Glaucoma.....Page 61

F) Axenfeld-Rieger Malformations.....Page 62

i) Clinical Description of AR.....Page 62

ii) Genetics of AR.....Page 63

G) References.....Page 65

## Chapter Two: Mapping of Axenfeld Rieger Malformations

A) Introduction.....Page 85

B) Materials and Methods.....Page 87

i) Clinical Analysis.....Page 87

ii) Linkage Analysis.....Page 98

C) Results.....Page 103

D) Discussion.....Page 110

E) References.....Page 114

## Chapter Three: *FOXF2* as a Candidate Gene for Axenfeld Rieger Malformations

A) Introduction.....Page 120

B) Materials and Methods.....Page 122

i) Direct Sequence Analysis.....Page 122

ii) SSCP.....Page 127

C) Results.....Page 127

D) Discussion.....Page 131

E) References.....Page 132

## Chapter Four: *BARX1* as a Candidate Gene for Axenfeld Rieger Malformations

A) Introduction.....Page 136

B) Materials and Methods.....Page 140

i) Screening of cDNA Library.....Page 140

ii) Characterization of the *BARX1* Gene...Page 144

iii) Northern Analysis.....Page 146

iiii) Radiation Hybrid Mapping.....Page 146

iiiii) Mutation Analysis.....Page 147

C) Results.....Page 148

i) Cloning of *BARX1*.....Page 148

ii) Genomic Structure of *BARX1*.....Page 151

iii) Northern Analysis.....Page 151

iiii) Chromosomal Localization.....Page 155

iiiii) Mutational Analysis.....Page 156

D) Discussion.....Page 158

i) Cloning of *BARX1*.....Page 158

ii) Northern Analysis.....Page 161

iii) Chromosomal Localization.....Page 161

iiii) Mutational Analysis.....Page 162

E) References.....Page 166

**Chapter Five: Characterization of Eight Patients with Terminal Deletions of Chromosome 6p25**

A) Introduction.....Page 172

B) Materials and Methods.....Page 174

i) Patient Reports.....Page 174

ii) Microsatellite Analysis.....Page 181

C) Results.....Page 182

i) Patients with Simple Deletions.....Page 182

ii) Patients with Unbalanced Translocations.....Page 186

D) Discussion.....Page 186

i) Genes Deleted in the 6p25 Region.....Page 186

ii) Genotype/Phenotype Correlation.....Page 195

iii) Evidence for Autosomal Dominant Deafness Locus.....Page 203

iiii) Evidence for an Eye Malformation Locus.....Page 204

E) References.....Page 206

Chapter Six: Discussion and Conclusions

A) Linkage Analysis.....Page 217

B) Deletion Patient Analysis.....Page 219

C) Mutational Analysis of Candidate Genes.....Page 220

D) Conclusions.....Page 223

E) References.....Page 225

**Appendix: Mutational Analysis of BARHL1 and BARX1 in Three New Patients With Joubert Syndrome**.....Page 229

## List of Tables

**Table 1-1** Germinal tissue of ocular structures.....Page 24

**Table 1-2** Known glaucoma loci and genes identified.Page 56

**Table 2-1** Variable expressivity of IGDA.....Page 95

**Table 2-2** Clinical findings of Family D.....Page 101

**Table 2-3** Two point LOD scores between chromosome 6 markers and IGDA in Families A and B...Page 105

**Table 2-4** LOD scores for 4q25 and 6p25 in Family C.Page 109

**Table 3-1** *FOXF2* primer sequences and conditions....Page 126

**Table 4-1** Primer pairs used to PCR amplify *BARX1*...Page 143

**Table 4-2** Intron/Exon boundaries for *BARX1*.....Page 152

**Table 4-3** Sequence alterations in *BARX1*.....Page 157

**Table 5-1** Clinical features of deletion patients in this study and from a survey of the literature.....Page 189

**Table5-2** Clinical features of patients with molecularly characterized terminal deletions.....Page 199

**Table 5-3** Clinical features of patients from other

published reports with molecularly characterized interstitial deletions.....Page 202

**Table A-1** Primer pairs used to amplify *BARHL1*.....Page 238

**Table A-2** Intron/Exon boundaries for *BARHL1*.....Page 243

## List of Figures


**Figure 1-1** Structures of the human eye.....Page 5

**Figure 1-2** Cell layers of the cornea.....Page 7

**Figure 1-3** Iridocorneal angle of the eye.....Page 10

**Figure 1-4** The trabecular meshwork.....Page 12

**Figure 1-5** The juxtacanalicular tissue.....Page 14

**Figure 1-6** Aqueous humor flow.....Page 18

**Figure 1-7** Schematic of the layers of the retina.....Page 20

**Figure 1-8** Three waves of neural crest derived mesenchyme invade the developing eye.....Page 26

**Figure 1-9** Morphogenesis of the optic primordia.....Page 29

**Figure 1-10** Origin and terminal position of migrating neural crest cells.....Page 31

**Figure 1-11** Morphogenesis of the murine optic cup.....Page 34

**Figure 1-12** Stages of lens induction.....Page 36

**Figure 1-13** Hierarchy of *Drosophila* genes involved in early eye development .....Page 45

**Figure 2-1** Photograph of an eye from an unaffected member of Family A.....Page 90

**Figure 2-2** Pedigree and affected eye photograph from Family A.....Page 92

**Figure 2-3** Pedigree and affected eye photograph from Family B.....Page 94

**Figure 2-4** Pedigree and affected eye photograph from Family C.....Page 97

**Figure 2-5** Pedigree and affected eye photograph from Family D.....Page 100

**Figure 2-6** Critical intervals for ARA and IGDA.Page 107

**Figure 3-1** Genetic mapping of IRID locus.....Page 124

**Figure 3-2** Schematic of *FOXF2* gene.....Page 129

**Figure 4-1** Schmatic of the human *BARX1* gene....Page 142

**Figure 4-2** Alignments of predicted human *BARX1* protein sequence with protein sequence of related Bar class proteins.....Page 150

**Figure 4-3** Autoradiographs of commercial Northern blots probed with *BARX1*....Page 154

**Figure 5-1** Schematic of the distal tip of human

chromosome 6p.....Page 185

**Figure 5-2** Schematic of extent of deletions for 8 patients in the literature with deletions characterized at a molecular level.....Page 198

**Figure A-1** Schematic of the *BARX1* coding region.....Page 237

**Figure A-2** Magnetic resonance imaging of patients 2 and 3.....Page 241

# List of Abbreviations

| | |
|---|---|
| °C | degrees Celcius |
| µCi | micro Curies |
| µL | micro Liters |
| µM | micro Molar |
| λZAP | bacteriophage vector |
| $^{32}P$ | radioactive phosphorous isotope 32 |
| $^{33}P$ | radioactive phosphorous isotope 33 |
| $^{35}S$ | radioactive sulphur |
| A | adenine |
| AR | Axenfeld Rieger |
| ARA | Axenfeld Rieger anomaly |
| ARS | Axenfeld Rieger syndrome |
| ASD | atrial septal defect |
| BARX1 | bar class homeobox gene 1 |
| BOR | Branchial-Oto-Renal |
| bp | base pairs |
| C | cytidine |
| cDNA | complementary DNA |
| CHLC | The Cooperative Human Linkage Center |
| cM | centi Morgans |
| C-section | cesarian section |
| CT | computed tonography |
| C-terminal | carboxy terminal |

| | |
|---|---|
| CYP1B1 | cytochrome P450 1B1 |
| dac | drosophila dachshund gene |
| DACH | mamalian dachshund gene |
| dATP | deoxyadenosine triphosphate |
| dCTP | deoxycytosine triphosphate |
| dGTP | deoxyguanosine triphosphate |
| dITP | deoxyinosine triphosphate |
| DMSO | dimethyl sulphoxide |
| DNA | deoxyribonucleic acid |
| dTTP | deoxythymidine triphosphate |
| E | embryonic day |
| ECM | extracellular matrix |
| EEG | electroencephalogram |
| ey | *Drosophila* gene eyeless |
| eya | *Drosophila* gene eyes absent |
| eyg | *Drosophila* gene eyes gone |
| FOXC1 | forkhead box C1 |
| FOXF2 | forkhead box F2 |
| G | guanine |
| GLC1 | primary open angle glaucoma loci A-F |
| GLC3 | primary congenital glaucoma loci |
| HCl | hydrochloric acid |
| IGDA | iridogoniodysgenesis anomaly |
| IGDS | iridogoniodysgenesis syndrome |
| IOP | intraocular pressure |
| LMX1B | LIM homeobox containing transcription factor1β |
| LOD | Log of odds |

| | |
|---|---|
| $MgCl_2$ | magnesium chloride |
| mL | milliliters |
| mM | millimolar |
| MRI | magnetic resonance imaging |
| MYOC | myocillin |
| NaCl | sodium chloride |
| NaOH | sodium hydroxide |
| ng | nanograms |
| N-terminal | amino terminal |
| PAX6 | paired box 6 |
| PCG | primary congenital glaucoma |
| PCR | polymerase chain reaction |
| PDA | patent ductus ateriosus |
| PFO | patent foramen ovale |
| PITX2 | pituitary transcription factor 2 |
| POAG | primary open angle glaucoma |
| RGC | retinal ganglion cell |
| RPE | retinal pigment epithelium |
| SDS | sodium dodecyl sulfide |
| sey | mouse small eye phenotype |
| SIX3 | mamalian homolog of *Drosophila* sine oculis gene |
| SM | salt magnesium |
| so | *Drosophila* sine oculis gene |
| SSC | sodium chloride and sodium citrate solution |
| SSCP | single strand conformation polymorphism |
| T | thymine |
| T5-T6 | thorasic vertebrae 5 and 6 |

| | |
|---|---|
| *Taq* | *Thermus aquaticus* |
| THC | tentative human contig |
| TIGR | trabecular meshwork glucocorticoid response |
| TIGR | The Institute for Genetic Research |
| TM | trabecular meshwork |
| toy | *Drosophila* gene twin of eyeless |
| Tris | Tris(hydroxymethyl)aminomethane |
| UTR | untranslated region |
| VSD | ventricular septal defect |

# CHAPTER 1

# INTRODUCTION

For many reasons, the eye has long been a favorite structure of developmental biologists. The eye is easily observed and extremely delicate. Therefore, even minor changes rarely go unnoticed. In addition, the eye is very important, as it is the one of our main sensory organs. However, eye malformations are usually not lethal and therefore the eye lends itself to genetic study more so than many other organs.

There are multiple reasons why vision loss may occur in one or both eyes. Glaucoma describes a group of disorders that arise, not as a single disease process, but as the result of many possible factors, both genetic and environmental. The importance of glaucoma research can be reflected in the quality of life for the estimated 13,000 (estimation extrapolated from Quigley and Vitale 1997) Canadians that will lose their vision to the disease each year and the cost to our medical system to treat this preventable vision loss.

Before understanding glaucoma, one must first be familiar with the histology of the eye, the tissues involved, and the locations, functions and interactions of these tissues. Before understanding the genetics of glaucoma it is also important to understand the

embryological origins of these tissues and the changes the germ layers undergo to form the mature eye.

## A) HISTOLOGY OF THE HUMAN EYE

The eye can be divided into three basic layers, the corneosclera, the uveal tract, and the inner retina (Sternberg 1997) (Figure 1-1). The sclera is the tough, white outer covering of the eye. The sclera provides the eye with some degree of protection while giving it structure and form. It is also important that the sclera be opaque so light is not able to enter the eye except by controlled means. The intended path for light entering the eye is through the cornea. The cornea is the anterior-most tissue of the eye and is continuous with the sclera. In direct contrast to the sclera, the cornea must be extremely transparent. The cornea also provides some degree of protection for the eye, however, the most important function of the cornea is the refraction of light entering the eye onto the lens. The cornea is composed of six layers (Figure 1-2). The outer surface of the cornea is the corneal epithelium. Directly underlying the corneal epithelium is a basal lamina, followed by Bowman's layer, the corneal stroma, Descemet's

**FIGURE 1-1. Structures of the human eye.**

The three basic layers of the eye: corneosclera, uveal tract, and retina. The corneosclera is made up of cornea and sclera. The uveal tract consists of iris, ciliary body, and choroid. The zonular fibers extend from the ciliary body to the lens. Other structures identified are the aqueous humor, the vitreous, the macula, and the optic nerve. Taken from Harding 1997.

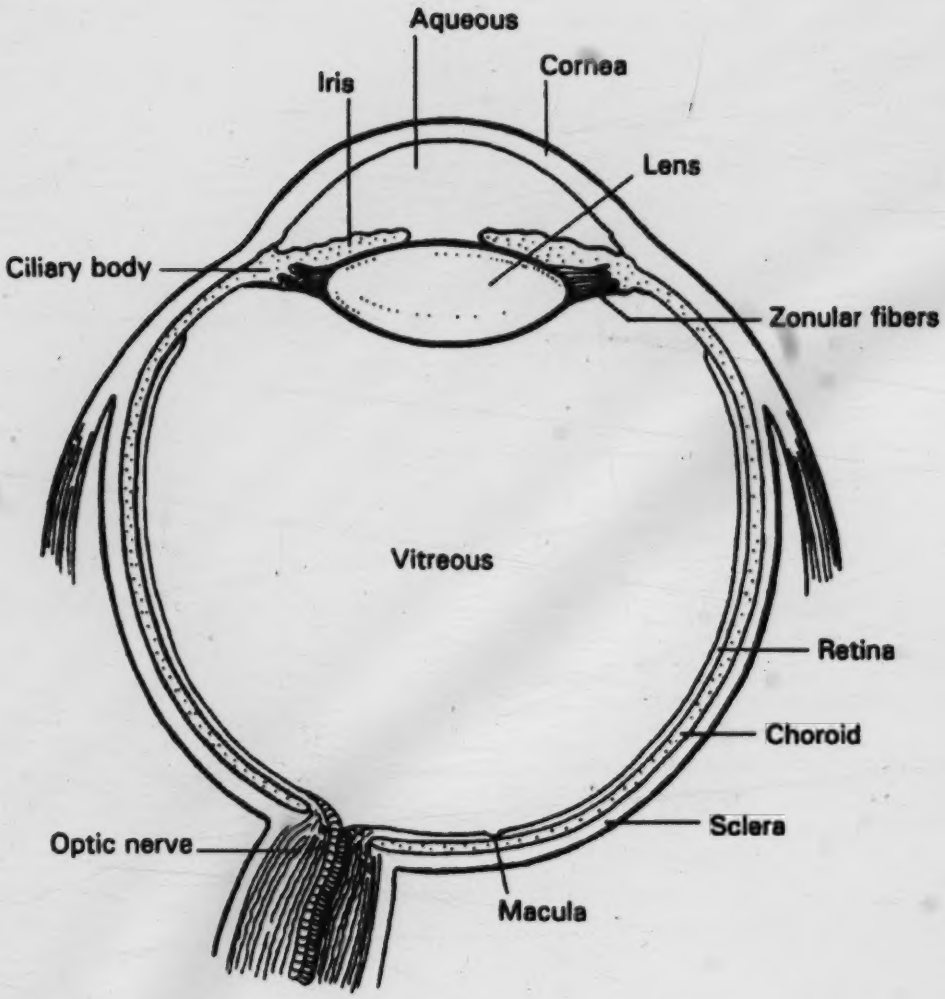
Aqueous
Cornea
Iris
Lens
Ciliary body
Zonular fibers
Vitreous
Retina
Choroid
Sclera
Optic nerve
Macula

**FIGURE 1-2. Cell layers of the cornea.**

The six morphological layers of the cornea are the epithelium, a basal lamina, Bowman's membrane, the corneal stroma, Descemet's membrane and the corneal endothelium. The basal membrane of the corneal epithelium is not identified in this figure. Keratocytes are mesenchymal cells that exist within the stroma. Taken from Harding 1997.

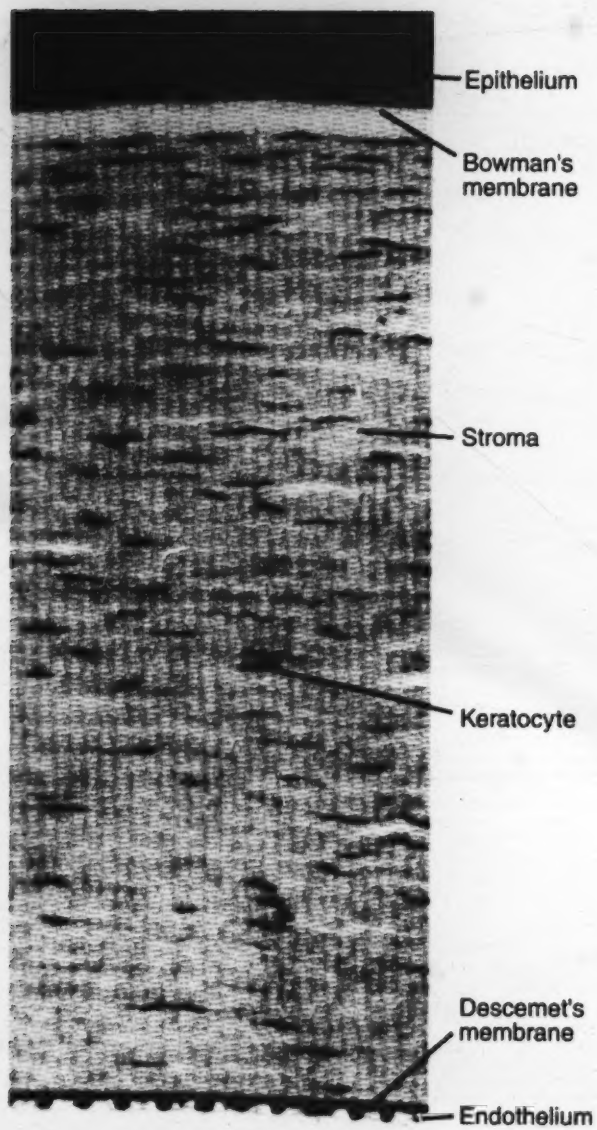
Epithelium
Bowman's membrane
Stroma
Keratocyte
Descemet's membrane
Endothelium

membrane and finally the corneal endothelium.

The junction between the cornea and sclera, the corneoscleral limbus, is the location of the trabecular meshwork (TM) and Schlemm's canal (Figure 1-3). The TM is a sieve-like structure through which fluid drains as it leaves the anterior chamber of the eye. The TM is comprised of three portions (Shields 1987) (Figure 1-4). The uveal meshwork is an irregularly sized rope-like meshwork, continuous with the iris, that the fluid must drain through first on its way out of the eye. The corneoscleral meshwork is a layer of sheets perforated with elliptical openings that directly underlies the uveal meshwork. The juxtacanalicular layer is connective tissue and endothelium that surrounds Schlemm's canal (Figure 1-5). As the fluid drains through the meshwork it is collected by Schlemm's canal and returned to the body's circulatory system.

The second layer of the eye is the uveal tract. The uveal tract consists of the iris, the ciliary body and the choroid (Figure 1-1). The uveal tract is heavily vascularized and supplies nutrients to much of the eye.

The iris is the colored part of the eye encircling the pupil. The basic function of the iris is to regulate the amount of light that

**FIGURE 1-3. Iridocorneal angle of the eye.**

The trabecular meshwork and Schlemm's canal are located at the angle of the anterior chamber of the eye. **C** cornea; **CB** ciliary body; **I** iris; **IP** iris process; **SC** Schlemm's canal; **SL** Schwalbe's line; **SS** scleral spur; **TM** trabecular meshwork. Taken from Jakobiec 1982.

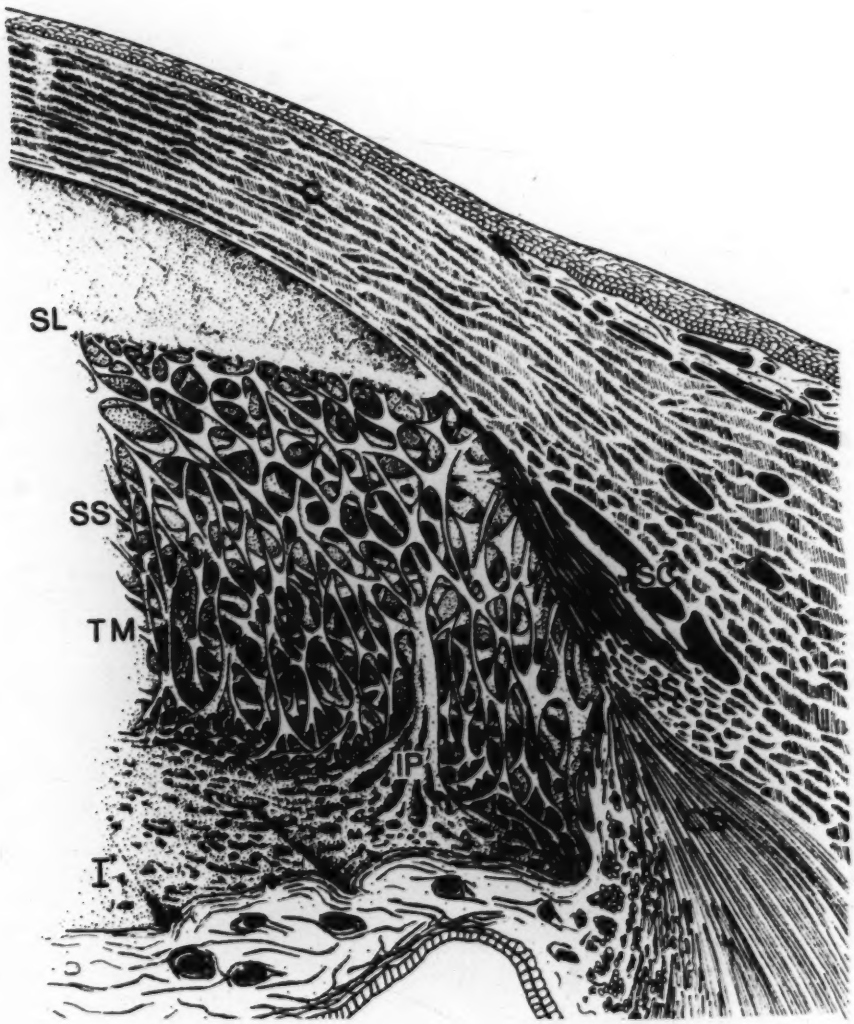
SL
SS
TM
SC
IP
I

**FIGURE 1-4. The trabecular meshwork.**

The rope-like strands of the uveal meshwork are easily observed (f). The perforated sheets of the corneoscleral meshwork are visable underneath the uveal meshwork (c). Schlemm's canal (a) lies beneath the uveal meshwork. An internal collector channel (c) opens into Schlemm's canal. The ciliary body (CB), ciliary muscle (i), scleral spur (d), Descemet's membrane (g), and an iris strand (h) are also visable. The corneal endothelium (j) is continuous with the trabecular endothelium. Taken from Spencer 1985.

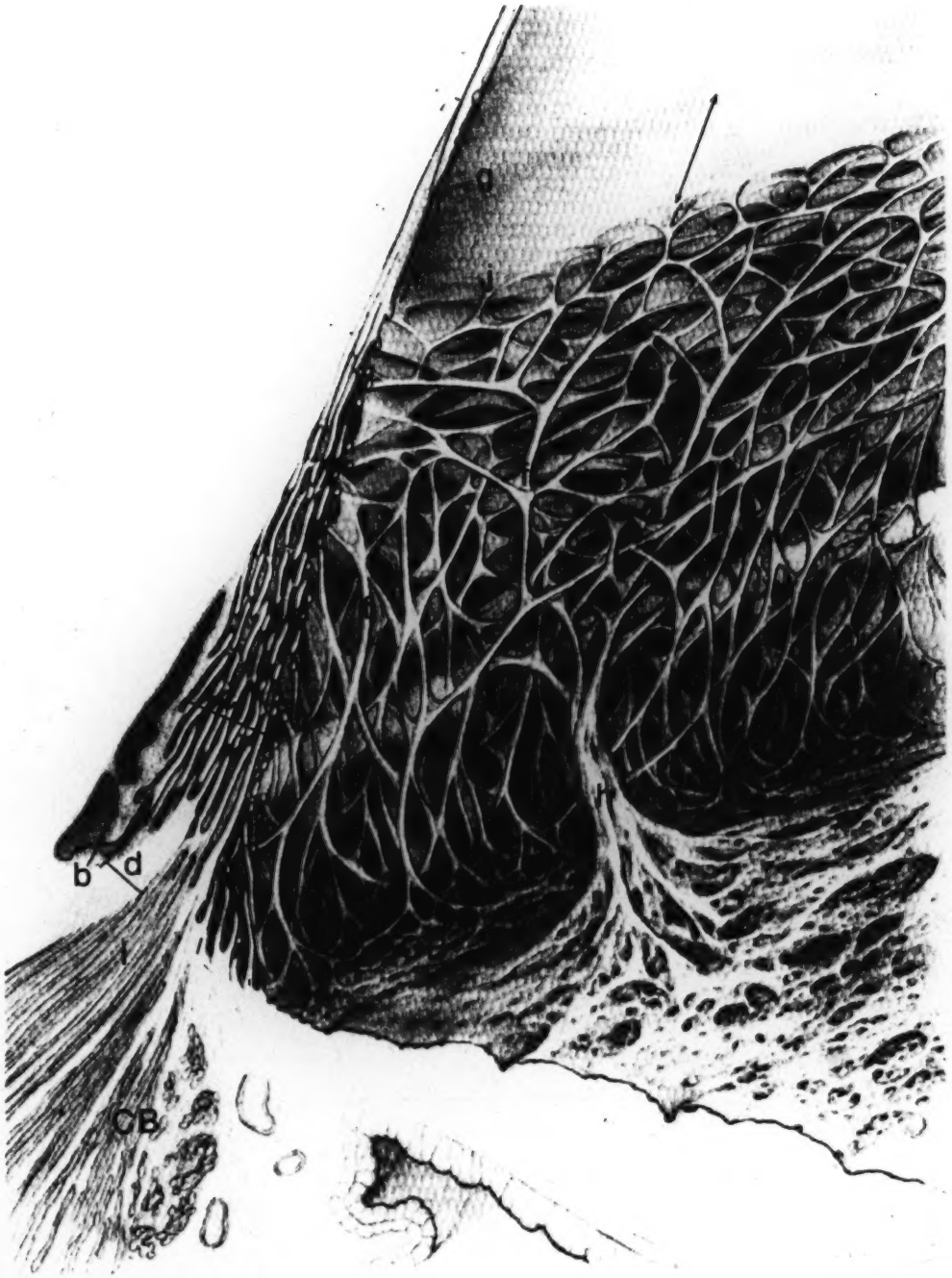
g
i
b
d
CB

**FIGURE 1-5. The juxtacanalicular tissue.**

Schlemm's canal (sc) is lined by an endothelium (e) that contains giant vacuoles (gv). An interior collector channel (icc) reaches into the corneoscleral trabecular sheets (cst). A trabecular space is indicated (ts) and Schlemm's canal is shown surrounded by a wall (a) separating the lumen from trabecular spaces. The exterior wall (ew) and interior wall (iw) of Schlemm's canal are also labeled. Taken from Spencer 1985.

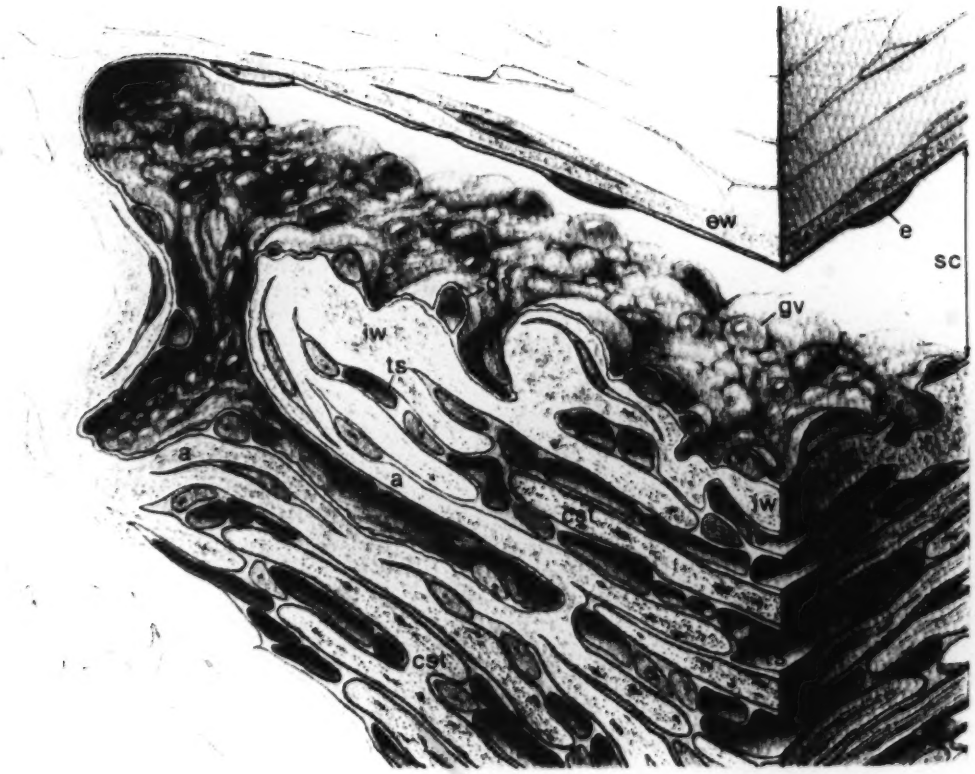
ew
e
sc
gv
iw
ts
a
a
iw
cst

reaches the retina. Structurally, the iris consists of a heavily pigmented posterior epithelial lining and the overlying stroma. The pigmentation of the stroma varies greatly and gives the eye its color, with dark eyed people having heavier pigmentation than those with lighter colored eyes. The stroma contains melanocytes, nerve cells, blood vessels, and smooth muscle. The sphincter pupillae is a bundle of circularly arranged smooth muscles that are able to constrict the pupil to reduce the amount of light that enters the posterior chamber of the eye. Dilator muscles also exist in the stroma which increase the aperture of the pupil to allow the entrance of more light.

The ciliary body is the middle segment of the uveal tract between the iris and the choroid. The functions of the ciliary body are twofold. First, the ciliary muscle is attached to the lens by zonules (Figure 1-1). Contraction and relaxation of the ciliary body change the shape of the lens and therefore controls the refraction of light onto the retina. The second major function of the ciliary body is the production of aqueous humor. Aqueous humor is the fluid that fills the anterior chamber of the eye. The ciliary body is heavily vascularized with arterial capillaries. Aqueous humor is produced by the ultrafiltration of plasma across capillary walls followed by active transport of necessary molecules across the ciliary epithelium

(Harding 1997). The main function of the aqueous humor is nourishment of the lens, cornea and trabecular meshwork. In conjunction with this, the aqueous humor is also responsible for removal of cellular debris from the anterior chamber. The requirement of transparency of the cornea and lens do not allow for vascularization and therefore the aqueous humor compensates for the lack of vascularization. The intraocular pressure of the anterior chamber of the eye is a function of the production of aqueous humor in the ciliary body and aqueous humor efflux mainly through the trabecular meshwork and Schlemm's canal (Figure 1-6). Minor drainage of aqueous humor occurs via uveoscleral outflow.

The choroid is the final component of the uveal tract. The outer surface of the choroid lies adjacent to the sclera and the inner surface to Bruch's membrane and the retinal pigment epithelium. The choroid is largely vascularized and provides nourishment for the retinal layers.

The retina can be divided into two main layers, the retinal pigment epithelium (RPE) and the neural retina. The neural retina is the portion of the eye responsible for receiving light and transmitting the information to the brain. The neural retina can be subdivided into seven distinct layers (Figure 1-7). The outermost

**FIGURE 1-6. Aqueous humor flow.**

The aqueous humor is produced in the posterior chamber by the ciliary body and flows over the lens, through the pupil into the anterior chamber. Outflow of aqueous humor from the anterior chamber is predominantly through the trabecular meshwork and Schlemm's canal. Taken from Epstein et al. 1997.

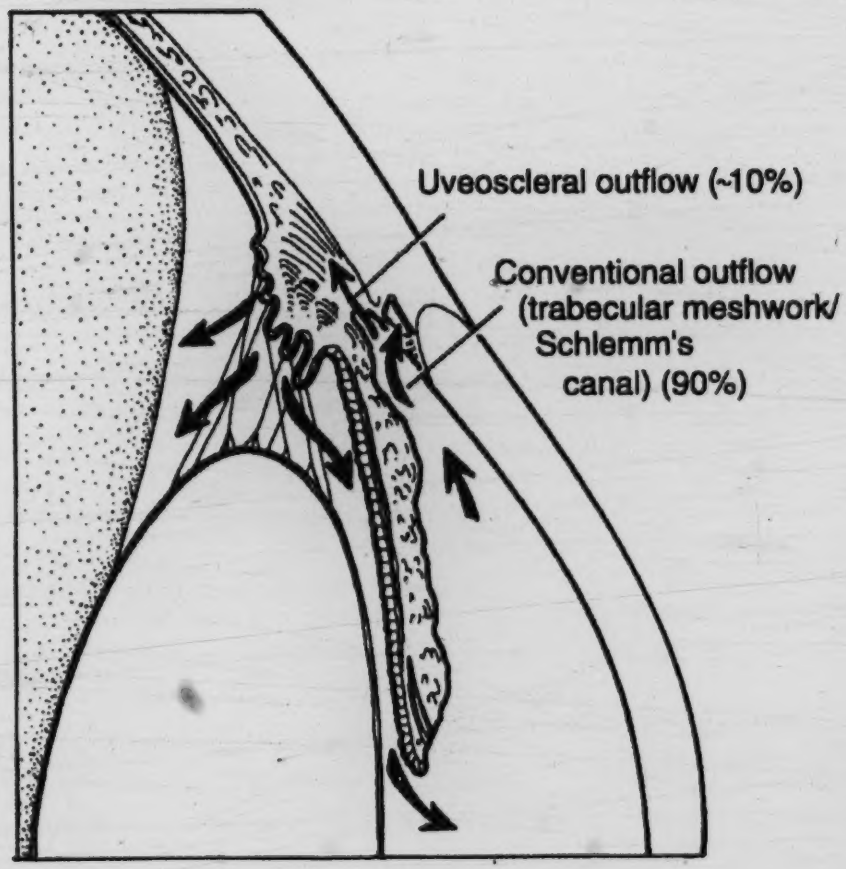
Uveoscleral outflow (~10%)
Conventional outflow
(trabecular meshwork/
Schlemm's
canal) (90%)

**FIGURE 1-7. Schematic of the layers of the retina.**

From bottom to top in the diagram are the outermost to innermost layers. The pigmented epithelium is shown adjacent to Bruch's membrane. The layers as one goes inward are: the rod and cone outer segments, the outer nuclear layer which contains the nuclei of photoreceptors, the outer plexiform layer, the inner nuclear layer, the inner plexiform layer, the ganglion cell layer, and the neural fiber layer. Taken from Jakobiec 1982.

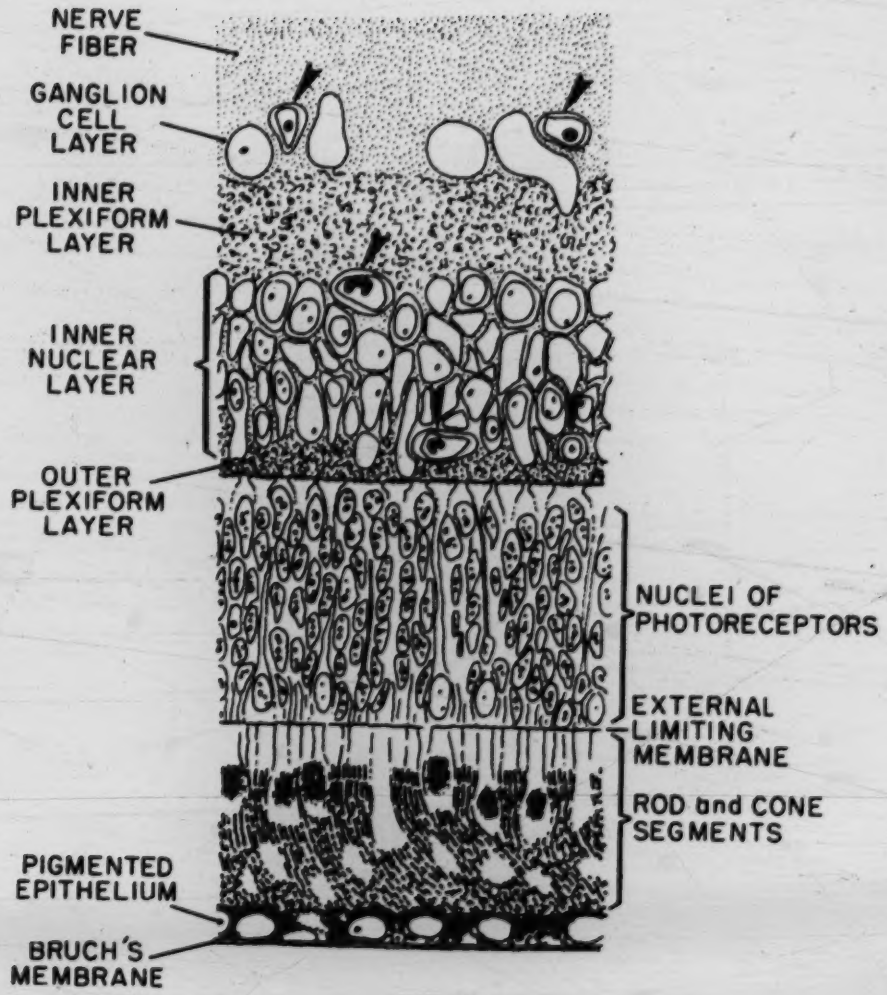
NERVE FIBER
GANGLION CELL LAYER
INNER PLEXIFORM LAYER
INNER NUCLEAR LAYER
OUTER PLEXIFORM LAYER
NUCLEI OF PHOTORECEPTORS
EXTERNAL LIMITING MEMBRANE
ROD and CONE SEGMENTS
PIGMENTED EPITHELIUM
BRUCH'S MEMBRANE

**TABLE 1-1. Germinal tissue origin of ocular structures**

| Germinal Tissue | Ocular Structure |
|---|---|
| Surface Ectoderm | Corneal epithelium |
| | Lens |
| | Conjunctiva |
| Neural Ectoderm | Retinal pigment epithelium |
| | Neural retina |
| | Iris posterior epithelium |
| | Iris sphincter and dilator muscles |
| | Ciliary epithelium |
| Neural Crest (Mesenchyme) | Choroid stroma |
| | Sclera |
| | Corneal endothelium |
| | Corneal stroma |
| | Trabecular meshwork |
| | Iris stroma |
| | Ciliary stroma |

**FIGURE 1-8. Three waves of neural crest derived mesenchyme invade the developing eye.**

Wave I forms corneal endothelium. Wave II forms corneal stroma. Wave III forms the iris stroma. Taken from Jakobiec 1982.

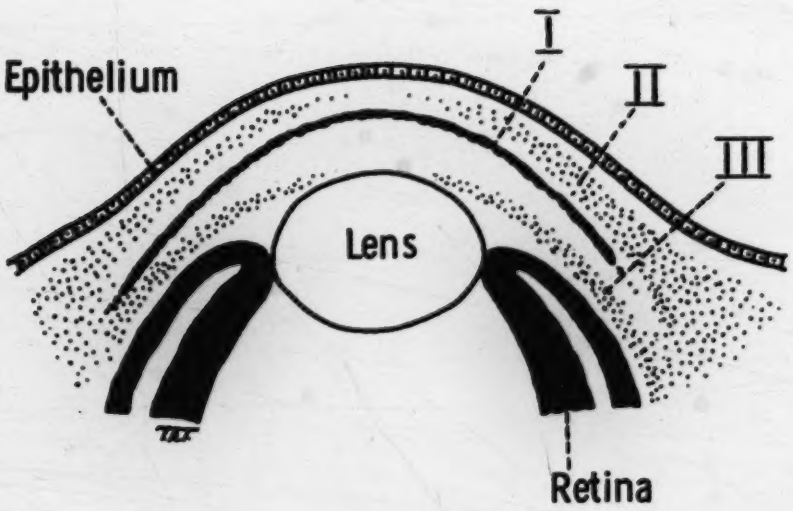
Epithelium
I
II
III
Lens
Retina

three segments, the prosencephalon, the mesencephalon and the rhombencephalon (anterior to posterior). In the fourth and fifth weeks, the prosencephalon divides into the telencephalon anteriorly and diencephalon posteriorly while the rhombencephalon divides into the metencephalon anteriorly and myelencephalon posteriorly. At this point the brain is divided into five segments; the telencephalon, the diencephalon, the mesencephalon, the metencephalon and the myelencephalon. The optic primordia first appear in the diencephalon near the telencephalon at E22 (embryonic day 22) (Barishak 1992) (Figure 1-9b). At E24 the optic pits move laterally toward the surface ectoderm. At E25 the optic primordia forms as an evagination of neural ectoderm tissue from the diencephalon (Jakobiec 1982) (Figure 1-9c).

Neural crest cells from the top and middle of the mesencephalon form as a delamination of surface ectoderm (Jakobiec 1982). The neural crest cells migrate laterally then ventrally from their original position until they reach their destinations at the maxillary process, the mandibular process and between the optic primordia and surface ectoderm (Figure 1-10).

The evaginating optic primordia approaches the overlying surface ectoderm. The optic stalk develops as the optic primordia

**FIGURE 1-9. Morphogenesis of the optic primordia.** Early mophogenesis of the optic primordia at E20 (A), E24 (B), and E26 (C). The inset frames in A), B), and C) show cross section drawings. The second inset frame (frontmost) in B) indicates the position of the optic pits as the neural groove closes. Taken from Jakobiec 1982.

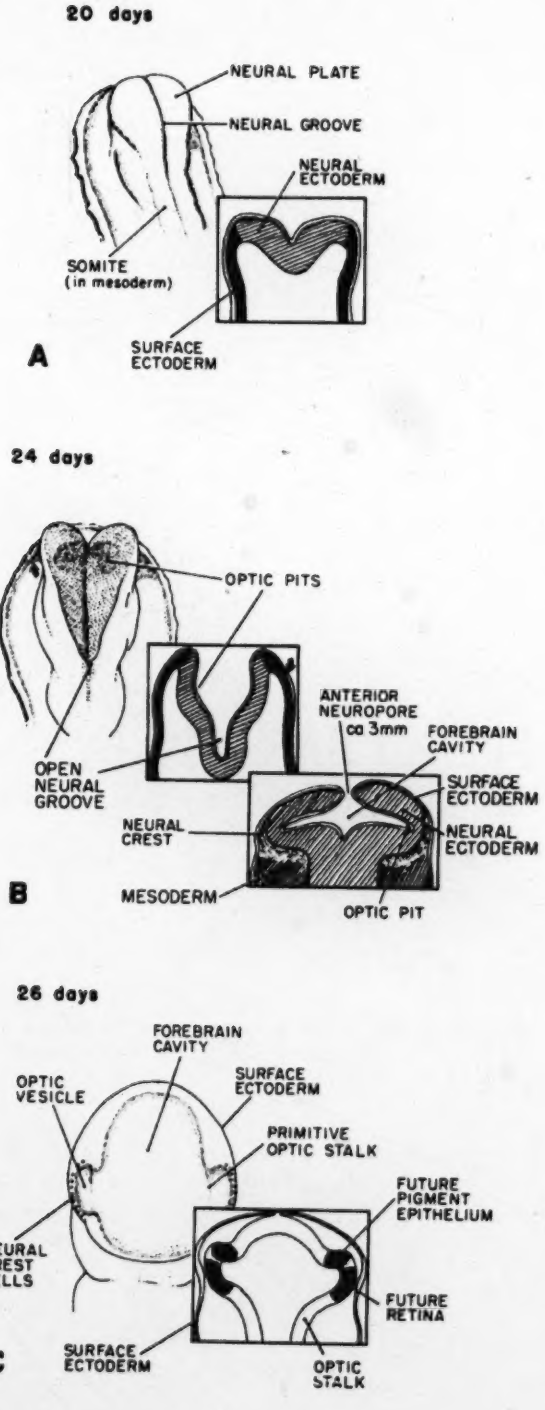
20 days
NEURAL PLATE
NEURAL GROOVE
NEURAL ECTODERM
SOMITE (in mesoderm)
SURFACE ECTODERM
A
24 days
OPTIC PITS
ANTERIOR NEUROPORE ca 3mm
FOREBRAIN CAVITY
OPEN NEURAL GROOVE
SURFACE ECTODERM
NEURAL CREST
NEURAL ECTODERM
MESODERM
OPTIC PIT
B
26 days
FOREBRAIN CAVITY
OPTIC VESICLE
SURFACE ECTODERM
PRIMITIVE OPTIC STALK
FUTURE PIGMENT EPITHELIUM
NEURAL CREST CELLS
FUTURE RETINA
SURFACE ECTODERM
OPTIC STALK
C

**FIGURE 1-10. Origin and terminal position of migrating neural crest cells.**

Murine embryo that has been fixed 22 hours after receiving a graft of $^{3}$H-thymidine-labeled neural crest cells. The graft is seen as two clusters of dots in the roof of the midbrain. These cells migrate laterally (into and out of the page) then ventrally (to the right) to occupy positions at the maxillary process, mandibular process and optic primordia. Taken from Jakobiec 1982.

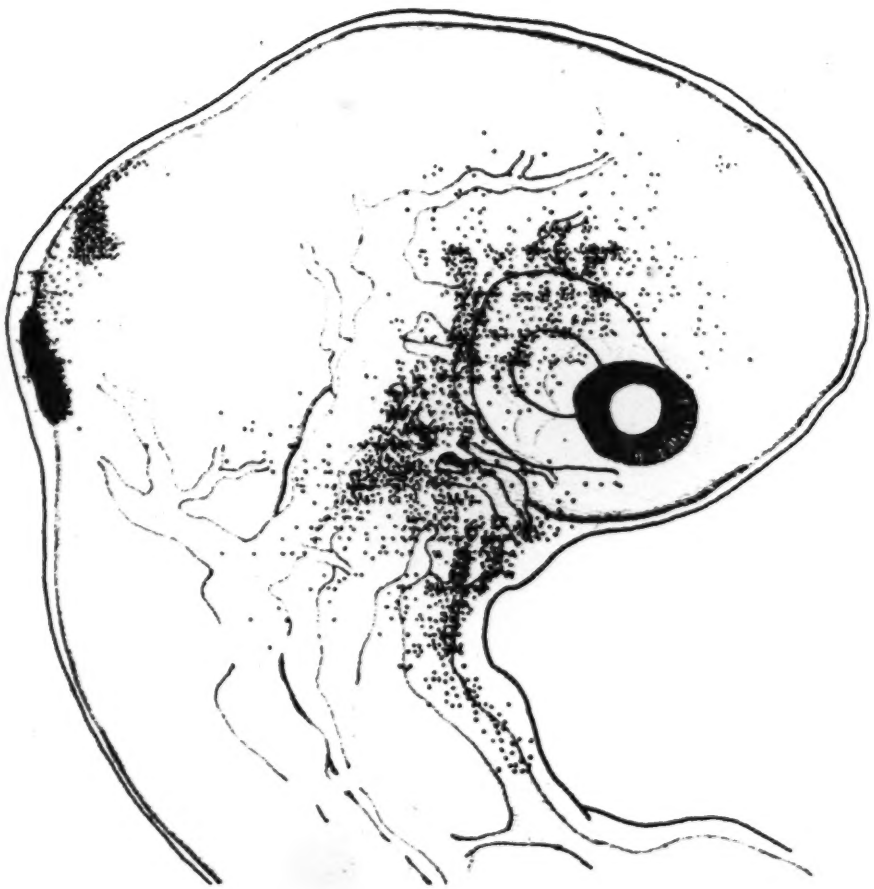

constricts giving rise to the optic vesicle (Figure 1-11). The optic stalk is the connection between the eye and what will become the third ventricle of the brain (Jakobiec 1982). As the neural ectoderm of the optic vesicle forms and approaches the overlying surface ectoderm, the optic vesicle is ensheathed by neural crest cells. Only a small region at the center of the optic vesicle is not covered by neural crest cells and this region makes contact with the surface ectoderm. The site of this contact is the site of lens induction.

Lens induction is a well-studied process that acts as a model for the reciprocal inductive process that occurs between tissues during organogenesis. The process of lens induction involves the surface ectoderm receiving a signal from the neural ectoderm of the optic cup. In response, a thickening of the surface ectoderm develops called the lens placode. The area of the lens placode undergoes rapid proliferation and the eventual invagination of this tissue, results in the lens placode forming the lens pit. The lens pit continues to invaginate to form the lens cup and the surface ectoderm begins to close. The lens cup deepens and a zone of necrosis displaces the lens cup as it closes and forms the lens vesicle (Fini 2000; Jakobiec 1982) (Figure 1-12). The lens vesicle is a single layer of epithelial cells covered with a basal lamina (Jakobiec

**FIGURE 1-11. Morphogenesis of the murine optic cup.**

A-F show the major morphogenetic changes that take place in murine eye development. Key stages are encroachment of optic vesicle on surface ectoderm (A) and (B), induction of the lens placode (C), folding of the optic cup (D), involution of lens pit (D), formation of lens vesicle (E), and constriction of optic stalk (F). The embryonic day of each stage is indicated at the bottom. Taken from Fini 2000.

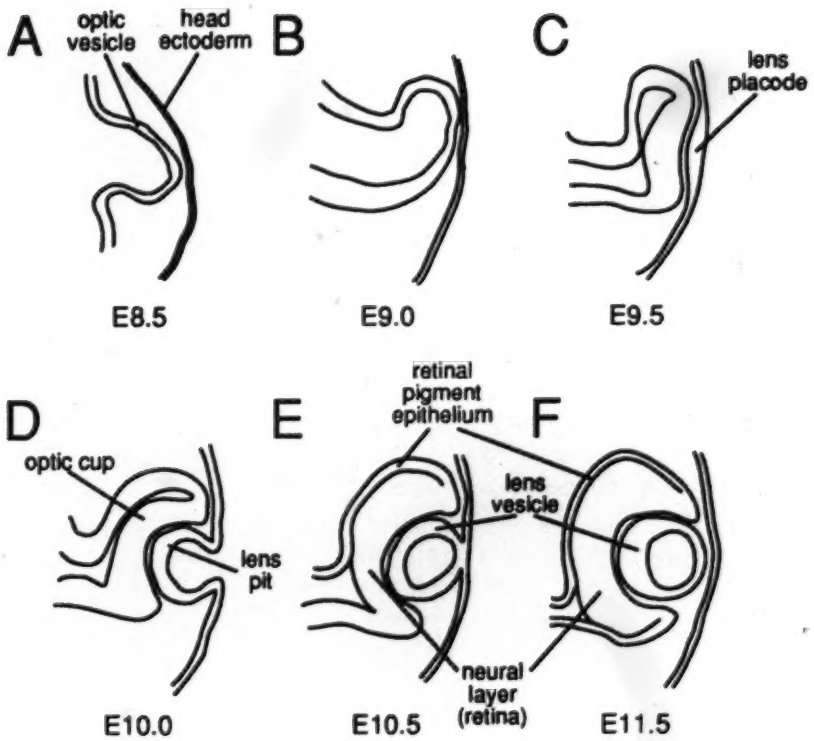
A
optic vesicle
head ectoderm
E8.5
B
E9.0
C
lens placode
E9.5
D
optic cup
lens pit
E10.0
E
retinal pigment epithelium
lens vesicle
neural layer (retina)
E10.5
F
E11.5

**FIGURE 1-12. Stages of lens induction.**

The morphogenetic stages of lens induction are shown. Induction of the surface ectoderm forms the lens placode. This invaginates to make the lens pit that seals off to form the lens vesicle. The lumen of the lens vesicle is eventually filled with lens fibers. Taken from Harding 1997.

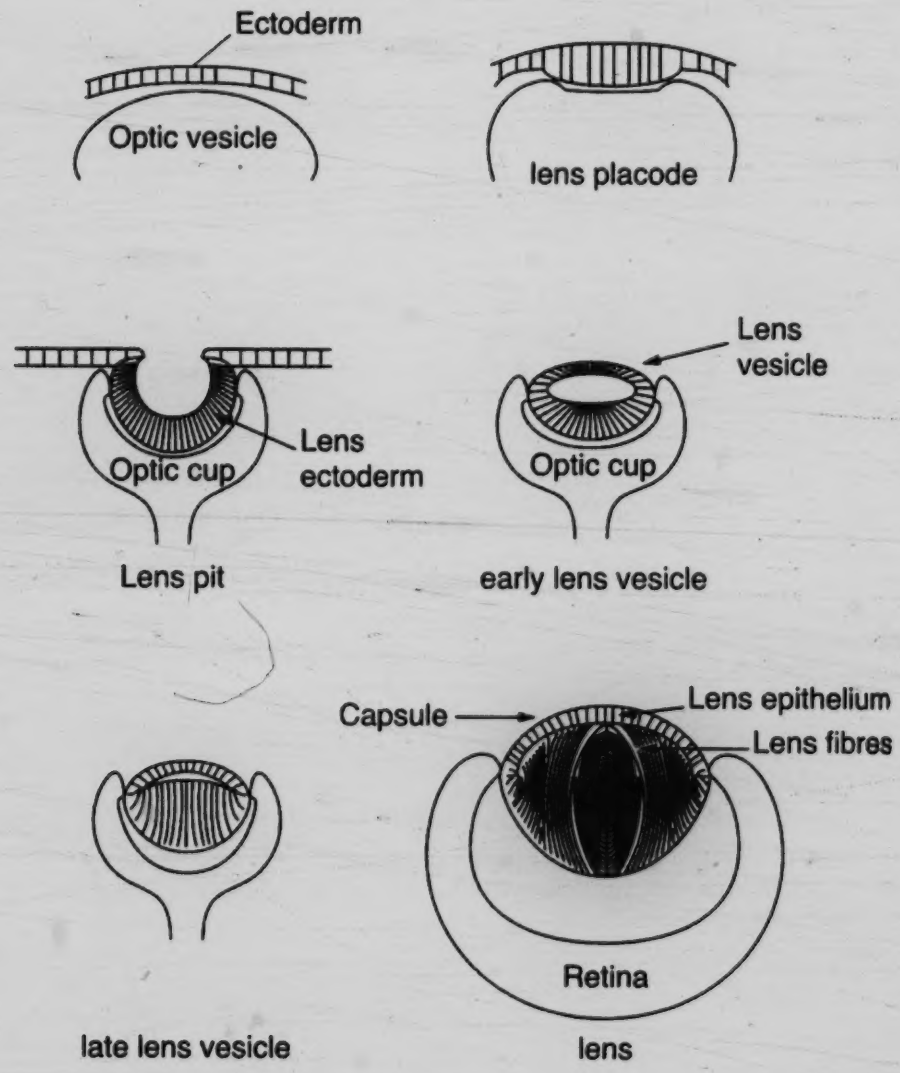
Ectoderm
Optic vesicle
lens placode
Lens
vesicle
Optic cup
Lens
ectoderm
Optic cup
Lens pit
early lens vesicle
Capsule
Lens epithelium
Lens fibres
Retina
late lens vesicle
lens

1982). The cells at the posterior of the lens vesicle elongate into the lumen of the lens vesicle and form the primary lens fibers. These cells undergo a number of ultrastructural changes (i.e. reduction of organelles) and begin to synthesize crystallins. The cells on the anterior pole of the lens vesicle remain proliferative. Cells from this layer begin to migrate laterally to an equatorial zone of transition where they undergo changes to become secondary lens fibers and also begin to synthesize crystallins.

Coincident with the process of lens induction and differentiation is the morphological beginning of retinal differentiation. As the neural ectoderm contacts the surface ectoderm, the wall of the optic vesicle thickens, flattens, and forms the retinal disc (Barishak 1992). The optic vesicle begins to invaginate and form the optic cup (Figure 1-12). The outer surface of the optic cup will form the RPE while the inner surface will form the neural retina.

Also coincident with the differentiation of the lens, in the fifth week of gestation, is the formation of the cornea. After the separation of the lens vesicle from the surface ectoderm, the surface ectoderm forms an epithelial layer two cells thick that is the primitive corneal epithelium (Barishak 1992). At about E40, the first wave of neural crest derived mesenchymal cells invades the

developing eye. These cells migrate over the lip of the optic cup and between the proliferative anterior lens epithelium and the corneal epithelium to form the corneal endothelium. A second wave of mesenchymal cells invades in two phases. The upper phase moves in between the corneal epithelium and the corneal endothelium to form the corneal stroma.

Formation of the iris stroma begins with the lower, or posterior, portion of the second wave of mesenchymal cells. These cells migrate and extend between the lens epithelium and corneal endothelium to form the pupillary membrane. At the apex of the angle formed by the anterior and posterior phases of the second wave is a mass of undifferentiated mesenchymal cells that are the primitive uveal trabecular meshwork (Jakobiec 1982). The remainder of the iris stroma forms as the third wave of neural crest cells invade the anterior chamber. The pupillary membrane will eventually atrophy and degenerate through resorption (Jakobiec 1982). Thus the iris stroma is composed of neural crest cells while the pigmented posterior epithelium and the pupillary sphincter and dilator muscles are of neural ectoderm origin (Table 1-1).

The choroid and sclera form as condensations of the periocular mesenchyme surrounding the optic cup. In contrast, the ciliary body develops with a neural ectodermal component. The

ciliary body forms near the lip of the optic cup. Neuroectoderm from the optic cup forms the ciliary epithelium. It is the ciliary epithelium that is responsible for the active transport of desired plasma constituents to produce aqueous humor. The stroma and ciliary muscle that controls the shape of the lens are both derived from mesenchyme.

In summary, the structures of the eye, though functioning in concert, develop as specific morphogenetic movements of three main tissue types, the surface ectoderm, the neural ectoderm, and neural crest derived mesenchyme.

## C) GENETICS OF OCULAR DEVELOPMENT

The marvels of the genetics of ocular development have been thrust into the limelight in the past decade. In this time it has been discovered that the complexities of the development of eyes as divergent as the compound eye of *Drosophila* and the eye of humans are the result of a common, conserved pathway. The discovery of this ancestral method of eye development is significant for understanding the evolutionary relationship between species. Of equal importance is the fact that *Drosophila* genetics can be used and applied extensively to the study of vertebrate eye development.

With this said, it is easiest to first look at the genes involved in *Drosophila* eye development and their epistatic relationships. One can then determine how well these results and predictions apply to vertebrate systems such as the mouse model of ocular development. The identification of homologues in mice and humans, and the involvement of mutations in these genes in human ocular disorders, has reinforced the concept of a conserved mechanism of eye development across phyla.

*Pax6*, a gene central to the excitement surrounding eye development, was first identified in mouse as the gene underlying the semidominant *small eye* (*Sey*) phenotype (Hill et al. 1991). Heterozygous *Sey*/+ mice have eyes that are smaller than normal, and often have a delay in closure of the optic fissure. In homozygous *Sey*/*Sey* mice, there is a complete absence of eyes and nasal cavities do not form (Hogan et al. 1986).

Aniridia in humans (OMIM# 106200) is clinically variable, ranging from mild iris hypoplasia to complete absence of the iris, and variably associated with cataracts, corneal opacification, and progressive glaucoma. Following the identification of the murine *pax6* gene causing *Sey*, the human *PAX6* gene was mapped near a locus for Aniridia (Ton et al. 1991) and mutations in *PAX6* were shown to cause Aniridia in humans (Glaser et al. 1992; Jordan et al.

1992). Since then, mutations in *PAX6* have been shown to cause a variety of ocular disorders including isolated foveal hypoplasia (Azuma et al. 1996), Peters' anomaly (Hanson et al. 1994), and autosomal dominant keratitis (Mirzayans et al. 1995). Additionally, a compound heterozygous individual with two nonsense alleles of *PAX6* has been described with severe craniofacial malformations, central nervous system malformations, and anophthalmia (Glaser et al. 1994) resembling *Sey/Sey* mice.

The major breakthrough indicating that there is a conserved mechanism of eye development between *Drosophila* and vertebrates came with the cloning of the gene responsible for the *eyeless* (*ey*) phenotype in *Drosophila* (Quiring et al. 1994). The *ey* gene is a *PAX6* orthologue showing 94% and 90% amino acid identity to the human *PAX6* gene in the two major DNA binding domains of the putative protein (Quiring et al. 1994). This finding was fundamental to the hypothesis that vertebrate and insect eyes develop using similar pathways. Further excitement was generated when it was established that ectopic expression of the *ey* gene was sufficient to induce the formation of complete and morphologically normal ectopic eyes (Halder et al. 1995). Furthermore, the targeted expression in *Drosophila*, of the mouse *pax6* gene was also able to induce ectopic *Drosophila* eye structures (Halder et al. 1995). A

vertebrate example of induction of ectopic eyes via exogenous *pax6* expression was provided when misexpression of *pax6* in *Xenopus* was shown to result in the formation of eyes that have a morphology characteristic of normal eyes (Chow et al. 1999). These results were considered proof of a common eye development pathway and evidence that *PAX6* is a "master control gene" for eye development.

**i) Genes Involved In Drosophila Ocular Development**

The concept of *PAX6* as a master control gene for eye development is debatable. First, the observation of *ey/PAX6* expression in tissues that do not form eyes indicates that the presence of *ey/PAX6* expression is not sufficient for eye development. Secondly, observation of more than just eye malformations in homozygous mutants indicate that *ey/PAX6* has a larger role in development than just that of directing eye development. Thus *ey/PAX6* is more than just an eye development gene and in eye development, *ey/PAX6* requires other factors.

Further evidence that *ey* is not the master control gene for eye development came with the identification of a second *Drosophila PAX6* homologue, *twin of eyeless* (*toy*) (Czerny et al. 1999). The *toy* gene is more closely related to vertebrate *PAX6* than *ey* is in terms conservation of sequence motifs, expression pattern, and affinity for

binding sites (Czerny et al. 1999). Furthermore, *toy* is upstream of *ey* in the pathway and acts to directly regulate *ey*. Attempts to identify *toy* and *ey* orthologues in other phyla suggest that a duplication event leading to distinct genes was restricted to insect evolution (Czerny et al. 1999).

Genes downstream of *ey* have also been identified. Identification of members of this developmental pathway largely revolved around the epistatic relationships between *ey* and the genes for a number of similar eye malformation phenotypes in *Drosophila*. Mutations in the Pax-like gene *eye gone* (*eyg*) (Jones et al. 1998; Jun et al. 1998), and the homeobox gene *sine oculis* (*so*) (Cheyette et al. 1994; Serikaku and O'Tousa 1994) cause small eye or eyeless phenotypes. Similarly, mutations in *eyes absent* (*eya*) (Bonini et al. 1993) or *dachshund* (*dac*) (Mardon et al. 1994) genes that both encode novel nuclear proteins, also cause small eye or eyeless phenotypes.

Based on epigenetic experiments, the pathway forms a feedback loop at the level of *ey* (Figure 1-13). The expression of *ey* is not required for *toy* expression and ectopic *toy* expression is able to induce *ey* expression, therefore, *ey* is downstream of *toy* (Czerny

**FIGURE 1-13. Hierarchy of *Drosophia* genes involved in early eye development.**

The *Drosophila* genes *toy* (*twin of eyeless*), *ey* (*eyeless*), *eyes absent* (*eya*), *sine oculis* (*so*), and *dachshund* (*dac*) can be arranged in a hierarchy based on their epigenetic relationships (see text). Taken from Treisman 1999.

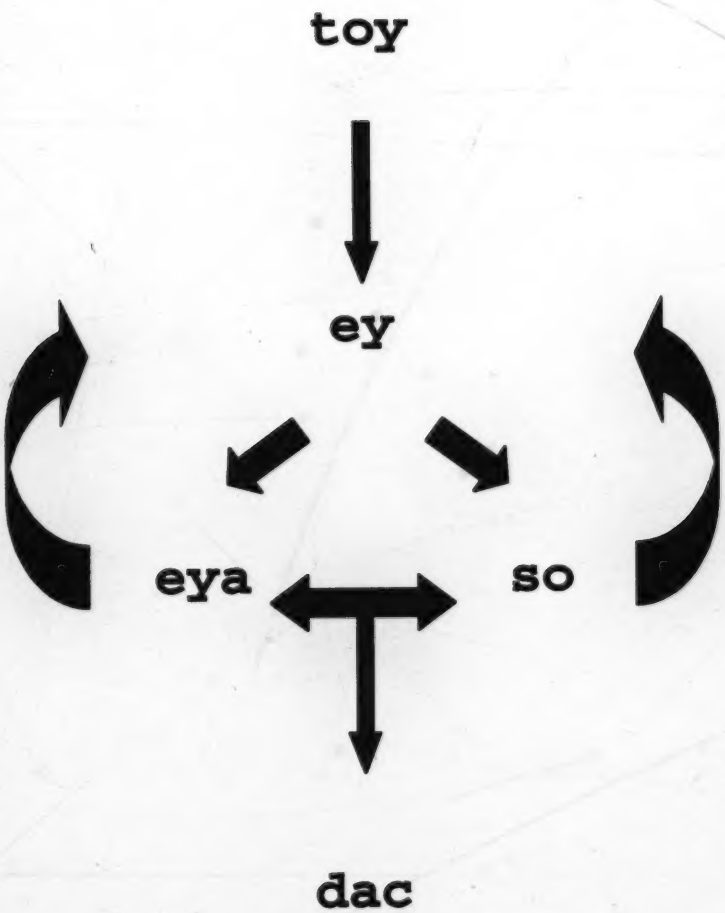
toy
ey
eya
so
dac

et al. 1999). The expression of *so*, and *eya* are not required for *ey* expression, however, *so* and *eya* expression require *ey* expression and therefore *so* and *eya* are downstream of *ey* (Halder et al. 1998). Both *so* and *eya* are independently activated by *ey*. The *so* and *eya* genes also activate each other and therefore are parallel in the pathway (Halder et al. 1998). Expression of *dac* requires expression of *eya* and *so* and therefore *dac* is downstream of *eya* and *so* (Pignoni et al. 1997). The ectopic expression of individual or combinations of these genes has also been shown to induce *ey* expression indicating a feedback loop (Desplan 1997; Lupo et al. 2000; Treisman 1999). Furthermore, the ectopic expression of individuals or combinations of downstream genes has also been shown to induce ectopic eye formation (Bonini et al. 1997; Pignoni et al. 1997; Shen and Mardon 1997).

### ii) Conserved Genes Involved In Mammalian Ocular Development

The *toy/ey* orthologue *PAX6* is important for mammalian eye development. *PAX6* is expressed in a number of areas of the developing vertebrate eye including the neural ectoderm of the evaginating optic vesicle and also the overlying surface ectoderm that opposes the optic vesicle. The first observable malformation in

the developing eye of the *pax6* mutant mouse (*Sey*) is the failure of induction of the lens. Co-culture experiments in rat suggest that it is the absence of *pax6* expression in the surface ectoderm that leads to the tissue not being competent to form lens rather than the inability of the optic cup to induce the lens placode that causes this observation (Fujiwara et al. 1994). At later stages *pax6* is thought to directly activate crystallins in the differentiated lens (Cvekl et al. 1994), and rhodopsin in the differentiated photoreceptor cells (Sheng et al. 1997). These results all lead to the conclusion that many of the pathways from broad determination of embryonic fields to terminal differentiation may all make use of the same factor and that temporally and spatially, *pax6* plays a number of roles.

Homologues for other members of the Drosophila pathway have also been identified in mice. *SIX3* is the human and murine orthologue of the *so* gene (Oliver et al. 1995). Expression of murine *six3* in the lens forming surface ectoderm requires *pax6* expression but expression in the optic vesicle does not (Oliver et al. 1995 and Xu, 1997 #2713). No knockouts of the *six3* gene have been described to date, however, transgenic fish expressing ectopic murine *six3* develop ectopic lenses at the otic placode (Oliver et al. 1996). *SIX3* is also associated with human disease as mutations in

the *SIX3* homeobox have been associated with holoprosencephaly at the HPE2 locus on chromosome 2p21 (Wallis et al. 1999).

The *eya* homologues are represented by family of three genes in mouse (*eya1*, *eya2*, and *eya3*) (Xu et al. 1997). Both *eya1* and *eya2* are expressed in the lens placode and are under *pax6* control (Xu et al. 1997). All three murine *eya* genes are able to rescue the *Drosophila eya* phenotype (Treisman 1999). Mice heterozygous for null alleles of *eya1* have hearing loss and renal malformations while those homozygous for the null allele lack ears and kidneys (Xu et al. 1999). Heterozygous mutations of the human *EYA1* gene have been shown to cause BOR (Branchio-Oto-Renal) syndrome (Abdelhak et al. 1997a; Abdelhak et al. 1997b). BOR syndrome is an autosomal dominant disorder with incomplete penetrance and variable expressivity. Mutations have also more recently been identified in patients with ocular malformations including Peters' anomaly, cataracts, iris anomaly and nystagmus (Azuma et al. 2000).

Vertebrate homologues for *dac* have recently been cloned (Hammond et al. 1998; Hammond et al. 1999; Kozmik et al. 1999). Murine *dach2* appears to be involved in muscle development while *dach1* is expressed in the periocular mesenchyme and the developing retina. To date, however, no mutations have been identified in human disorders.

## D) GLAUCOMA

One of the major consequences of Aniridia, caused by *PAX6* mutations in humans, is the onset of glaucoma in approximately 50% of cases (Nelson et al. 1984). Because of the high incidence of glaucoma in Aniridia patients, and patients with Peters' anomaly (OMIM #604229) and Axenfeld-Rieger (AR) malformations, these disorders are considered to be secondary or developmental glaucomas.

Glaucoma is not a single disease process, but a group of disorders related by some common features. These features include visual field loss and RGC death. Death of RGCs results in optic nerve head damage and optic nerve cupping and is the cause of visual field defects. Eventually, visual acuity is also lost. These features are frequently associated with an increase in intraocular pressure (IOP). A study on the prevalence of glaucoma predicted that at the turn of the century there were to be 67 million people with glaucoma worldwide and 6.7 million with blindness due to glaucoma (Quigley and Vitale 1997).

The observation that not all cases of glaucoma are associated with elevated IOP is a strong reminder that the etiology of glaucoma

is complex and largely unknown. It is possible that those cases of glaucoma that occur in patients whose IOPs are within normal limits have RGCs that are more susceptible to damage than those in the majority of the population. Patients in the majority of glaucoma cases experience elevated IOP and the problem usually lies within the aqueous humor drainage system of the anterior segment of the eye, although on rare occasions it is caused by aqueous humor hypersecretion (Spencer 1985). The outflow resistance may be caused at the site of drainage through the TM to Schlemm's canal, drainage between Schlemm's canal and the venous system, or at other locations in the eye.

**i) Aqueous Humor Dynamics**

An understanding of the dynamics of the aqueous humor gives insight as to how a various number of different ocular malformations may lead to elevated IOP and glaucoma. IOP is a function of the production of aqueous humor at the ciliary body, its outflow through the TM at the iridocorneal angle and the episcleral venous pressure. A uvealscleral drainage system exists but only accounts for approximately 10% of aqueous outflow and is relatively pressure independent and therefore not considered as a large contributor to IOP (Epstein et al. 1997) (Figure 1-6).

The aqueous humor is produced by the epithelium of the ciliary body (Epstein et al. 1997; Shields 1987). The ciliary epithelium consists of two layers of epithelial cells. The outer layer, adjacent to the ciliary stroma, is pigmented epithelium and is continuous with the RPE. The inner layer is nonpigmented epithelium and is continuous with both the neural retina and the posterior epithelium of the iris. Although both layers of the epithelium participate in aqueous humor production, the cells of the inner epithelium have larger and more numerous mitochondria suggesting that they are better equipped for the energy requirements of aqueous humor production (Epstein et al. 1997). The aqueous humor is produced by an ultrafiltration of plasma in the capillaries of the ciliary process. There is then active transport of constituents, such as glucose, citrate, lactate and ascorbate, across the epithelial barrier. This active transport produces a gradient and is followed by passive osmotic flow of fluid and electrolytes (Shields 1987).

The flow of aqueous humor then proceeds into the posterior chamber, through the aperture of the pupil and into the anterior chamber. There is some pupillary resistance to flow and the pressure in the posterior chamber is usually greater than that of the anterior chamber (Epstein et al. 1997). In extreme cases, pupillary

resistance can cause pupillary block angle closure glaucoma as the pressure in the posterior chamber pushes the iris anteriorly, closing off the iridocorneal angle.

At the iridocorneal angle, three layers of TM are present as discussed earlier (Figure 1-4). The aqueous humor percolates throughout the TM meeting with increased resistance with each layer. Finally, the aqueous humor is collected in Schlemm's canal and drains into the episcleral vein. The principle component of aqueous humor resistance is accounted for by the TM extracellular matrix (ECM) and the endothelial cells lining Schlemm's canal. It is in this drainage system that the problem is thought to lie in primary open angle glaucomas.

**ii) Classification of Glaucoma**

The glaucomas can be broadly separated into three major groups, primary glaucoma, secondary glaucoma and congenital glaucoma. Each of these groups can be further subdivided into open angle glaucoma and angle closure glaucoma based on the structure of the angle. All of the disorders I will be discussing are open angle glaucomas.

Primary open angle glaucoma (POAG) is the most common form of glaucoma (Shields 1987). Glaucoma is classified as primary

if there is no apparent initiating contribution from any ocular or other systemic disorder (Epstein et al. 1997; Ritch 1989). POAG usually develops with gradual onset in the 5th or 6th decade but may develop more abruptly in the 3rd or 4th decade (Epstein et al. 1997). POAG has a very large genetic component although other risk factors are also involved (i.e. increased age, myopia, hypertension, and diabetes) (Shields 1987). Although largely associated with elevated IOP, POAG also includes cases of low or normal tension glaucoma. As mentioned earlier, it is thought that individuals with normal tension glaucoma have RGCs that are more susceptible to death even with IOPs within what is considered the normal range (Spencer 1985). Recent reports also implicate roles for glutamate exitoxcity (Liu et al. 1999) and elevated nitric oxide levels (Chiou et al 2001; Liu et al 2000) in POAG.

Secondary or developmental glaucomas are those glaucomas that are able to be traced back to an underlying ocular or systemic defect. Aniridia, Peters'' anomaly and Axenfeld Rieger malformations are three of the most prominent examples of secondary glaucomas. The age of onset depends greatly on the underlying cause of the glaucoma and even within each example there is incomplete penetrance of the glaucoma and highly variable expressivity. All of these types of glaucoma are associated with elevated IOP.

Primary congenital glaucoma (PCG), also called primary infantile glaucoma or buphthalmos, is glaucoma present at birth or within three years after birth (Shields 1987; Spencer 1985). PCG is associated with TM malformations not associated with other anomalies (Ritch 1989). The buphthalmos described (Greek for "ox eye"), refers to the "ballooning" out of the eye due to the increased IOP. This occurs because the collagen fibers of the eye are very elastic in infants and allow enlargement of the globe (Ritch 1989). By approximately three years of age, the collagen has acquired its structural integrity and enlargement of the globe does not occur. PCG is also associated with photophobia (aversion to light), epiphoria (excessive tearing), and blepharospasm (spasms of the eyelids) (Shields 1987).

## E) GENETICS OF GLAUCOMA

The enigmatic etiology of glaucoma often precludes the use of functional candidate gene approaches to identify the underlying molecular basis of these disorders. Therefore, positional candidate gene approaches must be employed. To this end, large cohorts of families affected with the various types of glaucoma have been assembled by laboratories worldwide. The use of these families to

identify chromosomal regions that are linked to the disorders is the first step to identifying the genes involved and understanding the molecular basis of glaucoma.

**i) Primary Open Angle Glaucoma**

To date, six loci for POAG have been identified (Table 1-2). A recent genome wide scan for additional loci implicates four further chromosomal locations (Wiggs et al. 2000). Identification of a gene harboring mutations in patients with POAG glaucoma has only been successful for the *myocilin* gene (*MYOC*) at the *GLC1A* locus at 1q23 (Stone et al. 1997). The locus is usually considered to be responsible for a juvenile onset type of POAG, however, expressivity is largely variable (Morrisette 1995).

MYOC (also found in literature as TIGR-trabecular meshwork induced glucocorticoid response protein), has been independently isolated by several groups in various tissues. MYOC has been isolated from TM cells (Polansky et al. 1989), ciliary body (Escribanó et al. 1995; Ortego et al. 1997) and retina (Kubota et al. 1997). The three-exon gene codes for a putative protein with an N-terminal myosin-like domain and a C-terminal olfactomedin-like domain separated by a leucine zipper motif (Ortego et al. 1997).

**TABLE 1-2. Known glaucoma loci and genes identified**

| Glaucoma Classification | Locus | Location | Inheritance | Gene |
|---|---|---|---|---|
| **Primary open angle glaucoma** | | | | |
| | GLC1A | 1q24-25 | AD | *MYOC* |
| | GLC1B | 2cen-q13 | AD | unknown |
| | GLC1C | 3q21-24 | AD | unknown |
| | GLC1D | 8q23 | AD | unknown |
| | GLC1E | 10p15-14 | AD | unknown |
| | GLC1F | 7q35-36 | AD | unknown |
| **Primary congenital glaucoma** | | | | |
| | GLC3A | 2p21 | AR | *CYP1B1* |
| | GLC3B | 1p36 | AR | unknown |
| **Developmental glaucoma** | | | | |
| Aniridia | AN | 11p13 | AD | *PAX6* |
| Rieger syndrome | RIEG1 | 4q25 | AD | *PITX2* |
| Iris hypoplasia | RIEG1 | | AD | *PITX2* |
| Iridogoniodysgenesis syndrome | IRID2 | | AD | *PITX2* |
| Rieger syndrome | RIEG2 | 13q14 | AD | unknown |
| Iridogoniodysgenesis anomaly | IRID1 | 6p25 | AD | unknown |
| Axenfeld Rieger anomaly | | | AD | *FOXC1* |
| Iris hypoplasia | | | AD | *FOXC1* |
| Axenfeld Rieger syndrome | | | AD | *FOXC1* |
| Familial glaucoma iridogoniodysplasia | | | AD | unknown |
| Familial glaucoma with goniodysgenesis | | | AD | unknown |
| **Other loci** | | | | |
| Pigment dispersion | GPDS1 | 7q35-36 | AD | unknown |
| Pigment dispersion | GPDS2 | 18q11-21 | AD | unknown |
| Nail-Patella syndrome | NPS1 | 9q34 | AD | *LMXB1* |
| Pseudoexfoliation syndrome | | 2p16 | AD | unknown |

Modified from Craig and Mackey 1999.

The function of MYOC is unknown, although tissue and cellular localization and the study of mutant proteins are providing some understanding of *MYOC*'s function.

Results of Western blot analysis indicated the presence of MYOC protein in most eye structures including cornea, iris, TM, ciliary body, vitreous humor, retina and optic nerve (Karali et al. 2000). In the same study, immunohistochemistry indicated the presence of MYOC at the site of aqueous humor drainage in both uveal and corneoscleral meshwork cells, as well as in cells adjacent to Schlemm's canal. MYOC was also observed at the site of aqueous humor production in the cells of the ciliary epithelium. Furthermore, positive MYOC staining was also observed in the retina along the surface of rods and cones, in neurons of the inner and outer nuclear layers, and in the axons of RGC in the optic nerve (Karali et al. 2000). Thus, based on localization, it is difficult to ascertain if MYOC affects the production of aqueous humor, the drainage of aqueous humor, the susceptibility of RGC to damage, some combination of these factors or something else entirely.

Intracellular localization indicates MYOC associates with cytoplasmic filaments and microtubules (Mertts et al. 1999; Ueda et al. 2000), vesicles (Caballero et al. 2000; Ueda et al. 2000), and as

part of the ECM associated with trabecular beams (Ueda et al. 2000). The observation that MYOC is secreted by TM cells (Nguyen et al. 1998) and associates with trabecular beams suggests that MYOC's involvement in glaucoma is at the level of outflow. However, recent studies indicate that mutant MYOC proteins are not secreted from cultured TM cells and accumulate in the cell (Caballero et al. 2000; Jacobson et al. 2001). Furthermore, these proteins accumulate in association with intracellular vesicles and inhibit the secretion of normal MYOC proteins from the cell in a dominant negative fashion (Caballero et al. 2000; Jacobson et al. 2001). Based on these results, the effect of mutations in *myocilin* may be the reduced secretion of the protein into the ECM, or perhaps the general disruption of the secretion pathway influencing other secreted proteins. Finally, it may be the accumulation of non-secreted MYOC that damages the cells and is the primary effect of the glaucoma.

The credence of any hypothesis of MYOC's structural or functional role in glaucoma can be quickly tested by its ability to explain the homoallelic complementation of MYOC observed by Morissette and co-workers (Morissette et al. 1998). In this large pedigree, an autosomal dominant mutation of MYOC, K423E, segregates with POAG. However, in one branch of the family, two

heterozygous parents that are second degree cousins, have 10 children. Only two of the 10 children, aged 35-50, are affected with POAG, however children of one of the unaffected siblings were affected. Genotyping determined that of the 10 children of the original affected parents, three are homozygous for the normal allele and are unaffected. Three children are heterozygous for the normal and mutant alleles. Two of the heterozygous children are affected and one is not. The sibling that is not affected is the youngest of the 10 and is only 33 years of age and therefore may develop glaucoma. Four of the children are homozygous for the mutation and are clinically unaffected although one has affected, heterozygous children (Morissette et al. 1998). The net observation is that the K423E MYOC variant, when heterozygous, causes the disease, however, when the mutation is homozygous, the patients are unaffected. A point of importance is the observation that the K423E MYOC variant that segregates in this family is one of the five mutations tested for secretion. It was found that cultured TM cells transfected with K423E showed no secretion of the mutant protein and therefore no homoallelic complementation of this function in this model system (Jacobson et al. 2001). This suggests that the physiological effect of this variant does not involve secretion or

alternatively, that homoallelic complementation does not work in the in vivo system tested.

**ii) Primary Congenital Glaucoma**

In contrast to the six loci identified to date for autosomal dominant POAG, only two autosomal recessive loci have been identified for PCG (Table 1-2) (Akarsu et al. 1996; Sarfarazi et al. 1995). The *GLC3A* locus is the major PCG locus with approximately 87% of familial cases mapping to this locus. Families also exist that do not map to either locus suggesting the presence of a third PCG locus. PCG is familial in 10-40% of cases. In familial cases, variable penetrance of 40-100% is observed (Sarfarazi and Stoilov 2000). The wide variation in penetrance is attributable to differences in ethnicity with Slovakian Gypsies and Turkish families showing 100% penetrance (Sarfarazi and Stoilov 2000) but Saudi Arabian families having reduced penetrance (approximately 40%). Families with reduced penetrance appear to have an autosomal dominant modifier (Bejjani et al. 2000).

The cytochrome *P4501B1* (*CYP1B1*) gene has been identified as the PCG gene at the *GLC3A* locus at chromosome 2p21 (Stoilov et al. 1997). Members of the cytochrome P450 superfamily of genes are known to metabolize xenobiotics and play a role in oxidative

reactions of metabolites in a number of biosynthetic pathways (Sarfarazi and Stoilov 2000). To date no known substrate has been identified for *CYP1B1*. The identification of this substrate, and potentially the elucidation of a pathway necessary for the normal development of human TM will be an important step in the treatment of PCG and other glaucomas.

### iii) Secondary Glaucomas

Secondary or developmental glaucomas are associated with elevated IOP where the cause of the elevated IOP is apparently a result of malformations of ocular structures. Secondary glaucomas are also often associated with other systemic abnormalities. A wide variety of secondary glaucomas exist (Craig and Mackey 1999). Genes have been identified for a limited number of these, including the *PAX6* gene for Aniridia (Jordan et al. 1992) (and a variety of other related disorders discussed earlier), the LIM homeobox-containing transcription factor *LMX1B* for nail-patella-syndrome (OMIM# 161200) (Vollrath et al. 1998) and the bicoid-related homeobox-containing transcription factor *PITX2* for Axenfeld-Rieger syndrome (OMIM# 180500) (Semina et al. 1996) and, as I discuss later, *FOXC1* for other AR malformations. The goal of my research has been to identify genes involved in Axenfeld-Rieger eye

malformations. Therefore this is the secondary glaucoma I will discuss in detail.

## F) AXENFELD-RIEGER MALFORMATIONS

### i) Clinical Description of Axenfeld Rieger

In 1920, Axenfeld described a condition of posterior embryotoxon, which is a prominent and anteriorly displaced Schwalbe's line (Axenfeld 1920). In 1935, Rieger described this same condition with associated iris and angle malformations (Rieger 1935). Iris malformations may include hypoplasia, corectopia, polycoria and peripheral anterior synechia (PAS) (Wiggs 1995). Although iridocorneal adhesions obstruct the angle, the TM is usually normal and the condition is considered to be open angle. The major consequence for patients with these eye malformations is the development of late adolescent or early adult glaucoma in approximately 50% of individuals (Wiggs 1995).

In some cases of AR malformation, the patients present with associated systemic, non-ocular features, including midface abnormalities (including maxillary hypoplasia and hypertelorism), dental anomalies (hypodontia and microdontia) and redundant periumbilical skin (Wiggs 1995). Although historically these

disorders have been clinically described as Axenfeld-Rieger Anomaly (ARA) (for those presenting with only ocular features), and Axenfeld-Rieger syndrome (ARS) (for those with ocular and non-ocular features), the elucidation of the underlying molecular events indicates a single spectrum of heterogeneous disorders, the AR malformations. The clinically related but distinct disorders of iridogoniodysgenesis anomaly/syndrome, iridogoniodysplasia, and iris hypoplasia should also be considered part of this spectrum of disorders (Alward 2000).

**ii) The Genetics Of Axenfeld-Rieger Malformations**

The AR malformations are inherited as autosomal dominant heterogeneous disorders with loci at 4q25 (Heon et al. 1995; Murray et al. 1992), 13q14 (Phillips et al. 1996) and 16q24 (Nishimura et al. 2000). To date no genes have been identified for the loci at 13q14 or 16q24. The bicoid-related homeobox transcription factor gene *PITX2* has been cloned and mutations identified in patients with a variety of AR malformation phenotypes (Alward et al. 1998; Kulak et al. 1998; Semina et al. 1996). Although extreme variable expressivity occurs, the basic underlying molecular mechanism for the disorders is the haploinsufficiency of *PITX2* (Kozlowski and Walter 2000). Recently, a possible

downstream target for the PITX2 protein has been identified (Hjalt et al. 2001). The characterization of further targets of the PITX2 protein will demonstrate the role PITX2 plays in ocular development as well as its role in development of other tissues affected by AR malformations. Of peripheral interest is the role of murine *pitx2* in the establishment of laterality and left right asymmetry (Lin et al. 1999; Lu et al. 1999).

Only approximately 15% of AR malformations are caused by mutations in the PITX2 gene (Kulak et al. 1998). The identification of additional genes underlying Axenfeld Rieger malformations has been the focus of my research.

**E) REFERENCES**

1) Abdelhak S, Kalatzis V, Heilig R, Compain S, Samson D, Vincent C, Levi-Acobas F, et al (1997a) Clustering of mutations responsible for branchio-oto-renal (BOR) syndrome in the eyes absent homologous region (eyaHR) of EYA1. Hum Mol Genet 6:2247-55.

2) Abdelhak S, Kalatzis V, Heilig R, Compain S, Samson D, Vincent C, Weil D, et al (1997b) A human homologue of the Drosophila eyes absent gene underlies branchio-oto-renal (BOR) syndrome and identifies a novel gene family. Nat Genet 15:157-64.

3) Akarsu AN, Turacli ME, Aktan SG, Barsoum-Homsy M, Chevrette L, Sayli BS, Sarfarazi M (1996) A second locus (GLC3B) for primary congenital glaucoma (Buphthalmos) maps to the 1p36 region. Hum Mol Genet 5:1199-203.

4) Alward WL (2000) Axenfeld-rieger syndrome in the age of molecular genetics. Am J Ophthalmol 130:107-15.

5) Alward WL, Semina EV, Kalenak JW, Heon E, Sheth BP, Stone EM, Murray JC (1998) Autosomal dominant iris hypoplasia is caused by

a mutation in the Rieger syndrome (RIEG/PITX2) gene. Am J Ophthalmol 125:98-100.

6) Axenfeld TH (1920) Embryotoxon cornea posterius. Klin Monatsbl Augenheilkd 65:381-382

7) Azuma N, Hirakiyama A, Inoue T, Asaka A, Yamada M (2000) Mutations of a human homologue of the Drosophila eyes absent gene (EYA1) detected in patients with congenital cataracts and ocular anterior segment anomalies. Hum Mol Genet 9:363-6.

8) Azuma N, Nishina S, Yanagisawa H, Okuyama T, Yamada M (1996) PAX6 missense mutation in isolated foveal hypoplasia. Nat Genet 13:141-2.

9) Barishak YR (1992) Embrylogy of the Eye and Its Adnexae. In: Straub W (ed) Developments in Ophthalmology. Vol. 24. Karger, Basel

10) Bejjani BA, Stockton DW, Lewis RA, Tomey KF, Dueker DK, Jabak M, Astle WF, et al (2000) Multiple CYP1B1 mutations and incomplete penetrance in an inbred population segregating primary

congenital glaucoma suggest frequent de novo events and a dominant modifier locus. Hum Mol Genet 9:367-74.

11) Bonini NM, Bui QT, Gray-Board GL, Warrick JM (1997) The Drosophila eyes absent gene directs ectopic eye formation in a pathway conserved between flies and vertebrates. Development 124:4819-26.

12) Bonini NM, Leiserson WM, Benzer S (1993) The eyes absent gene: genetic control of cell survival and differentiation in the developing Drosophila eye. Cell 72:379-95.

13) Caballero M, Rowlette LL, Borras T (2000) Altered secretion of a TIGR/MYOC mutant lacking the olfactomedin domain. Biochim Biophys Acta 1502:447-60.

14) Cheyette BN, Green PJ, Martin K, Garren H, Hartenstein V, Zipursky SL (1994) The Drosophila sine oculis locus encodes a homeodomain-containing protein required for the development of the entire visual system. Neuron 12:977-96.

15) Chiou SH, Chang CJ, Hsu WM, Kao CL, Liu JH, Chen WL, Tsai DC, Wu CC, Chou CK (2001) Elevated nitric oxide level in aqueous humor of patients with acute angle-closure glaucoma. Ophthalmologica 215:113-6.

16) Chow RL, Altmann CR, Lang RA, Hemmati-Brivanlou A (1999) Pax6 induces ectopic eyes in a vertebrate. Development 126:4213-22.

17) Craig JE, Mackey DA (1999) Glaucoma genetics: where are we? Where will we go? Curr Opin Ophthalmol 10:126-34.

18) Cvekl A, Sax CM, Bresnick EH, Piatigorsky J (1994) A complex array of positive and negative elements regulates the chicken alpha A-crystallin gene: involvement of Pax-6, USF, CREB and/or CREM, and AP-1 proteins. Mol Cell Biol 14:7363-76.

19) Czerny T, Halder G, Kloter U, Souabni A, Gehring WJ, Busslinger M (1999) twin of eyeless, a second Pax-6 gene of Drosophila, acts upstream of eyeless in the control of eye development. Mol Cell 3:297-307.

20) Desplan C (1997) Eye development: governed by a dictator or a junta? Cell 91:861-4.

21) Epstein DL, Allingham RR, Shuman JS (1997) Chandler and Grant's Glaucoma. Williams & Wilkins, Baltimore.

22) Escribano J, Ortego J, Coca-Prados M (1995) Isolation and characterization of cell-specific cDNA clones from a subtractive library of the ocular ciliary body of a single normal human donor: transcription and synthesis of plasma proteins. J Biochem (Tokyo) 118:921-31.

23) Fini ME (2000) Vertebrate Eye Development. In: W. Hennig LN, U. Scheer (ed) Results and Problems in Cell Differentiation. Vol. 31. Springer-Verlag, Berlin.

24) Fujiwara M, Uchida T, Osumi-Yamashita N, Eto K (1994) Uchida rat (rSey): a new mutant rat with craniofacial abnormalities resembling those of the mouse Sey mutant. Differentiation 57:31-8.

25) Glaser T, Jepeal L, Edwards JG, Young SR, Favor J, Maas RL (1994) PAX6 gene dosage effect in a family with congenital

cataracts, aniridia, anophthalmia and central nervous system defects. Nat Genet 7:463-71.

26) Glaser T, Walton DS, Maas RL (1992) Genomic structure, evolutionary conservation and aniridia mutations in the human PAX6 gene. Nat Genet 2:232-9.

27) Halder G, Callaerts P, Flister S, Walldorf U, Kloter U, Gehring WJ (1998) Eyeless initiates the expression of both sine oculis and eyes absent during Drosophila compound eye development. Development 125:2181-91.

28) Halder G, Callaerts P, Gehring WJ (1995) Induction of ectopic eyes by targeted expression of the eyeless gene in Drosophila. Science 267:1788-92.

29) Hammond KL, Hanson IM, Brown AG, Lettice LA, Hill RE (1998) Mammalian and Drosophila dachshund genes are related to the Ski proto- oncogene and are expressed in eye and limb. Mech Dev 74:121-31.

30) Hammond KL, Lettice LA, Hill RE, Lee M, Boyle S, Hanson IM (1999) Human (DACH) and mouse (Dach) homologues of Drosophila dachshund map to chromosomes 13q22 and 14E3, respectively. Genomics 55:252-3.

31) Hanson IM, Fletcher JM, Jordan T, Brown A, Taylor D, Adams RJ, Punnett HH, et al (1994) Mutations at the PAX6 locus are found in heterogeneous anterior segment malformations including Peters' anomaly. Nat Genet 6:168-73.

32) Harding JJ (1997) Biochemistry of the Eye. Chapman and Hall, London.

33) Heon E, Sheth BP, Kalenak JW, Sunden SL, Streb LM, Taylor CM, Alward WL, et al (1995) Linkage of autosomal dominant iris hypoplasia to the region of the Rieger syndrome locus (4q25). Hum Mol Genet 4:1435-9.

34) Hill RE, Favor J, Hogan BL, Ton CC, Saunders GF, Hanson IM, Prosser J, et al (1991) Mouse small eye results from mutations in a paired-like homeobox- containing gene. Nature 354:522-5.

35) Hjalt TA, Amendt BA, Murray JC (2001) PITX2 Regulates Procollagen Lysyl Hydroxylase (PLOD) Gene Expression. Implications for the pathology of rieger syndrome. J Cell Biol 152:545-552.

36) Hogan BL, Horsburgh G, Cohen J, Hetherington CM, Fisher G, Lyon MF (1986) Small eyes (Sey): a homozygous lethal mutation on chromosome 2 which affects the differentiation of both lens and nasal placodes in the mouse. J Embryol Exp Morphol 97:95-110.

37) Jacobson N, Andrews M, Shepard AR, Nishimura D, Searby C, Fingert JH, Hageman G, et al (2001) Non-secretion of mutant proteins of the glaucoma gene myocilin in cultured trabecular meshwork cells and in aqueous humor. Hum Mol Genet 10:117-125.

38) Jakobiec FA (1982) Ocular Anatomy, Embryology, and Teratology. Harper and Row Publishers, Philadelphia.

39) Jones NA, Kuo YM, Sun YH, Beckendorf SK (1998) The Drosophila Pax gene eye gone is required for embryonic salivary duct development. Development 125:4163-74.

40) Jordan T, Hanson I, Zaletayev D, Hodgson S, Prosser J, Seawright A, Hastie N, et al (1992) The human PAX6 gene is mutated in two patients with aniridia. Nat Genet 1:328-32.

41) Jun S, Wallen RV, Goriely A, Kalionis B, Desplan C (1998) Lune/eye gone, a Pax-like protein, uses a partial paired domain and a homeodomain for DNA recognition. Proc Natl Acad Sci U S A 95:13720-5.

42) Karali A, Russell P, Stefani FH, Tamm ER (2000) Localization of myocilin/trabecular meshwork--inducible glucocorticoid response protein in the human eye. Invest Ophthalmol Vis Sci 41:729-40.

43) Kozlowski K, Walter MA (2000) Variation in residual PITX2 activity underlies the phenotypic spectrum of anterior segment developmental disorders. Hum Mol Genet 9:2131-9.

44) Kozmik Z, Pfeffer P, Kralova J, Paces J, Paces V, Kalousova A, Cvekl A (1999) Molecular cloning and expression of the human and mouse homologues of the Drosophila dachshund gene. Dev Genes Evol 209:537-45.

45) Kubota R, Noda S, Wang Y, Minoshima S, Asakawa S, Kudoh J, Mashima Y, et al (1997) A novel myosin-like protein (myocilin) expressed in the connecting cilium of the photoreceptor: molecular cloning, tissue expression, and chromosomal mapping. Genomics 41:360-9.

46) Kulak SC, Kozlowski K, Semina EV, Pearce WG, Walter MA (1998) Mutation in the RIEG1 gene in patients with iridogoniodysgenesis syndrome. Hum Mol Genet 7:1113-7.

47) Lin CR, Kioussi C, O'Connell S, Briata P, Szeto D, Liu F, Izpisua-Belmonte JC, et al (1999) Pitx2 regulates lung asymmetry, cardiac positioning and pituitary and tooth morphogenesis. Nature 401:279-82.

48) Liu B, Neufeld AH (2001) Nitric oxcide synthase-2 in human optic nerve head astrocytes induced by elevated pressure in vitro. Arch Ophthalmol 119:240-5.

49) Liu H, Cao Y, Basbaum AI, Mazarati AM, Sankar R, Wasterlain CG (1999) Resistance to exitotoxin-induced seizures and neuronal

death in mice lacking the preprotachykinin A gene. PNAS 96:12096-101.

50) Lu MF, Pressman C, Dyer R, Johnson RL, Martin JF (1999) Function of Rieger syndrome gene in left-right asymmetry and craniofacial development. Nature 401:276-8.

51) Lupo G, Andreazzoli M, Gestri G, Liu Y, He RQ, Barsacchi G (2000) Homeobox genes in the genetic control of eye development. Int J Dev Biol 44:627-36.

52) Mardon G, Solomon NM, Rubin GM (1994) dachshund encodes a nuclear protein required for normal eye and leg development in Drosophila. Development 120:3473-86.

53) Mertts M, Garfield S, Tanemoto K, Tomarev SI (1999) Identification of the region in the N-terminal domain responsible for the cytoplasmic localization of Myoc/Tigr and its association with microtubules. Lab Invest 79:1237-45.

54) Mirzayans F, Pearce WG, MacDonald IM, Walter MA (1995) Mutation of the PAX6 gene in patients with autosomal dominant keratitis. Am J Hum Genet 57:539-48.

55) Morissette J, Clepet C, Moisan S, Dubois S, Winstall E, Vermeeren D, Nguyen TD, et al (1998) Homozygotes carrying an autosomal dominant TIGR mutation do not manifest glaucoma. Nat Genet 19:319-21.

56) Murray JC, Bennett SR, Kwitek AE, Small KW, Schinzel A, Alward WL, Weber JL, et al (1992) Linkage of Rieger syndrome to the region of the epidermal growth factor gene on chromosome 4. Nat Genet 2:46-9.

57) Nelson LB, Spaeth GL, Nowinski TS, Margo CE, Jackson L (1984) Aniridia. A review. Surv Ophthalmol 28:621-42.

58) Nguyen TD, Chen P, Huang WD, Chen H, Johnson D, Polansky JR (1998) Gene structure and properties of TIGR, an olfactomedin-related glycoprotein cloned from glucocorticoid-induced trabecular meshwork cells. J Biol Chem 273:6341-50.

59) Nishimura DY, Searby CC, Borges AS, Carani JCE, Betinjane AJ, Stone EM, Susanna R, et al (2000) Identification of a Fourth Rieger Syndrome Locus at 16q24. Am J Hum Genet 67:383.

60) Oliver G, Loosli F, Koster R, Wittbrodt J, Gruss P (1996) Ectopic lens induction in fish in response to the murine homeobox gene Six3. Mech Dev 60:233-9.

61) Oliver G, Mailhos A, Wehr R, Copeland NG, Jenkins NA, Gruss P (1995) Six3, a murine homologue of the sine oculis gene, demarcates the most anterior border of the developing neural plate and is expressed during eye development. Development 121:4045-55.

62) Ortego J, Escribano J, Coca-Prados M (1997) Cloning and characterization of subtracted cDNAs from a human ciliary body library encoding TIGR, a protein involved in juvenile open angle glaucoma with homology to myosin and olfactomedin. FEBS Lett 413:349-53.

63) Phillips JC, del Bono EA, Haines JL, Pralea AM, Cohen JS, Greff LJ, Wiggs JL (1996) A second locus for Rieger syndrome maps to chromosome 13q14. Am J Hum Genet 59:613-9.

64) Pignoni F, Hu B, Zavitz KH, Xiao J, Garrity PA, Zipursky SL (1997) The eye-specification proteins So and Eya form a complex and regulate multiple steps in Drosophila eye development. Cell 91:881-91.

65) Polansky JR, Kurtz RM, Alvarado JA, Weinreb RN, Mitchell MD (1989) Eicosanoid production and glucocorticoid regulatory mechanisms in cultured human trabecular meshwork cells. Prog Clin Biol Res 312:113-38.

66) Quigley HA, Vitale S (1997) Models of open-angle glaucoma prevalence and incidence in the United States. Invest Ophthalmol Vis Sci 38:83-91.

67) Quiring R, Walldorf U, Kloter U, Gehring WJ (1994) Homology of the eyeless gene of Drosophila to the Small eye gene in mice and Aniridia in humans. Science 265:785-9.

68) Rieger H (1935) Beitrage zur Kenntnis seltener Missbildungen der Iris, II: uber Hypoplasie des Irisvorderblattes mit Verlagerung und Entrundung der Pupille. Albrecht von Graefes Arch Klin Exp Ophthalmol 133:602-635.

69) Ritch R, Shields M.B., Krupin, T. (1989) The Glaucomas. Vol. 2. The C.V. Mosby Company, St. Louis.

70) Sarfarazi M, Akarsu AN, Hossain A, Turacli ME, Aktan SG, Barsoum-Homsy M, Chevrette L, et al (1995) Assignment of a locus (GLC3A) for primary congenital glaucoma (Buphthalmos) to 2p21 and evidence for genetic heterogeneity. Genomics 30:171-7.

71) Sarfarazi M, Stoilov I (2000) Molecular genetics of primary congenital glaucoma. Eye 14:422-8.

72) Semina EV, Reiter R, Leysens NJ, Alward WL, Small KW, Datson NA, Siegel-Bartelt J, et al (1996) Cloning and characterization of a novel bicoid-related homeobox transcription factor gene, RIEG, involved in Rieger syndrome. Nat Genet 14:392-9.

73) Serikaku MA, O'Tousa JE (1994) sine oculis is a homeobox gene required for Drosophila visual system development. Genetics 138:1137-50.

74) Shen W, Mardon G (1997) Ectopic eye development in Drosophila induced by directed dachshund expression. Development 124:45-52.

75) Sheng G, Thouvenot E, Schmucker D, Wilson DS, Desplan C (1997) Direct regulation of rhodopsin 1 by Pax-6/eyeless in Drosophila: evidence for a conserved function in photoreceptors. Genes Dev 11:1122-31.

76) Shields MB (1987) Textbook of Glaucoma. Williams and Wilkins, Baltimore.

77) Spencer WH (1985) Ophthalmic Pathology: An Atlas and Textbook. Vol. 1. W.B. Saunders Company, Philadelphia.

78) Sternberg SS (1997) Histology for Pathologists. Lippencott-Raven Publishers, Philadelphia, pp 315-336.

79) Stoilov I, Akarsu AN, Sarfarazi M (1997) Identification of three different truncating mutations in cytochrome P4501B1 (CYP1B1) as the principal cause of primary congenital glaucoma (Buphthalmos) in families linked to the GLC3A locus on chromosome 2p21. Hum Mol Genet 6:641-7.

80) Stone EM, Fingert JH, Alward WL, Nguyen TD, Polansky JR, Sunden SL, Nishimura D, et al (1997) Identification of a gene that causes primary open angle glaucoma. Science 275:668-70.

81) Ton CC, Hirvonen H, Miwa H, Weil MM, Monaghan P, Jordan T, van Heyningen V, et al (1991) Positional cloning and characterization of a paired box- and homeobox- containing gene from the aniridia region. Cell 67:1059-74.

82) Treisman JE (1999) A conserved blueprint for the eye? Bioessays 21:843-50.

83) Ueda J, Wentz-Hunter KK, Cheng EL, Fukuchi T, Abe H, Yue BY (2000) Ultrastructural localization of myocilin in human trabecular meshwork cells and tissues. J Histochem Cytochem 48:1321-30.

84) Vollrath D, Jaramillo-Babb VL, Clough MV, McIntosh I, Scott KM, Lichter PR, Richards JE (1998) Loss-of-function mutations in the LIM-homeodomain gene, LMX1B, in nail- patella syndrome. Hum Mol Genet 7:1091-8.

85) Wallis DE, Roessler E, Hehr U, Nanni L, Wiltshire T, Richieri-Costa A, Gillessen-Kaesbach G, et al (1999) Mutations in the homeodomain of the human SIX3 gene cause holoprosencephaly. Nat Genet 22:196-8.

86) Wiggs JL (1995) Molecular Genetics of Ocular Disease. Wiley-Liss.

87) Wiggs JL, Allingham RR, Hossain A, Kern J, Auguste J, DelBono EA, Broomer B, et al (2000) Genome-wide scan for adult onset primary open angle glaucoma. Hum Mol Genet 9:1109-17.

88) Xu PX, Adams J, Peters H, Brown MC, Heaney S, Maas R (1999) Eya1-deficient mice lack ears and kidneys and show abnormal apoptosis of organ primordia. Nat Genet 23:113-7.

89) Xu PX, Woo I, Her H, Beier DR, Maas RL (1997) Mouse Eya homologues of the Drosophila eyes absent gene require Pax6 for expression in lens and nasal placode. Development 124:219-31.

# CHAPTER TWO
# MAPPING OF AXENFELD-RIEGER MALFORMATIONS

Portions of this chapter have been previously published in:

Mears AJ, Mirzayans F, Gould DB, Pearce WG, and Walter MA (1996). Autosomal dominant iridogoniodysgenesis anomaly maps to 6p25. American Journal of Human Genetics 59(6):1321-1327.

Gould DB, Mears AJ, Pearce WG, and Walter MA (1997). Autosomal dominant Axenfeld-Rieger anomaly maps to 6p25. American Journal of Human Genetics 61(3):765-768.

Mirzayans F, Gould DB, Heon E, Billingsley GD, Cheung JC, Mears AJ, and Walter MA (2000). Axenfeld-Rieger syndrome resulting from mutation of the FKHL7 gene on chromosome 6p25. European Journal of Human Genetics 8(1):71-74.

## A) INTRODUCTION

One of the most powerful techniques used to identify genes involved in inherited disorders is positional cloning (Collins 1990). Positional cloning starts by identifying the chromosomal region containing a particular trait. The markers that flank the region define the "critical interval" for the trait. Genes within the critical interval are then considered positional candidates based solely on the fact that they lie within the critical interval. Genes whose putative protein function may be involved in the observable phenotype of the trait being mapped may also be considered functional candidates. Steps are taken to prove or disprove the involvement of such genes with the trait.

The ability to map a disease locus to a critical interval of manageable size depends on two factors. The first is access to a high density of polymorphic markers in the region. With the human genome sequence now largely available, these are easily obtained. The second factor is access to families affected with the disorder of interest. Obtaining clinically-characterized familial samples is the single most valuable resource for linkage analysis. The definition of the critical interval requires recombination events between the disease locus and the polymorphic markers being tested. The larger a family is, the more opportunity there is for recombination events,

and, therefore, the more useful the family is for refining a critical interval.

Genetic linkage analysis asks the question "Is a particular allele of a polymorphic marker associated with the disease phenotype more often than is expected by chance?". By examining the inheritance of alleles of a marker, and knowing the inheritance of the disorder in the pedigree, an algorithm can can be used to determine what the odds are of getting the observed pattern if the two loci are linked and what the odds are of getting the observed pattern if the two loci are not linked. A ratio of these two values (odds of observed pattern if loci are linked versus odds if they are not linked) greater than 1000:1 is considered evidence of linkage. This ratio is expressed as a logarithmic value (called the LOD score for "Log of odds") and, therefore, a LOD value of 3 or greater is considered evidence of linkage. If the LOD score is -2 or lower (100:1 odds against linkage), then linkage between the two loci is excluded (Morton 1955). I used genetic linkage analysis to identify chromosomal regions responsible for anterior segment malformations.

Clinically, the breakdown of the four related anterior segment malformations IGDA (iridogoniodysgenesis anomaly OMIM#601631), IGDS (iridogoniodysgenesis syndrome

OMIM#137600), ARA (Axenfeld Rieger anomaly (OMIM# 601090.0009), and ARS (Axenfeld Rieger syndrome) are as follows. IGDA and IGDS eye malformations are relatively mild and include iris hypoplasia and malformations of the iridocorneal angle. IGDA presents with ocular features alone, while IGDS presents with ocular features associated with systemic findings including midface anomalies, dental anomalies, and redundant periumbilical skin. ARA and ARS eye malformations are similar to the IGD malformations but may also include a prominent and/or displaced Schwalbe's line that may be associated with iris adhesions, corectopia, and polycoria. ARA presents only with the ocular features while ARS presents with ocular features associated with the same non-ocular features of IGDA.

The purpose of my work described below was to genetically map the disease loci for three small pedigrees each segregating with a clinically distinct type of autosomal dominant Axenfeld-Reiger malformation. This work was done in conjunction with collaborators who mapped three additional families.

## B) MATERIALS AND METHODS

### i) Clinical Analysis

Individuals from families A (Figure 2-2a) and B (Figure 2-3a) were examined with standard slit-lamp and gonioscopic procedures by refering physicians. Detailed descriptions of the clinical methodologies have been reported elsewhere (Pearce et al. 1983; Wyatt et al. 1983). IOPs were considered abnormal at greater than 21mm Hg.

Family members with congenital iris hypoplasia and/or goniodysgenesis were diagnosed as affected. Iris hypoplasia can be observed in the eyes from patients in both family A (Figure 2-2b) and family B (Figure 2-3b) when compared to an eye from an unaffected patient (Figure 2-1). Elevated IOP (and subsequent risk of glaucoma) is observed in approximately 74% of IGDA patients (Table 2-1). The age of onset of glaucoma, its severity, and management in IGDA patients have all been discussed in the literature (Jerndal 1972; Weatherill and Hart 1969; Wyatt et al. 1983).

Clinical examinations of 13 members of family C (Figure 2-4a) revealed 7 to be affected with ARA. Individuals diagnosed with ARA had a prominent and anteriorly displaced Schwalbe's line, iris stromal hypoplasia, and corectopia (Figure 2-4b). Non-ocular features of ARS (including jaw, dental, and umbilical anomalies) were not present.

**FIGURE 2-1. Photograph of an eye from an unaffected member of Family A.**

The right eye of unaffected member VI:5 of Family A. Taken from Mears et al. 1996.

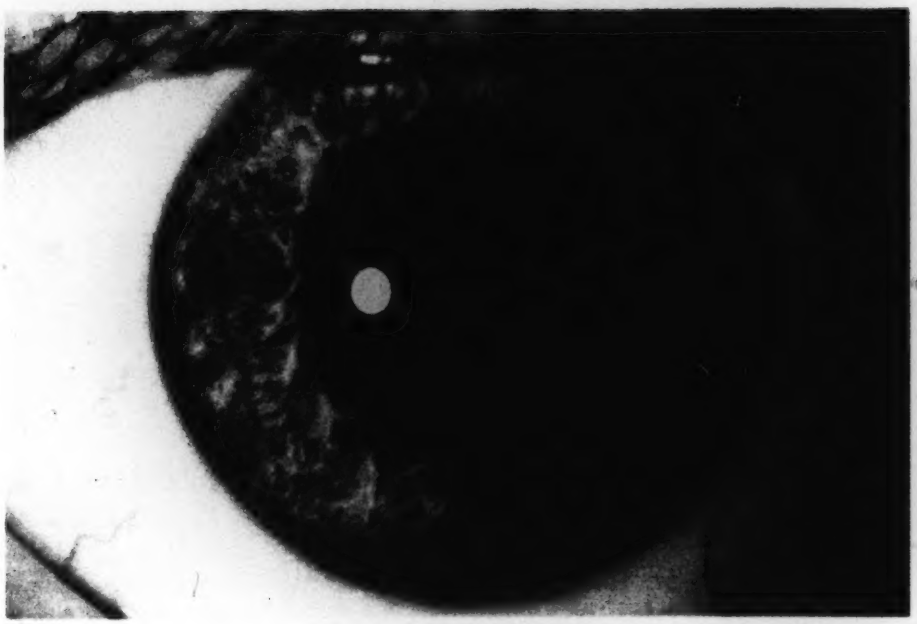

**FIGURE 2-2. Pedigree and affected eye photograph from Family A.**

**A)** Family A with autosomal dominant IGDA. Affected individuals are indicated with filled symbols. A diagonal line through a symbol indicates the individual is deceased. Males are indicated with squares. Females are indicated with circles. DNA samples were available for individuals 1, 2, 7, 10, and 17 for generation IV; 2-11, 13-20, and 22-24 for generation V; 1-13 and 15 for generation VI; and 1-7 for generation VII. Taken from Mears et al. 1996.

**B)** The right eye from affected member VI:3 of Family A with IGDA. Note the marked iris stromal hypoplasia with exposure of the pupilary sphincter muscle compared to the normal eye in Figure 2-1. Taken from Mears et al. 1996.

A)

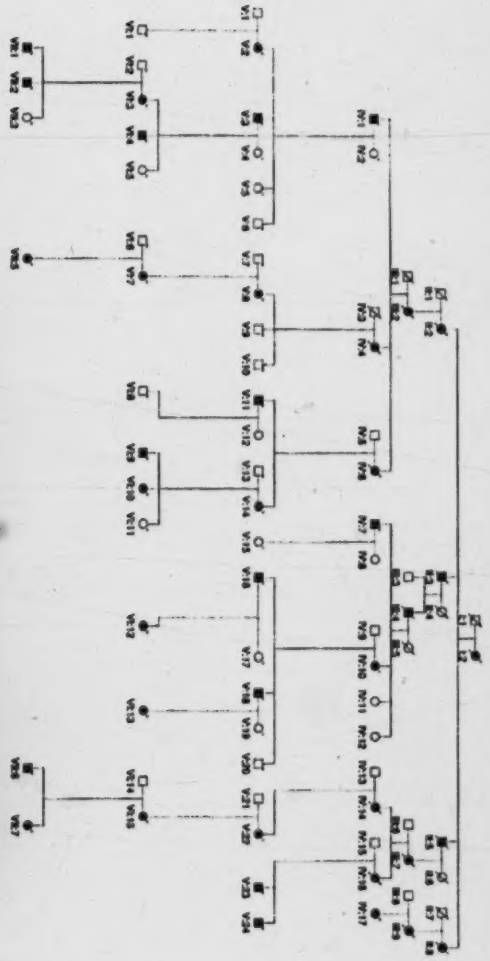

B)

**FIGURE 2-3. Pedigree and affected eye photograph from Family B.**

**A)** Family B with autosomal dominant IGDA. Affected individuals are indicated with filled symbols. A diagonal line through a symbol indicates the individual is deceased. Males are indicated with squares. Females are indicated with circles. Plus signs indicate individuals for whom DNA samples were available. Taken from Mears et al. 1996.

**B)** The left eye from affected member III:2 of Family B with IGDA. Note the marked iris stromal hypoplasia with exposure of the pupilary sphincter muscle compared to the normal eye in Figure 2-1. Also note the similarity to the eye in Figure 2-1b. Taken from Mears et al. 1996.

A)

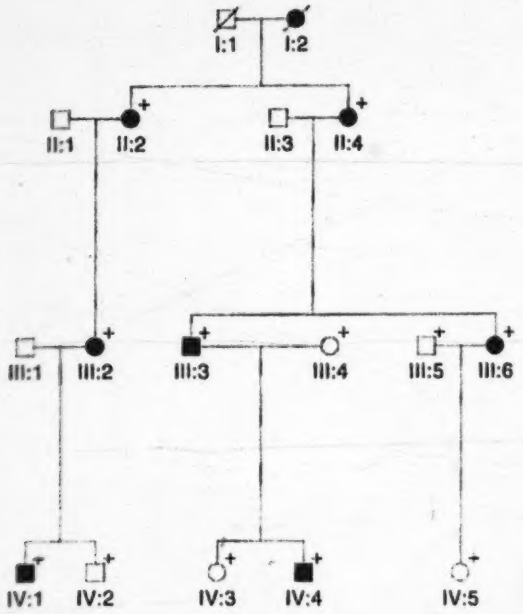
I:1
I:2
II:1
II:2
II:3
II:4
III:1
III:2
III:3
III:4
III:5
III:6
IV:1
IV:2
IV:3
IV:4
IV:5

B)

## Table 2-1

**Variable expressivity of IGDA**

| Clinical features | | | Publication | | | |
|---|---|---|---|---|---|---|
| Abnormal angle | Elevated IOP[1] | Iris hypoplasia | Jerndal 1983 | Weatherill and Hart 1969 | Pearce et al. 1983* | % of total |
| + | + | + | 27/37 | 16/30 | 16/22 | 66 |
| + | - | + | 10/37 | 7/30 | 2/22 | 21 |
| + | + | - | 0/37 | 4/30 | 0/22 | 5 |
| + | - | - | 0/37 | 3/30 | 1/22 | 5 |
| - | + | + | 0/37 | 0/30 | 3/22 | 3 |

Summary of previous reports of clinical variability of IGDA. (+) indicates presence of IGDA clinical feature, (-) absence. * data includes families A and B described in this study. [1] Intraocular pressure (IOP) was considered elevated if greater than 21 mm Hg at time of examination.

**FIGURE 2-4. Pedigree and affected eye photograph from Family C.**

**A)** Family C with autosomal ARA. Individuals who were examined and affected are denoted with filled symbols. Individuals who were examined and not affected are denoted with "N". Open symbols represent individuals who were not examined. A diagonal line indicates the individual is deceased. Males are indicated with squares. Females are indicated with circles. Individual II:5 is deceased and was not examined, but is presumed to have been affected, because he has an affected son (III:9) and ARA has not been reported with non-penetrance. Taken from Gould et al. 1997.

**B)** The right eye of affected member II:1 of Family C with ARA. Note the prominent, centrally displaced Schwalbe's line that is detached from the cornea and crosses the anterior chamber, in addition to marked iris stromal hypoplasia and a superiorly displaced pupil. This is in contrast to the normal eye in Figure 2-1. Taken from Gould et al. 1997.

A)

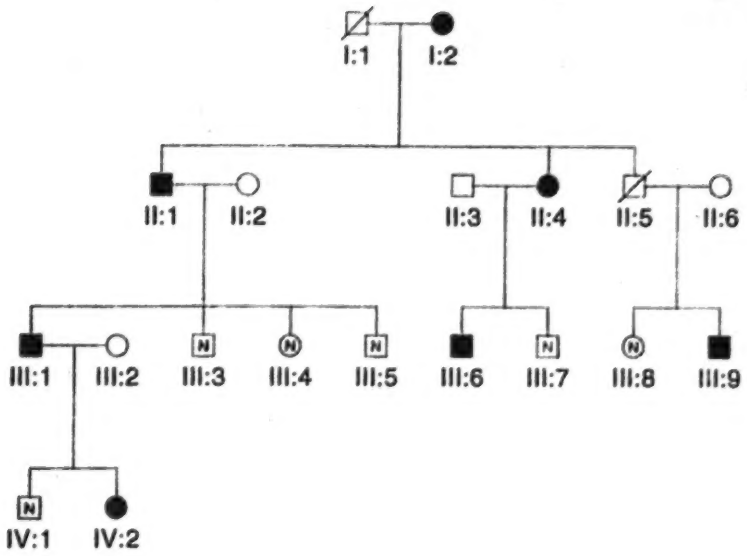
I:1
I:2
II:1
II:2
II:3
II:4
II:5
II:6
III:1
III:2
III:3
III:4
III:5
III:6
III:7
III:8
III:9
IV:1
IV:2

B)

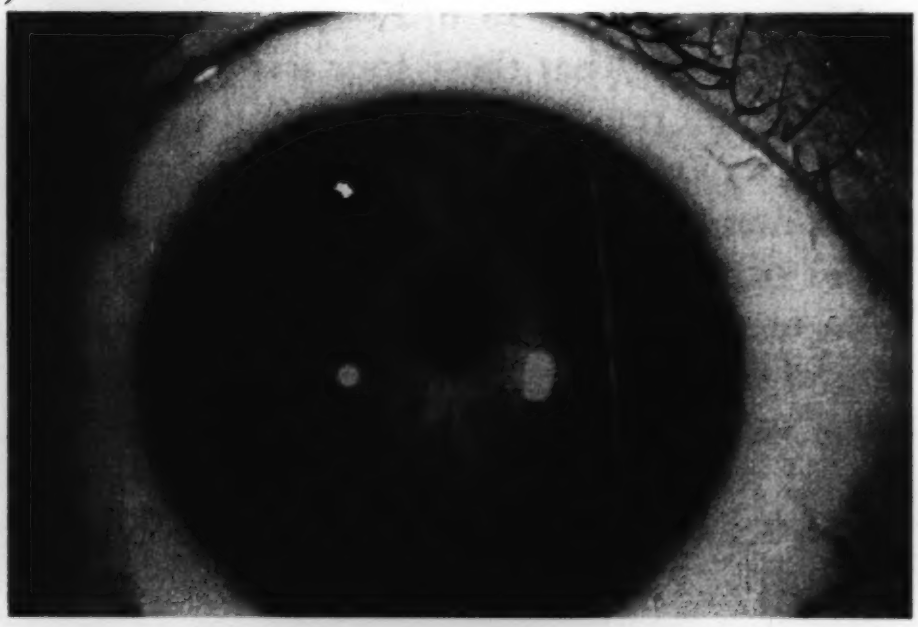

Clinical examinations of 15 patients of family D (Figure 2-5a) revealed nine members over three generations affected with ARS. Affected individuals presented with a variable degree of iris hypoplasia, corectopia, and a prominent, anteriorly displaced Schwalbe's line to which peripheral iris strands were attached bridging the iridocorneal angle (Figure 2-5b). Non-ocular features associated with ARS were also observed in most of the affected individuals (Table 2-2).

The study and collection of blood samples from all individuals included in this report were approved by the Research Ethics Board of the Faculty of Medicine of the University of Alberta (Families A, B, and C) or by the Toronto Hospital Committee for Research on Human Subjects (Family D).

**ii) Linkage Analysis**

Microsatellite analysis was performed using oligonucleotide primers obtained from Research Genetics (Huntsville, AL, USA). Polymerase chain reaction (PCR) amplification involved direct incorporation of $^{35}$S-dATP into PCR products. Reactions were performed with 20mM Tris-HCl; 50mM KCl; 1.5mM $MgCl_2$; 200$\mu$M each of dCTP, dGTP, and dTTP; 25$\mu$M dATP; 5$\mu$Ci $^{35}$S-dATP; and

**FIGURE 2-5. Pedigree and affected eye photograph from Family D.**

**A)** Family D with autosomal dominant ARS. Affected individuals are indicated with filled symbols. Males are indicated with squares. Females are indicated with circles. Taken from Mirzayans et al. 2000.

**B)** The left eye of affected member I:1 of Family D with ARS. Note the marked iris stromal hypoplasia and slight correctopia (displaced pupil) compared to the normal eye in Figure 2-1. Taken from Mirzayans et al. 2000.

A)

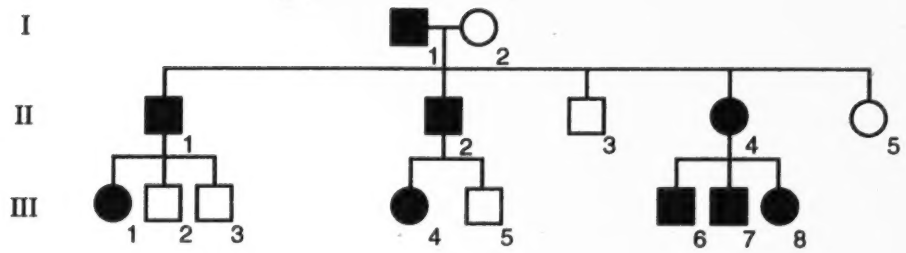


B)

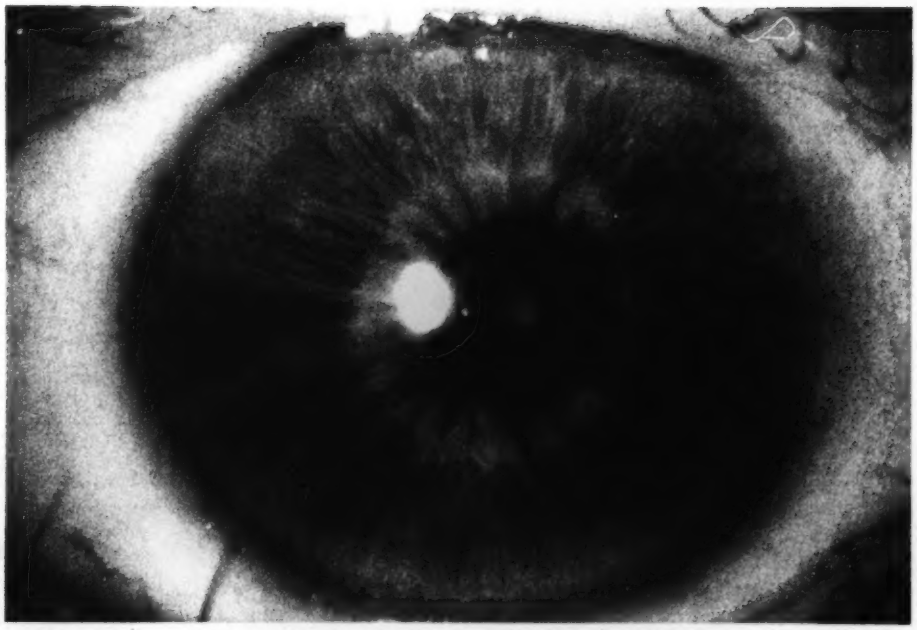

**Table 2-2. Clinical findings of Family D.**

| PEDIGREE NO. | I-1 | II-1 | II-2 | II-4 | III-1 | III-4 | III-6 | III-7 | III-8 | |
|---|---|---|---|---|---|---|---|---|---|---|
| DATE OF BIRTH | 1940 | 1960 | 1962 | 1964 | 1993 | 1981 | 1979 | 1984 | 1988 | |
| OCULAR FINDINGS* | | | | | | | | | | |
| Post. embryotoxon | + | + | + | + | + | + | + | + | + | |
| Iris hypoplasia | | + | + | + | + | + | + | + | + | +/- |
| Gonioscopy | | PAS | PAS | IP | IP | IP | nd | IP | nd | nd |
| Glaucoma | - | + | - | - | - | - | - | - | - | |
| NON-OCULAR FINDINGS | | | | | | | | | | |
| flat midface | + | + | + | - | - | - | - | - | + | |
| microdontia | + | + | + | - | - | - | - | - | + | |
| hypertelorism | + | + | - | - | + | - | + | - | + | |
| umbilical abn. | + | - | + | - | - | - | - | - | - | |
| Other | | - | - | - | - | - | - | - | CD | HL |

PAS peripheral anterior synechia
IP iris process
nd not done
CD cardiac defect
HL hearing loss

NOTE TO USERS

Page (s) not included in the original manuscript is unavailable from the author or university. The manuscript was microfilmed as received.

102-104

This reproduction is the best copy available.

UMI

**Table 2-3. Two-point lod scores between chromosome 6 markers and IGDA in families A and B**

| | Recombination fraction (θ) | | | | | | |
|---|---|---|---|---|---|---|---|
| Locus | 0.00 | 0.05 | 0.10 | 0.20 | 0.40 | $Z_{max}$ | $\theta_{max}$ |
| D6S1600 | 11.14 | 10.28 | 9.28 | 7.05 | 2.20 | 11.14 | 0.00 |
| D6S967 | 12.33 | 11.19 | 10.01 | 7.51 | 2.28 | 12.33 | 0.00 |
| D6S1617 | 11.53 | 10.65 | 9.61 | 7.29 | 2.23 | 11.53 | 0.00 |
| D6S477 | 6.25 | 8.73 | 8.18 | 6.42 | 2.02 | 8.78 | 0.03 |
| D6S277 | 6.00 | 8.48 | 7.94 | 6.21 | 1.97 | 8.53 | 0.03 |
| D6S1006 | -6.06 | 4.23 | 4.58 | 4.03 | 1.36 | 4.58 | 0.10 |

**FIGURE 2-6. Critical intervals for ARA and IGDA.**

This schematic of chromosome 6 indicates the critical interval for the ARA and IGDA loci. Cumulative genetic distances (in centiMorgans from the telomere) are indicated to the left of each marker. Key recombinant individuals are represented with the family and pedigree number at the top. The disease status is indicated at the bottom. Blackened rectangles indicate the region cosegregating with the disease in the respective families.

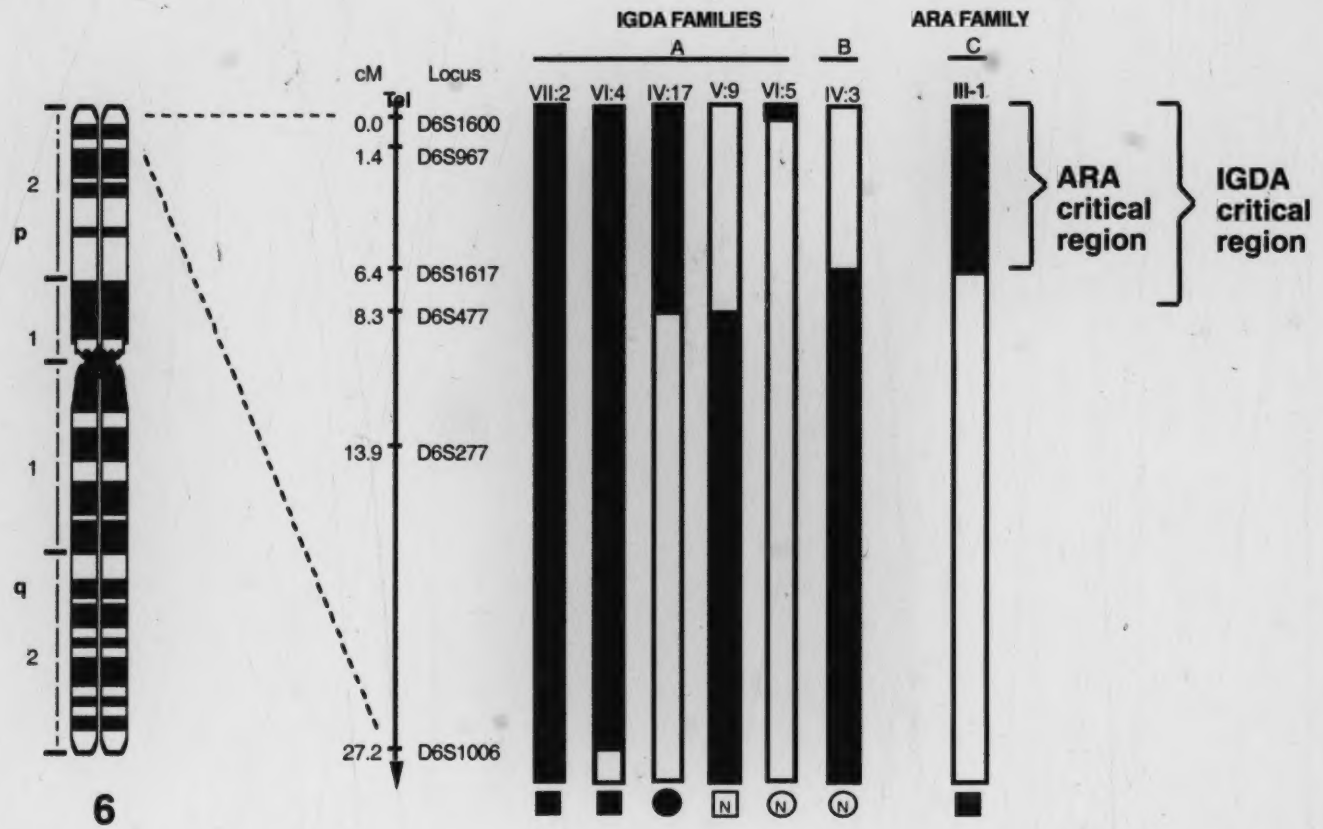
IGDA FAMILIES
A
B
ARA FAMILY
C
cM
Locus
Tel
0.0
D6S1600
1.4
D6S967
6.4
D6S1617
8.3
D6S477
13.9
D6S277
27.2
D6S1006
VII:2
VI:4
IV:17
V:9
VI:5
IV:3
III-1
ARA critical region
IGDA critical region
2
p
1
1
q
2
6

I carried out linkage analysis on 13 members of Family C, of which 7 were affected. Linkage to the ARS locus at 4q25 (Murray et al. 1992) was excluded by examination of polymorphic markers in the region (Table 2-4). Linkage was demonstrated however to the locus at 6p25. A maximum LOD score of 3.31 was obtained with marker D6S344 at a maximum recombination fraction of Theta=0.00 (Table 2-4). This result suggested that ARA and IGDA may be allelic, however, it does not exclude the possibility of two separate, closely linked, genes underlying the two phenotypes.

A key recombinant in Family C (individual III:1) indicates that the ARA critical interval is a 6.4cM region flanked by markers D6S1600 and D6S1617 (Figure 2-6).

Linkage analysis was conducted on 14 members of Family D, of which 9 were affected. Linkage of the ARS phenotype in this family to the locus at 4q25 (Murray et al. 1992) was excluded by examination of three polymorphic markers in the 4q25 region, D4S3240, D4S2623, and D4S406 (data not shown). Examination of six polymorphic markers (D13S894, D13S1288, D13S1253, D13S1248, D13S263, and D13S325) that span the *RIEG2* critical region at 13q14 (Phillips et al. 1996) was consistent with exclusion of the *RIEG2* gene (data not shown). In contrast, complete linkage

Table 2-4. LOD scores for 4q25 and 6p25

| | LOD SCORE AT θ= | | | | | | |
|---|---|---|---|---|---|---|---|
| ARA vs. 4q25 LOCI | | | | | | | |
| **LOCUS** | **.00** | **.05** | **.10** | **.20** | **.40** | $Z_{MAX}$ | $\theta_{MAX}$ |
| D4S3256 | -7.68 | -2.93 | -2.07 | -1.12 | -0.22 | - | - |
| D4S2623 | -8.48 | -1.70 | -1.03 | -0.44 | -0.05 | - | - |
| ARA vs. 6p25 LOCI | | | | | | | |
| **LOCUS** | **.00** | **.05** | **.10** | **.20** | **.40** | $Z_{MAX}$ | $\theta_{MAX}$ |
| D6S1600 | 1.51 | 1.39 | 1.25 | 0.96 | 0.32 | 1.51 | 0.00 |
| D6S942 | 2.60 | 2.35 | 2.08 | 1.51 | 0.34 | 2.60 | 0.00 |
| D6S344 | 3.31 | 3.03 | 2.74 | 2.13 | 0.74 | 3.31 | 0.00 |
| D6S967 | 2.88 | 2.62 | 2.35 | 1.76 | 0.49 | 2.88 | 0.00 |
| D6S1617 | -7.68 | 0.57 | 0.72 | 0.69 | 0.29 | 0.74 | 0.13 |
| D6S1713 | -5.59 | 1.38 | 1.48 | 1.34 | 0.57 | 1.48 | 0.10 |
| D6S477 | -6.45 | 1.05 | 1.20 | 1.14 | 0.46 | 1.22 | 0.13 |

of ARS in this family to polymorphic loci at 6p25 was observed. A maximum LOD score of 2.71 at a recombination fraction of Theta=0.00 was obtained with marker D6S344. Positive LOD scores of 2.41 at Theta=0.00 were also found with D6S1600 and D6S967. The small size of Family D together with only partially informative markers precludes the maximum LOD scores from reaching the critical value of 3.00 required to indicate significant linkage. However, the suggestion of possible linkage was sufficient for this family to be included in mutational screens for candidate genes in the critical interval.

## D) DISCUSSION

This work demonstrates two significant findings. The first is the mapping of a new locus for anterior segment malformations and secondary glaucoma to chromosome 6p25. The second significant finding is that the clinically-separable disorders of IGDA (Families A and B), ARA (Family C), and ARS (Family D) all map to the same region. This indicates that these disorders are either allelic variants of the same gene, or alternatively, that two or more genes exist in close proximity at 6p25. Both of these alternatives are very interesting.

Originally, ARS was mapped to the RIEG1 locus at 4q25 (Murray et al. 1992). Subsequently, two families with IGD eye malformations were also mapped to this locus (Heon et al. 1995; Walter et al. 1996). Both of these families had affected members who showed non-ocular features although variable expressivity for non-ocular features was demonstrated in one of the families (Heon et al. 1995). Two other families, one with ARA (Legius et al. 1994) and one with IGDA (Family A from this study) (Walter et al. 1996) were excluded from linkage to this locus and the popular hypothesis was that there would be one locus, 4q25, for the syndromic forms and one locus for the ocular-only forms.

The *PITX2* gene has been identified as the gene mutated in families mapping to 4q25 (Alward et al. 1998; Kulak et al. 1998; Semina et al. 1996). To date, no *PITX2* mutations have been identified in families without systemic findings.

The results of mapping IGDA to 6p25 (Families A and B) by Dr. Mears and me (Mears et al. 1996), and my mapping of ARA to 6p25 (Family C) (Gould et al. 1997), were consistent with the hypothesis regarding the genetic distinction of the disorders based on the presence or absence of non-ocular findings. My mapping of an ARS family (Family D) (Mirzayans et al. 2000) to this region was the first

example of co-localization of syndromic and non-syndromic forms of the disorders.

The results of this work indicate the minimal critical interval for the two IGDA families (Families A and B) is 8.3cM and the minimal critical interval for the ARA family (Family C) is 6.4cM. Other members of our lab have identified a gene located within this critical interval, *FOXC1* (formerly *FREAC3* and *FKHL7*), as the gene mutated in both the ARA family (Family C) (Mears et al. 1998) and the ARS family (Family D) (Mirzayans et al. 2000). The entire coding region of *FOXC1* was also sequenced in Family A and Family B and no mutations were detected (Mears et al. 1998). One explanation for this is that the AR and IGD malformations mapping to this region are genetically distinct and that at least one more gene exists within the critical region that underlies the phenotype observed in Family A and Family B.

The physical size of the critical interval is roughly 250-300 kb. Efforts of the human genome project to sequence this region are still underway as a gap still exists in the known sequence. Based only on the physical size of the region, one might expect about 5 genes to be present within this interval. The availability of the full sequence through this region will allow an exhaustive search for genes in the

critical interval that may be involved in the remaining AR families that map to 6p25.

**E) REFERENCES**

1) Alward WL, Semina EV, Kalenak JW, Heon E, Sheth BP, Stone EM, Murray JC (1998) Autosomal dominant iris hypoplasia is caused by a mutation in the Rieger syndrome (RIEG/PITX2) gene. Am J Ophthalmol 125:98-100.

2) Collins FS (1990) Identifying human disease genes by positional cloning. Harvey Lect. 86:149-64

3) Gould DB, Mears AJ, Pearce WG, Walter MA (1997) Autosomal dominant Axenfeld-Rieger anomaly maps to 6p25. Am J Hum Genet 61:765-8.

4) Heon E, Sheth BP, Kalenak JW, Sunden SL, Streb LM, Taylor CM, Alward WL, et al (1995) Linkage of autosomal dominant iris hypoplasia to the region of the Rieger syndrome locus (4q25). Hum Mol Genet 4:1435-9.

5) Jerndal T (1972) Dominant goniodysgenesis with late congenital glaucoma. A re- examination of Berg's pedigree. Am J Ophthalmol 74:28-33.

6) Jerndal T (1983) Congenital glaucoma due to dominant goniodysgenesis. A new concept of the heredity of glaucoma. Am J Hum Genet 35:645-51.

7) Kulak SC, Kozlowski K, Semina EV, Pearce WG, Walter MA (1998) Mutation in the RIEG1 gene in patients with iridogoniodysgenesis syndrome. Hum Mol Genet 7:1113-7.

8) Legius E, de Die-Smulders CE, Verbraak F, Habex H, Decorte R, Marynen P, Fryns JP, et al (1994) Genetic heterogeneity in Rieger eye malformation. J Med Genet 31:340-1.

9) Mears AJ, Jordan T, Mirzayans F, Dubois S, Kume T, Parlee M, Ritch R, et al (1998) Mutations of the forkhead/winged-helix gene, FKHL7, in patients with Axenfeld-Rieger anomaly. Am J Hum Genet 63:1316-28.

10) Mears AJ, Mirzayans F, Gould DB, Pearce WG, Walter MA (1996) Autosomal dominant iridogoniodysgenesis anomaly maps to 6p25. Am J Hum Genet 59:1321-7.

11) Mirzayans F, Gould DB, Heon E, Billingsley GD, Cheung JC, Mears AJ, Walter MA (2000) Axenfeld-Rieger syndrome resulting from mutation of the FKHL7 gene on chromosome 6p25. Eur J Hum Genet 8:71-4.

12) Morton NE (1955) Sequential test for the detection of linkage. American Journal of Human Genetics 8:80-96.

13) Murray JC, Bennett SR, Kwitek AE, Small KW, Schinzel A, Alward WL, Weber JL, et al (1992) Linkage of Rieger syndrome to the region of the epidermal growth factor gene on chromosome 4. Nat Genet 2:46-9.

14) Nichols BE, Sheffield VC, Stone EM (1993) A user-friendly Hypercard interface for human linkage analysis. Comput Appl Biosci 9:757-9.

15) Nishimura DY, Searby CC, Borges AS, Carani JCE, Betinjane AJ, Stone EM, Susanna R, et al (2000) Identification of a Fourth Rieger Syndrome Locus at 16q24. Am J Hum Gene67:383.

16) Pearce WG, Wyatt HT, Boyd TA, Ombres RS, Salter AB (1983) Autosomal dominant iridogoniodysgenesis: genetic features. Can J Ophthalmol 18:7-10.

17) Phillips JC, del Bono EA, Haines JL, Pralea AM, Cohen JS, Greff LJ, Wiggs JL (1996) A second locus for Rieger syndrome maps to chromosome 13q14. Am J Hum Genet 59:613-9.

18) Semina EV, Reiter R, Leysens NJ, Alward WL, Small KW, Datson NA, Siegel-Bartelt J, et al (1996) Cloning and characterization of a novel bicoid-related homeobox transcription factor gene, RIEG, involved in Rieger syndrome. Nat Genet 14:392-9.

19) Sheffield VC, Stone EM, Alward WL, Drack AV, Johnson AT, Streb LM, Nichols BE (1993) Genetic linkage of familial open angle glaucoma to chromosome 1q21-q31. Nat Genet 4:47-50.

20) Terwilliger JD, Ott J (1994) Handbook of human genetic linkage. Johns Hopkins University Press, Baltimore.

21) Ton CC, Hirvonen H, Miwa H, Weil MM, Monaghan P, Jordan T, van Heyningen V, et al (1991) Positional cloning and

characterization of a paired box- and homeobox- containing gene from the aniridia region. Cell 67:1059-74.

22) Walter MA, Mirzayans F, Mears AJ, Hickey K, Pearce WG (1996) Autosomal-dominant iridogoniodysgenesis and Axenfeld-Rieger syndrome are genetically distinct. Ophthalmology 103:1907-15.

23) Weatherill JR, Hart CT (1969) Familial hypoplasia of the iris stroma associated with glaucoma. Br J Ophthalmol 53:433-8.

24) Wyatt HT, Pearce WG, Boyd TA, Ombres RS, Salter AB (1983) Autosomal dominant iridogoniodysgenesis: glaucoma management. Can J Ophthalmol 18:11-4.

# CHAPTER THREE

# *FOXF2* AS A CANDIDATE GENE FOR AXENFELD-RIEGER MALFORMATIONS

## A) INTRODUCTION

In an effort to identify genes within the critical interval that we had mapped to 6p25, our lab established collaborations with two investigators who also had families with AR malformations that map to 6p25. The first, Family E, is an extremely large pedigree described as having familial glaucoma iridodysplasia mapping to 6p25 (Jordan et al. 1997). Upon clinical inspection, this family looks phenotypically identical to Family A with IGDA. The second family, Family F, a large family described with familial glaucoma with goniodysgenesis, also mapped to 6p25 (Morissette et al. 1997).

The *PITX2* gene at 4q25 and *PAX6* gene at 11p13 are both developmentally regulated transcription factors with highly conserved DNA binding domains. Therefore, the identification of a developmentally regulated transcription factor within the critical interval would be considered a very attractive positional and functional candidate gene. The localization of six members of the forkhead family of transcription factors revealed that one of these mapped to chromosome 6p25 (Larsson et al. 1995). Direct sequence analysis of the *FOXC1* (Forkhead box C1) gene (formerly *FREAC3* and *FKHL7*) in affected members of all six of the families we

had collected, revealed disease causing mutations in Family C (Mears et al. 1998) and Family D (Mirzayans et al. 2000).

Coincident with the identification of *FOXC1* mutations by members of our lab, a second group also identified mutations in *FOXC1* in patients with anterior segment malformations (Nishimura et al. 1998). The mouse *Foxc1* gene (formerly *Mf1*) has been shown to cause autosomal recessive congenital hydrocephalus (*ch*) (Kume et al. 1998), and mice heterozygous for targeted disruptions of *Foxc1* have a phenotype resembling AR malformations (Hong et al. 1999; Smith et al. 2000). Recently, duplications of the region containing *FOXC1* have also been demonstrated to be involved in iris hypoplasia and glaucoma (Lehmann et al. 2000; Nishimura et al. 2001).

The absence of mutations in the coding region of *FOXC1* in four of our families has three possible explanations. The first is that a second gene exists within the critical region that is mutated in these families. The second explanation is that these families each have a mutation with *FOXC1* regulatory elements. The third explanation is that it is a duplication event in these families that is responsible for the phenotype.

While the third possibility is being explored (F. Mirzayans personal communication), evidence exists that perhaps one of the

first two explanations is more likely at least for Family E. A key recombination event in an affected individual (VIII:24) in Family E suggests that the critical interval can be refined and *FOXC1* is not a part of the refined interval (Figure 3-1). Based on this result it still cannot be determined if the mutation in this family is in a second gene within the new critical interval, or in a *FOXC1* regulatory element distal to the gene.

*FOXF2* (Forkhead box F2), another member of the forkhead family of transcription factors that *FOXC1* belongs to, lies within the refined critical region at 6p25.3 (Blixt et al. 1998). Due to its chromosomal position and homology to *FOXC1*, *FOXF2* is a very strong candidate gene for anterior segment eye malformations mapping to 6p25 that are not due to mutations in *FOXC1*.

## B) MATERIALS AND METHODS

### i) Direct Sequence Analysis

The DNA sequence for *FOXF2* was provided by Dr. Peter Carlsson. Dr. Alan Mears designed primers to amplify both exons of

**FIGURE 3-1. Genetic mapping of IRID locus.**

This schematic of chromosome 6 indicates the critical interval for the IRID locus. Cumulative genetic distances (in centiMorgans from the telomere) are indicated to the left of each marker. Key recombinant individuals are represented with the family and pedigree number at the top. The disease status of these individuals is indicated at the bottom. Blackened rectangles indicate the region cosegregating with the disease in the respective families.

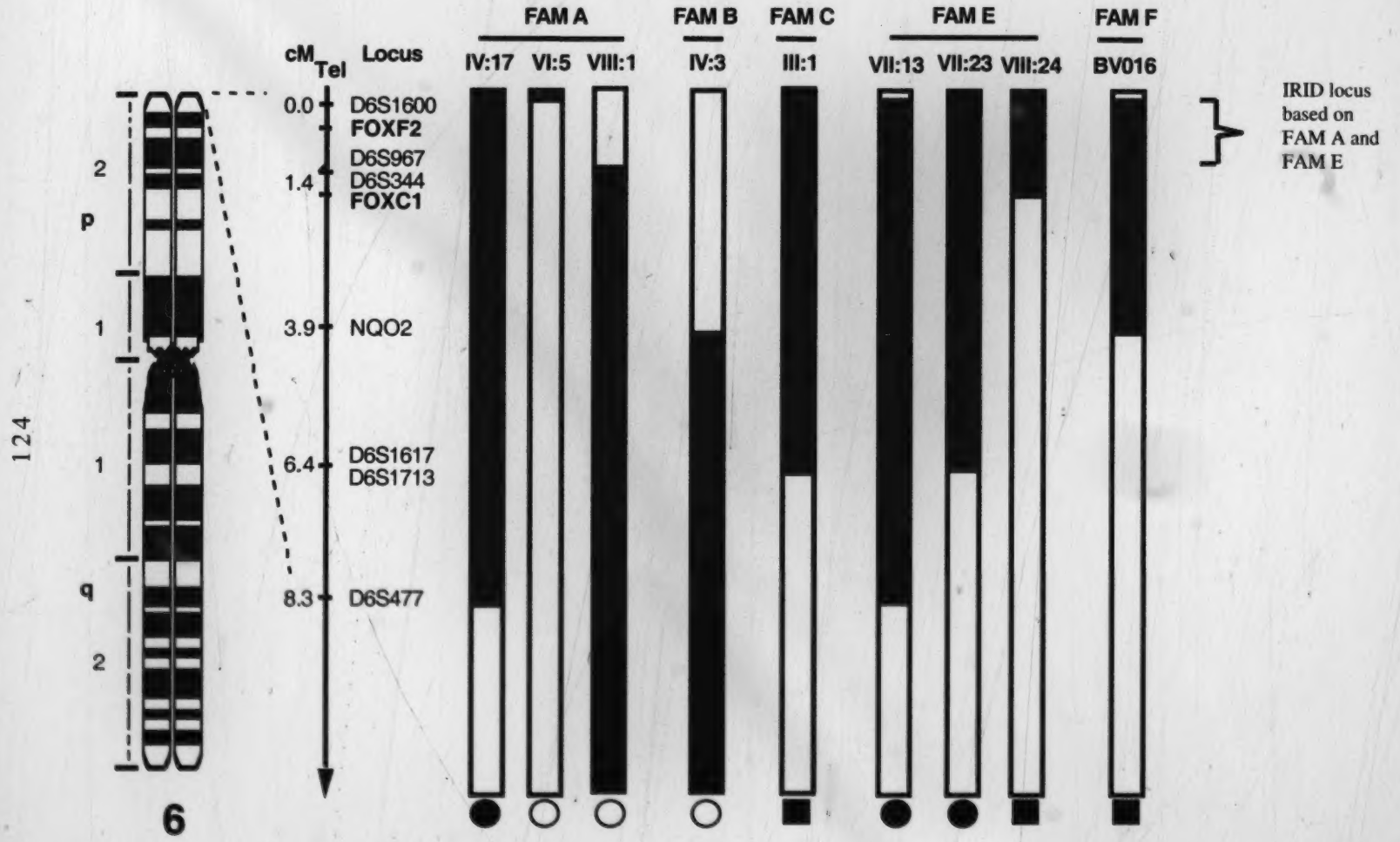
FAM A
FAM B
FAM C
FAM E
FAM F
cM
Tel
Locus
IV:17
VI:5
VIII:1
IV:3
III:1
VII:13
VII:23
VIII:24
BV016
0.0
D6S1600
FOXF2
D6S967
1.4
D6S344
FOXC1
3.9
NQO2
6.4
D6S1617
D6S1713
8.3
D6S477
IRID locus based on FAM A and FAM E
p
q
2
1
1
2
6

coding sequence and the intron/exon boundaries (Table 3-1). I empirically determined the conditions used to amplify genomic DNA from affected members from Families A, B, E, and F. The conditions appear in Table 3-1. PCR was performed with 20mM Tris-HCl, 50mM KCl, 1.5mM $MgCl_2$, 200$\mu$M each of dCTP, dTTP, dATP, and dGTP, and 60ng of each primer. Dimethyl sulfoxide (DMSO) was added to the reactions to alleviate secondary-structure problems created by the high GC content of *FOXF2*. Each reaction was overlaid with light mineral oil to prevent evaporation. A "hot start" step was used in which samples were subjected to a denaturing step of 5 minutes at 96°C, during which time 1 unit of *Taq* DNA polymerase and sufficient water were added to produce a final total reaction volume of 25$\mu$L. The reactions consisted of 35 cycles of denaturing at 94°C for 30 seconds, annealing at the primer specific temperature for 30 seconds, extension at 72°C for 30 seconds and a final elongation step of 72°C for 5 minutes. PCR products were size separated on 1% agarose gels to ensure a single product was amplified. PCR products were then excised from the gel and purified with QIAquick columns (QIAGEN) and then were directly sequenced via $^{33}P$ cycle sequencing (Amersham). Sequencing reactions were size-separated on gels of 6% acrylamide and 7M urea prior to drying and used for autoradiography.

**TABLE 3-1. *FOXF2* primer sequences and conditions.**

| Primer Name | Primer Sequence (5′-3′) | Product Size (bp) | Conditions |
|---|---|---|---|
| Primer 2F | AGAGGAGCTGAGGGAGGC | 675 | 5% DMSO @ 61°C |
| Primer 2R | TCGTTGAGCGAGAGATTGTG | | |
| Primer 3F | GAGTTCATGTTCGAGGAGGG | 461 | 5% DMSO @ 57°C |
| Primer 3R | GTGTAGGGAGAGTGGCATT | | |
| Primer 4F | TACTCGTACATCGCGCTCAT | 377 | 5% DMSO @ 57°C |
| Primer 4R | CTGGAAGTCGAAGCCCTG | | |
| Primer 5F | ACCCGGGTTCCACCTACAT | 450 | 5% DMSO @ 57°C |
| Primer 5R | GCCCTCAGACCTCCTAGCTT | | |
| Primer 6F | GGGTCCCAGATGACCACC | 202 | 5% DMSO @ 60°C |
| Primer 6R | AATTGGAGGAGGACGAGGA | | |
| Primer 7F | GCACAGCAGCACCTTTTGTA | 352 | 5% DMSO @ 57°C |
| Primer 7R | GTGCATGTGACTTGAATCCGT | | |

**ii) Single-Strand Conformation Polymorphism (SSCP)**

SSCP analysis was conducted using direct incorporation of $^{35}$S-dATP into the 6F/6R PCR product as described in Chapter 2. The products were subjected to electrophoresis on 6% acrylamide gels under nondenaturing conditions at 4°C. The gel was dried and used for autoradiography.

## C) RESULTS

The sequencing of the coding region in Families A, B, E, and F, did not reveal any disease-causing mutations. Three polymorphisms were identified. The polymorphisms and their relative positions in the gene are indicated on Figure 3-2. The first polymorphism is an A33del alteration. The published sequence has nine GCC trinucleotide repeats that code for a polyalanine stretch in the protein. Affected members from Families A, B, and E were homozygous for nine repeats. The affected member from Family F that was sequenced was determined to be heterozygous with one allele having eight repeats and one allele having nine repeats.

**FIGURE 3-2. Schematic of *FOXF2* gene.**

The coding region of the *FOXF2* gene is indicated with open boxes. The Forkhead box is indicated with shading. The intron is indicated with a dashed line. 5'UTR and 3'UTR are indicated as thick black lines. The relative positions of three observed sequence alterations are indicated above the coding region.

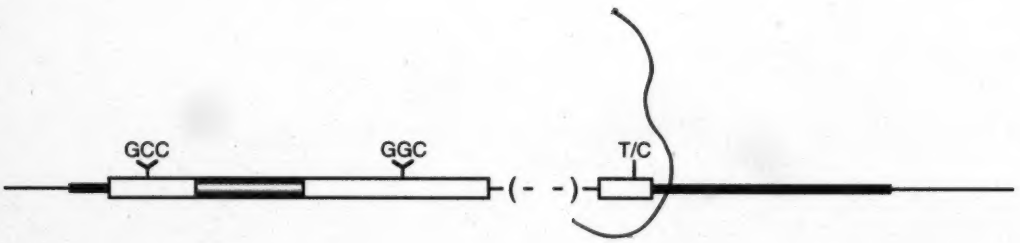
GCC
GGC
T/C
(- -)

Examination of the inheritance pattern of this sequence alteration in the family demonstrated that the alteration did not segregate with the disease. This is evidence that the alteration is a polymorphism and not a disease-causing mutation.

The second polymorphism, G302del, was also found in a trinucleotide repeat. Affected members of Families E and F are homozygous for five repeats of a GGC trinucleotide repeat that codes for a polyglycine stretch in the FOXF2 protein (the protein actually has a stretch of six glycine residues however the first is not coded by GGC). Affected members from Families A and B, were heterozygous with alleles of four and five repeats. This polymorphism was tested by SSCP analysis in 20 normals. The allele frequencies were 57.5% (23/40) for the $GGC_{(5)}$ allele, and 42.5% (17/40) for the $GGC_{(4)}$ allele.

The final polymorphism is a T1284C single nucleotide polymorphism in the second exon. The alteration was observed in a heterozygous state in Families A, B, and F. The single nucleotide change is a T to C at the third position of a tyrosine codon. This is a silent alteration that does not change the amino acid encoded. As silent substitutions are not likely to be disease-causing mutations, an allele frequency in a sample of controls was not calculated.

## D) DISCUSSION

*FOXF2* is both a positional and functional candidate gene for AR malformations that map to chromosome 6p25. *FOXF2* lies within the critical interval determined by familial linkage analysis. Secondly, mutations in a paralogous gene *FOXC1* has been shown to cause AR malformations. Primers were generated to span the whole coding sequence and the intron/exon boundaries of this two exon gene. Families with AR malformations that map to 6p25 and do not have mutations within the *FOXC1* gene were screened by direct sequence analysis. No disease-causing mutations were found, however three polymorphisms were identified. I conclude that *FOXF2* mutations do not cause AR malformations in these families.

**E) REFERENCES**

1) Blixt A, Mahlapuu M, Bjursell C, Darnfors C, Johannesson T, Enerback S, Carlsson P (1998) The two-exon gene of the human forkhead transcription factor FREAC-2 (FKHL6) is located at 6p25.3. Genomics 53:387-90.

2) Hong HK, Lass JH, Chakravarti A (1999) Pleiotropic skeletal and ocular phenotypes of the mouse mutation congenital hydrocephalus (ch/Mf1) arise from a winged helix/forkhead transcriptionfactor gene. Hum Mol Genet 8:625-37.

3) Jordan T, Ebenezer N, Manners R, McGill J, Bhattacharya S (1997) Familial glaucoma iridogoniodysplasia maps to a 6p25 region implicated in primary congenital glaucoma and iridogoniodysgenesis anomaly. Am J Hum Genet 61:882-8.

4) Kume T, Deng KY, Winfrey V, Gould DB, Walter MA, Hogan BL (1998) The forkhead/winged helix gene Mf1 is disrupted in the pleiotropic mouse mutation congenital hydrocephalus. Cell 93:985-96.

5) Larsson C, Hellqvist M, Pierrou S, White I, Enerback S, Carlsson P (1995) Chromosomal localization of six human forkhead genes, freac-1 (FKHL5), - 3 (FKHL7), -4 (FKHL8), -5 (FKHL9), -6 (FKHL10), and -8 (FKHL12). Genomics 30:464-9.

6) Lehmann OJ, Ebenezer ND, Jordan T, Fox M, Ocaka L, Payne A, Leroy BP, et al (2000) Chromosomal duplication involving the forkhead transcription factor gene FOXC1 causes iris hypoplasia and glaucoma. Am J Hum Genet 67:1129-35.

7) Mears AJ, Jordan T, Mirzayans F, Dubois S, Kume T, Parlee M, Ritch R, et al (1998) Mutations of the forkhead/winged-helix gene, FKHL7, in patients with Axenfeld-Rieger anomaly. Am J Hum Genet 63:1316-28.

8) Mirzayans F, Gould DB, Heon E, Billingsley GD, Cheung JC, Mears AJ, Walter MA (2000) Axenfeld-Rieger syndrome resulting from mutation of the FKHL7 gene on chromosome 6p25. Eur J Hum Genet 8:71-4.

9) Morissette J, Falardeau P, Dubois S, Bergeron J, Vonvk P, Cote G, Anctil J-P, et al (1997) A common gene for developmental and

familial open-angle glaucomas confined on chromosome 6p25. Am J Hum Genet Supplement:A286.

10) Nishimura DY, Searby CC, Alward WL, Walton D, Craig JE, Mackey DA, Kawase K, et al (2001) A Spectrum of FOXC1 Mutations Suggests Gene Dosage as a Mechanism for Developmental Defects of the Anterior Chamber of the Eye. Am J Hum Genet 68:364-372.

11) Nishimura DY, Swiderski RE, Alward WL, Searby CC, Patil SR, Bennet SR, Kanis AB, et al (1998) The forkhead transcription factor gene FKHL7 is responsible for glaucoma phenotypes which map to 6p25. Nat Genet 19:140-7.

12) Smith RS, Zabaleta A, Kume T, Savinova OV, Kidson SH, Martin JE, Nishimura DY, et al (2000) Haploinsufficiency of the transcription factors FOXC1 and FOXC2 results in aberrant ocular development. Hum Mol Genet 9:1021-32.

# CHAPTER FOUR

# *BARX1* AS A CANDIDATE GENE FOR AXENFELD-RIEGER MALFORMATIONS

The majority of this chapter has been previously published in:

Gould DB, and Walter MA (2000). Cloning, characterization, localization, and mutational screening of the human BARX1 gene. Genomics 68(3):336-342.

## A) INTRODUCTION

A second and more indirect method of identifying candidate genes is to examine genes in regions of conserved synteny with the mouse. Genes known in mice that map to regions with conserved synteny to a given critical interval of a trait, are potentially positional candidates for the trait. The human orthologues of murine positional or functional candidate genes must first be mapped in humans to determine if they are located within the critical interval. Finally, a mutation screen can determine if mutations in this gene cause the disease of interest.

A region on mouse chromosome 13 (from 9.00cM to 31.00cM) has conserved synteny to human chromosome 6p. A homeobox-containing gene, *Barx1*, is located on mouse chromosome 13 (21.00cM) and flanked by regions with conserved synteny to human chromosome 6p25. Based on this conserved synteny, I decided to clone, map, and determine the expression pattern of the human *BARX1* gene. I then screened *BARX1* for mutations in patients with AR malformations.

The Bar subclass of homeodomain-containing proteins was first identified with the cloning of the *BarH1* and *BarH2* genes as the duplicated genes underlying the *Bar* phenotype in *Drosophila*

*melanogaster* and the *Om(1D)* phenotype in *Drosophila ananassae*, (Higashijima et al. 1992; Kojima et al. 1991). Both *BarH1* and *BarH2* contain a novel change at a previously invariant amino acid residue within the highly conserved homeodomain. All other known metazoan homeodomain proteins have a phenylalanine at position 49 of the 60 amino acid homeodomain, however *BarH1* and *BarH2* have a tyrosine residue at this position.

Higashijima and co-workers demonstrated that *BarH1* and *BarH2* are required for ommatidia development during the third instar larva stage and are specifically coexpressed in R1/R6 photoreceptors and later in pigment cells (Higashijima et al. 1992). It was later concluded that *BarH1* and *BarH2* are also functionally redundant, and act as a homeotic switch between fates of two different types of sensory neurons (Higashijima et al. 1992). In 1993 Kojima and co-workers demonstrated that the *Bar* phenotype in *D. melanogaster* can be caused by the over expression of *BarH1* and *BarH2* at third instar larva stage, by suppressing the progression of the morphogenetic furrow as it traverses the eye disc epithelium from posterior to anterior, and also by inhibiting the re-initiation of normal ommatidal differentiation (Kojima et al. 1993).

The known expression pattern of the *Bar* genes in *Drosophila* was subsequently shown to include photoreceptors and glial cells

and neurons of external sensory organs to include the developing notum (Sato et al. 1999). Bar expression boundaries were observed to be determined by the expression boundaries of two secreted factors, *Decapentaplegic* and *Wingless*.

The first vertebrate member of the Bar homeodomain subclass, *Barx1*, was cloned from mice by its ability to bind sequence found in the *Ncam* promoter (Tissier-Seta et al. 1995). *Barx1* shares the hallmark tyrosine at position 49 of the homeodomain, however, it shows only 61% and 62% identity to the *BarH1* and *BarH2* homeodomains respectively. Mouse *Barx1* shows higher overall homology to a hydra homeobox gene, *Cnox3*, with which it shares an atypical valine residue at position 7 of the homeodomain as well as the characteristic tyrosine at position 49 (Tissier-Seta et al. 1995). Expression of the mouse *Barx1* was observed most notably in craniofacial mesenchyme as well as in the developing stomach and at low levels in the proximal region of the forelimbs and the hindlimbs. Of particular note was the dynamic expression in the developing molars and absence of expression in developing incisors (Tissier-Seta et al. 1995).

Chick *Barx1* was cloned from a stage 24 head, cDNA library (Barlow et al. 1999). The chick *Barx1* amino acid sequence is identical to the mouse over the 60 residue homeodomain and 93%

identical overall. Expression of the chick *Barx1* is similar to the expression observed of the mouse *Barx1*, with the major domains of expression being in the developing stomach, branchial arches, and the proximal limb buds. Unlike the mouse *Barx1*, chick *Barx1* expression was observed in epithelium of the maxillary and mandibular primordia and of the frontonasal mass.

A second mouse *Barx* gene, *Barx2*, has been cloned (Jones et al. 1997). An identical 17 amino acid residue stretch was identified between mouse *Barx1* and mouse *Barx2* that lies 8 and 7 amino acids 3' of the respective homeodomains (Jones et al. 1997). The chick *Barx1* is identical at 16 of the 17 amino acids in this region (Jones et al. 1997). The human *BARX2* gene has recently been cloned (Hjalt and Murray 1999). *BARX2* has 100% identity within the homeodomain to mouse *Barx2* and chick *Barx2b* and 87% identity to the homeodomains of mouse and chick *Barx1* genes.

Other members of the Bar subclass of homeodomain proteins have also been cloned in rat, *MBH1* (Saito et al. 1998); Xenopus *Xbr-1*, and *XBH1*, *XBH2* (Papalopulu and Kintner 1996; Patterson et al. 2000); and chick, *Barx2b*, (Smith and Tabin 1999). *BARX1* is the third member of this class of proteins characterized in humans (*BARX2* and *BARHL1* were previously identified). Based on the role of *Bar* genes in eye development in *Drosophila*, the expression

pattern of murine *Barx1* in craniofacial mesenchyme, and the location of murine *Barx1* to a region of conserved synteny to human 6p25, I considered the human *BARX1* gene to be a candidate gene for AR malformations.

## B) MATERIALS AND METHODS

### i) Screening of cDNA library by hybridization.

A tentative human contig (THC219746) from the TIGR database was identified with homology to the published mouse *Barx1* sequence. Primer sets F and G (Figure 4-1 and Table 4-1) were used to amplify products in a human fetal craniofacial cDNA λZAPII phage library received from Dr. Jeff Murray. Bacterial cells were transfected with the bacteriophage library and plated. Plaques were then transferred to Hybond N nylon membrane by briefly placing the membrane on the surface of the bacterial lawn then sequentially soaking for 7 minutes in each of denaturing solution (0.5M NaOH, 1.5M NaCl), neutralizing solution (1.5M NaCl, 0.5M Tris, pH 7.5) and rinsing solution (2X SSC). Membranes were dried at room temperature then baked for 3 hours at 80°C before prehybridization. Prehybridization was performed with 15 mL of hybridization solution (Church and Gilbert 1984) for 3 hours at 65°C.

**FIGURE 4-1. Schematic of the human *BARX1*.**

Large boxes indicate *BARX1* exons. Thin lines indicate intronic sequences and are not to scale. Intronic sizes are indicated above the thin lines. The 5' and 3' UTRs are indicated by diagonal shading. The homeobox is indicated by black boxes. Vertical arrows at the top indicate the position and nucleotide change in all sequence alterations, and the effect on the amino acid appears in brackets for the two coding sequence alterations identified. Vertical arrows at the bottom indicate the positions of the upstream in-frame stop, the predicted start methionine and the predicted stop codon. Horizontal arrows indicate the relative locations of primer pairs A through G. The thick black line indicates the fragment of BARX1 used to probe Northern blots. Taken from Gould and Walter 2000.

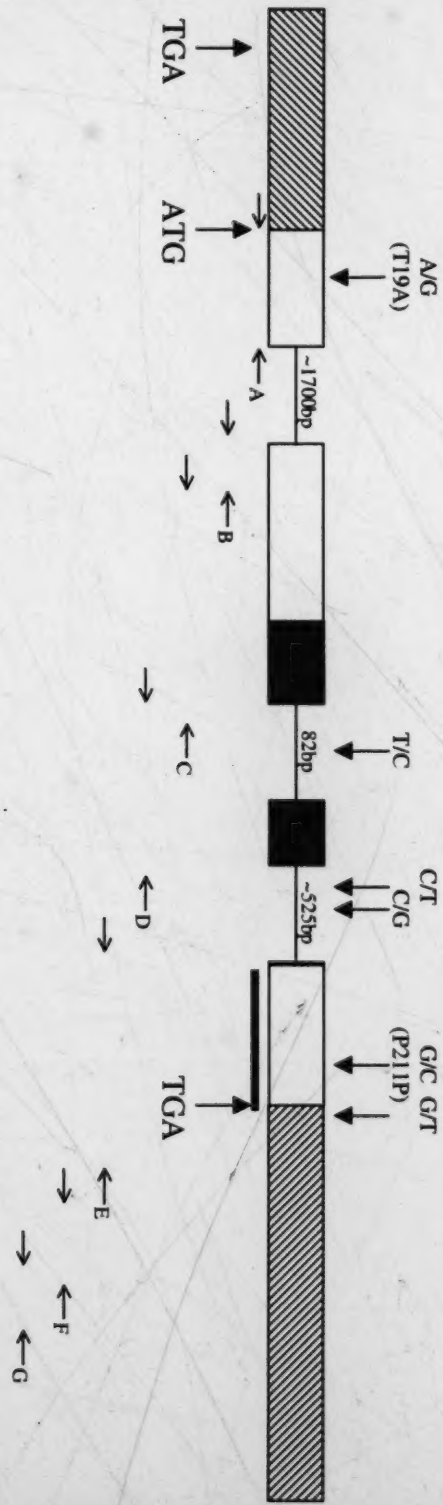
TGA
ATG
A/G
(T19A)
~1700bp
A
B
C
82bp
T/C
D
C/T
C/G
~525bp
G/C G/T
(P21P)
TGA
E
F
G

**Table 4-1 Primer Pairs Used to PCR Amplify BARX1**

| Primer Set | Primer Oligonucleotide (5'-3') | | Product Size (bp) | Annealing Temperature (°C) |
|---|---|---|---|---|
| | Forward | Reverse | | |
| A | gcagcctatcgcagcttc | ttcagctcgctgtctccc | 211 | 59 |
| B | gtagctcacccgggtcct | CAGCAACGCAGAGCTCAG | 119 | 59 |
| C | GTGTTCAAGTTCCCACTG | aaggcaagtgaccacactgg | 321 | 56-53* |
| D | CAGAAGTACCTTTCCACG | aaggccttagtggggagaaa | 287 | 56-53* |
| E | cctcatatggaccctgcact | gtaaacttcttggacgcgga | 370 | 60-58* |
| F | tccgcgtccaagaagtttac | agtctcccaggttagagccc | 137 | 58 |
| G | caaacggaaggacacagacc | acggagctcagggtagagac | 117 | 58 |

Primers from non-coding regions are shown in lower case.
* Indicates touchdown conditions

Hybridization was done with 15 mL of fresh hybridization solution overnight at 65°C. Post hybridization washes were done with 2XSSC, 0.2%SDS for 45 minutes at 65°C. Membranes were hybridized with the PCR product of primer pair F that had been isolated from a 1% agarose gel using the QIAquick gel extraction protocol (Qiagen, Mississauga, Ontario, Canada) and $^{32}P$ dCTP-labeled using a random priming DNA labeling kit (GibcoBRL, Gaithersburg, MD, USA), followed by nucleotide removal using the Qiagen nucleotide removal protocol. Plaques that were positive by hybridization were picked and placed in 0.5 mL of SM buffer with 2.3 mg/mL chloramphenicol and re-plated on 100mm plates. The hybridizations were then repeated. Positive plaques from secondary plates were converted to pBluescript phagemids from the λZAPII phage using the Stratagene (La Jolla, CA, USA) *in vivo* excision protocol.

**ii) Characterization of the BARX1 gene.**

Sequence analysis of the *BARX1* cDNA was carried out using a $^{33}P$ dideoxy terminator sequencing kit (Amersham Pharmacia Biotech Baie d'Urfe, QB, Canada). Fragments used for sequence analysis were amplified (as described in Chapter 3) using primers and conditions listed in Table 4-1 prior to separation on a 1% agarose

gel and isolation by QIAquick cleaning of amplification products. Amplification reactions using primer pairs with "touchdown" conditions were carried out for 5 cycles at the high annealing temperature followed by 30 cycles at the low annealing temperature. All other amplification reactions were conducted for 30 cycles at the specified annealing temperature (Table 4-1). Cycle sequencing was carried out according to manufacturer's recommendations using dGTP terminator master mix. In the event that sequence compressions were observed, reactions were repeated with dITP termination mix. All dGTP sequencing reactions were size-separated on gels of 6% acrylamide (19:1; acrylamide:bis), 7 M urea, and dITP sequencing reactions were either size-separated on these gels or gels including 30% formamide. Formamide gels were treated with 20% methanol, 5% acetic acid prior to drying. The *BARX1* exon/intron boundaries were identified by sequence differences between genomic and cDNA sequence following observed differences in amplification product size. Start and stop codons were identified by analysis of the raw sequence in all possible open reading frames with GeneWorks 2.2.1 (IntelliGenetics Inc.). The *BARX1* cDNA sequence has been deposited in Genbank (accession number AF213356).

**iii) Northern blot analysis.**

A 709 bp *Pst* I fragment (Figure 4-1) corresponding to exon four of *BARX1* and containing no homeobox sequence was size-separated on a 1% agarose gel, isolated and $^{32}$P-dCTP labeled using a random priming DNA labeling kit as described previously. The fragment was isolated from the pBluescript vector and therefore also includes 15 nucleotides of vector sequence at the 3' end. Hybridization to three commercially available Northern blots (Human Multiple Tissue Northern Blot, Human Multiple Tissue Northern Blot II, and Human Fetal Multiple Tissue Northern Blot II), (Clontech, Palo Alto, CA) was performed. ExpressHyb solution (Clontech) was used for prehybridization (68°C for 30 minutes) and hybridization (68°C for one hour) prior to washing with 2XSSC, 0.1%SDS (50°C for 45 minutes). Biomax film (Kodak, Rochester, NY, USA) was then exposed to the Northern blots for a minimum of 16 hours. ß-actin was used as an RNA loading control according to manufacturer's recommendations (Clontech).

**iiii) Radiation Hybrid mapping of BARX1.**

The GeneBridge 4 radiation hybrid panel (Research Genetics, AL, USA) was screened with primer pair C (Table 4-1) to determine the chromosomal localization of *BARX1*. The PCR products were

analyzed by electrophoresis on 3% agarose gels and scored according to manufacturer's recommendations and submitted for interpretation to http:/www-genome.wi.mit.edu/. To confirm these results primers were tested on a human chromosome 9q cell line (GM64063) and products were size-separated on a 1% agarose gel.

**iiiii) Mutation Analysis in Patients.**

DNA was obtained from 55 patients with various ocular malformations. Thirty-six patients had Axenfeld-Rieger, 17 patients had Iridogoniodysgenesis, one patient had Peters' anomaly and one patient had congenital hereditary endothelial dystrophy. The entire *BARX1* coding region, including all intron/exon boundaries, were amplified and screened for mutations using primer pairs and conditions in Table 4-1 (primer pairs A-E). For primer sets A,B,C, and D, mutational analysis was conducted by SSCP using direct incorporation of $^{35}S$ dATP as described in Chapter 2. Products were subjected to electrophoresis on 6% acrylamide gels under non-denaturing conditions at 4°C. Biomax film (Kodak) was then exposed for a minimum of 16 hours. For primer set E, products were amplified, separated on 1% agarose and isolated with Qiagen columns as described above. Products were then sequenced directly using fluorescent forward and reverse primers (LI-COR, Lincoln, NE,

USA) and a thermo sequenase fluorescent primer cycle sequencing kit (Amersham Pharmacia Biotech). Products were analyzed on a LI-COR 4200 DNA sequencer. The re-sequencing of any ambiguities was confirmed by manual $^{33}P$ dideoxy terminator sequencing.

## C) RESULTS

### i) Cloning *BARX1*

Sequence from the murine *Barx1* gene was used *in silico* to identify a human THC (THC219746). Primer pairs F and G (Table 4-1) were generated from the THC and used to determine the expression profile by amplification of eight cDNA libraries. An amplification product was obtained in a human fetal craniofacial library and an adult human iris library but not in lymphoblast, fibroblast, choroid/retina, retinal pigment epithelium, kidney or fetal liver (data not shown). A human craniofacial cDNA library was subsequently screened to identify the human *BARX1* cDNA. A positive clone, by hybridization with the *BARX1* primer set F PCR product, was isolated. The sequence of the *BARX1* cDNA was determined and compared to the sequences of other known genes of the Bar subclass (Figure 4-2a and Figure 4-2b).

**FIGURE 4-2. Alignments of predicted human BARX1 protein sequence with protein sequence of related Bar class genes.**

**(A)** The full-length human BARX1 predicted protein sequence aligned with the partial predicted protein sequences of chick Barx1 and mouse Barx1. Identities are shown by dashes and differences are indicated by what the amino acid is in the chick or mouse sequence. The homeodomain is indicated by a box. The polyalanine tract is underlined. The potential nuclear localization sequence is indicated by a line above the sequence. The 17 amino acid stretch conserved in Barx genes is indicated by bold type.

**(B)** Sequence of the human BARX1 homeodomain aligned with the homeodomains of 7 related Bar class homeodomains. Identities are shown as dashes and differences are indicated by the amino acid that appears at this position in the other sequence. Amino acid sequence identity to the human sequence for the homeodomain is indicated as a percent following each sequence. Taken from Gould and Walter 2000.

**A**

```
      1          15 16          30 31          45 46          60 61          75 76          90
Human MIEEILTEPPGPKGA APATAAAAAGELLKF GVQALLAARPFHSHL AVLKAEQAAVFKFPL APLGCSGLSSALLAA GPGLPGAAGAPHLPL
Chick                ANERPP-SCSSS -CRRCCRPG-Y---- --------------- --------G------ ---M--P---S----
Mouse                             SAYRRCWPPGPY--- --------------- --------G------ ---M--P---S----

      91         105 106        120 121        135 136        150 151        165 166        180
Human ELHVRGKLEAAGPGE PGTKAKKGRRSRTVF TELQLMGLEKRFEKQ KYLSTPDRIDLAESL GLSQLQVKTWYQNRR MKWKKIVLQGGGLES
Chick --QL--------S-- --S---------- --------------- --------------- --------------- ---------------
Mouse --QL--------S-- --A---------- --------------- --------------- --------------- ---------------

      181        195 196        210 211        225
Human PTKPKGRPKKNSIPT SEQLTEQERAKDAEK PAEVPGEPSDRSRED
Chick --------------S ----S------ET-- -P-S-----ERQQ-E
Mouse ---------------- ----------ET-- -A-T-------NC--
```

150

**B**

```
Human BARX1          GRRSRTVFTELQLMGLEKRFEKQKYLSTPDRIDLAESLGLSQLQVKTWYQNRRMKWKKIV
Chick Barx1          ------------------------------------------------------------    100%
Mouse Barx1          ------------------------------------------------------------    100%
Human BARX2          P-----I----------K-Q----------L---Q----T----------------M-      87%
Chick Barx2b         P-----I----------K-Q----------L---Q----T----------------M-      87%
Mouse Barx2          P-----I----------K-Q----------L---Q----T----------------M-      87%
Drosophila BarH2     Q-KA--A--DH--QT---S--R-----VQ--ME--NK-E--DC----------T---RQT    62%
Drosophila BarH1     Q-KA--A--DH--QT---S--R-----VQE-QE--HK-D--DC----------T---RQT    60%
```

**ii) Genomic Structure of *BARX1***

Intron/exon boundaries for *BARX1* were determined by PCR amplification of genomic DNA. Amplification products that were larger in genomic than cDNA were sequenced for the presence of an intron. Three introns were found (Figure 4-1 and Table 4-2). The first and third introns were not entirely sequenced. Their sizes are approximately 1700 bp and 525 bp respectively as determined by agarose gel size-separation. The second intron is 82 bp and was fully sequenced. The sequence of the splice sites (Table 4-2) is in good agreement with published consensus sequence (Senapathy et al. 1990).

**iii) Northern Analysis of *BARX1***

The coding fragment of exon 4 of *BARX1* was used to probe five different multi-tissue Northern blots from Clontech (Figure 4-3). A transcript of approximately 1.6 Kb was observed at highest levels in testes, skeletal muscle and heart. A smaller band was also observed in pancreas however the significance of this band is not known.

**Table 4-2 Intron/Exon Boundaries for BARX1**

| Splice Donors | Splice Acceptors |
|---|---|
| EXON 1.....ACAGCCACCTGGgtacgtgtggcg.....Intron 1 | Intron 1.....ctttcttcgcagCCGTGCTGAAGG.....EXON 2 |
| EXON 2.....CACGCCGGACAGgtagggcggtac.....Intron 2 | Intron 2.....tgctctttccagAATAGATCTTCG.....EXON 3 |
| EXON 3.....TGGAAGAAAATAgtgagtgtgcct.....Intron 3 | Intron 3.....tcccccgtgcagGTGCTGCAGGGC.....EXON 4 |

Invarient bases are underlined.

**FIGURE 4-3. Autoradiographs of commercial Northern Blots probed with BARX1.**

All three membranes were hybridized with the *BARX1* probe indicated in Figure 4-3. The probe was a 709bp *Pst* I product generated by digesting the *BARX1* cDNA. Tissue of origin for RNA is listed above each lane. Size markers for RNA are listed down the left side. β-Actin was used as a loading control. The *BARX1* transcript is indicated on the right and is approximately 1.6Kb and found predominantly in testes and heart. Taken from Gould and Walter 2000.

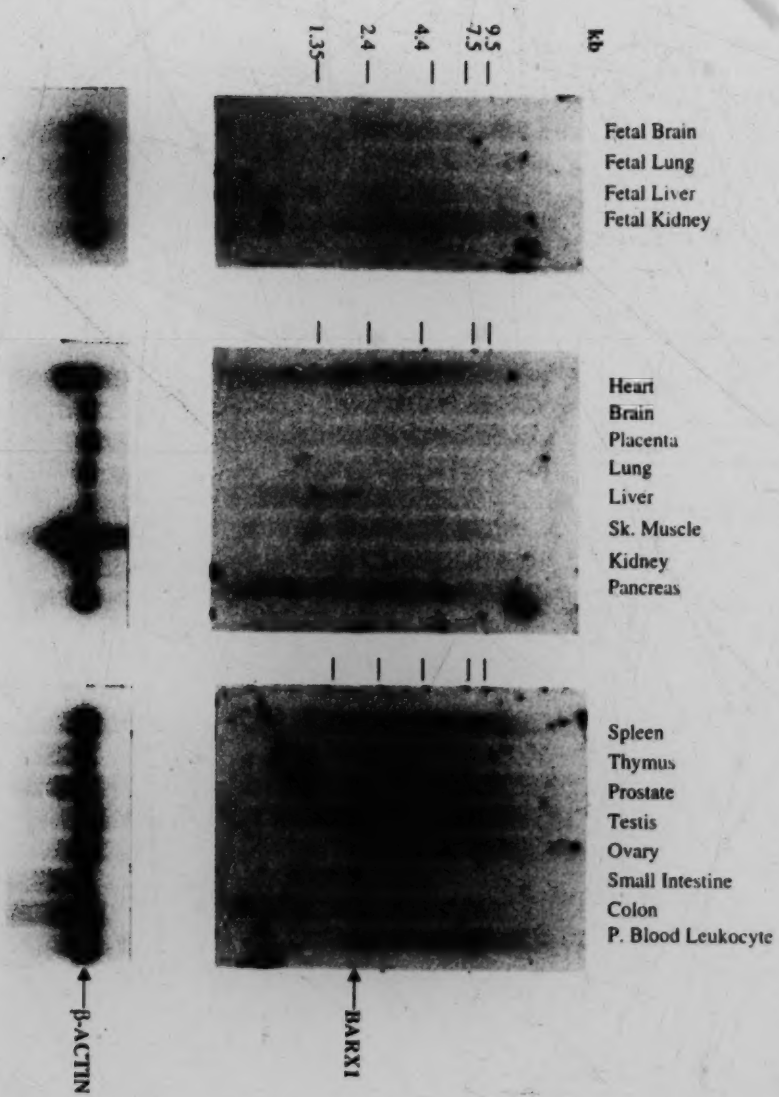
kb
9.5
7.5
4.4
2.4
1.35
Fetal Brain
Fetal Lung
Fetal Liver
Fetal Kidney
Heart
Brain
Placenta
Lung
Liver
Sk. Muscle
Kidney
Pancreas
Spleen
Thymus
Prostate
Testis
Ovary
Small Intestine
Colon
P. Blood Leukocyte
β-ACTIN
BARX1

**iiii) Chromosomal Localization of *BARX1***

Based on the location of *BARX1* to mouse chromosome 13 in a region of synteny with human chromosome 6p25, various primer sets, and combinations of sets, were used to PCR amplify a series of contiguous bacterial artificial chromosomes (BACs) and yeast artificial chromosomes (YACs) from chromosome 6p25. All results were negative (data not shown).

Primer pair C (Table 4-1) was used to amplify a human/hamster radiation hybrid panel (Research Genetics). The products were size-separated by gel electrophoresis on a 3% agarose gel and scored as present (1), absent (0) or ambiguous (2). The resulting code (010000000010000000000000010000000100000011000000010000001000100001001100000110200010122200001100 0) was submitted to the Whitehead Institute website for interpretation (http:/www.genome.wi.mit.edu). *BARX1* was localized to chromosome 9q12 between markers WI-3028 and WI-9330.

To confirm the result of the radiation hybrid mapping, primer pair C (Table 4-1) was used to amplify DNA isolated from a human/rodent somatic cell line, containing chromosome 9q as its

only human component. A positive result was observed by size separation of products on a 1% agarose gel (data not shown).

**iiiii) Mutational Analysis of *BARX1***

In light of the localization of *BARX1* to 9q12, *BARX1* was no longer a candidate gene for the AR malformations that map to 6p25. However, based on its expression pattern in developing head mesenchyme and teeth in mice, *BARX1* is still a strong candidate for AR malformations for which the genetic basis has not been mapped. To examine the possibility of *BARX1* involvement in AR malformations, DNA samples were collected from 55 patients diagnosed with ARS or other related malformations of the anterior segment of the eye. Primers were used to span all coding regions and splice sites (Figure 4-1 and Table 4-1). DNA was isolated and mutational analysis of the entire coding region and intron/exon boundaries was conducted by either SSCP (exons 1,2 and 3) or direct sequence analysis (exon 4). No disease-causing mutations were identified, however, six sequence alterations were observed (Figure 4-1 and Table 4-3).

**Table 4-3** **Sequence Alterations In BARX1**

| Nucleotide Change | Amino Acid Change | Allele Frequency (patient & control) | Position |
|---|---|---|---|
| A to G | T19A | 14% | Nucleotide 55 |
| T to C | Non-coding | .6% | 40bp 3' of intron 2 donor |
| C to T | Non-coding | 26% | 30bp 3' of intron 3 donor |
| C to G | Non-coding | .6% | 50bp 3' of intron 3 donor |
| G to C | P211P | 18% | Nucleotide 633 |
| G to T | Non-coding | 3.6% | 17bp 3' of stop codon |

## D) DISCUSSION

### i) Cloning *BARX1*

A human *BARX1* cDNA was cloned from a human fetal craniofacial library. We conclude that the 1469 bp cDNA is full length because there is an in-frame stop codon 5' of the first methionine (Figure 4-1) and there is a polyadenylated tail following the stop codon. The predicted *BARX1* protein is 226 amino acids. The putative initiation codon differs from the hypothesized initiation codon in the murine *Barx1* gene (Tissier-Seta et al. 1995) and in chick *Barx1* (Barlow et al. 1999), resulting in a larger open reading frame. The fact that the human transcript contains a single nucleotide alteration that changes the speculated mouse start methionine to a leucine is evidence that this codon may not be the start methionine in mouse. Neither the mouse nor the chick *Barx1* cDNA clones have sequence that extends 5' to include the region containing the human start codon. Mouse and chick *Barx1* do not have stop codons upstream of their putative start codons. As well, the nucleotide sequence between the three genes is highly conserved 5' of the mouse putative initiation codon. The human *BARX1* and chick *Barx1* are 91% identical through this region at a nucleotide

level. However, four reading frame changes occur between the chick *Barx1* and human *BARX1*, 3' of the human start codon. This could most easily be explained by a sequencing error in the chick *Barx1* gene due to the high G/C content in this region. Re-sequencing with dITP to address the high G/C content of the human *BARX1* gene in both directions allowed resolution of the human *BARX1* sequence. We cannot rule out that the genes are divergent at this point, however this explanation is unlikely because of the 91% identity at the nucleotide level between the human and chick *Barx1* genes in this region. Also, the human *BARX2* gene uses an analogous start codon to that of the human *BARX1* (GenBank AF171219). These data are all consistent with the use, in human, mouse, and chick, of the start codon identified in the human *BARX1* gene (Figure 4-1).

The human *BARX1* gene is identical to both the mouse and chick *Barx1* genes throughout the 60 amino acid homeodomain (Figure 4-2b). Overall, human BARX1 is 91% identical to mouse and 89% identical to chick at an amino acid level (Figure 4-2a) and 87% identical to the mouse gene and 84% identical to the chick gene at a nucleotide level. The human BARX1 also shares an identical 17 amino acid stretch 3' of the homeodomain (Figure 4-2a) with human BARX2, mouse Barx1 and Barx2, and chick Barx1 (16 of 17 residues) and Barx2b. The biological significance of this domain is not

known, however similar proline, serine threonine rich domains have been shown to be involved in protein/protein interactions of other transcription factors (Glaser et al. 1994).

BARX1 has a polyalanine stretch upstream of the homeodomain (Figure 4-2a). The mouse *Barx1* sequence does not extend far enough 5' to determine if this polyalanine tract exists and the chick Barx1 sequence also ends near this point. However, the mouse Barx2 does have a polyalanine stretch (Jones et al. 1997). In BARX1, 8 of 10 residues are alanine and in mouse Barx2, 9 of 10 residues are alanine. Mouse Barx2 has been shown to have repressor qualities (Jones et al. 1997) for which the polyalanine stretch has been implicated (Hanna-Rose and Hansen 1996).

Finally, a putative nuclear localization signal exists at the amino terminal end of the homeodomain, represented by the strongly basic hexapeptide KAKKGR (Figure 4-2a) (Boulikas 1994). The presence, in BARX1, of a homeodomain, highly conserved proline, serine, threonine domain, and the polyalanine potential repressor domain, are all consistent with human BARX1 having a role in the nucleus as a transcriptional activator, repressor or both.

**ii) Northern analysis of *BARX1***

Hybridization of *BARX1* to Northern blots revealed a 1.6 Kb band in testes, skeletal muscle and heart. This result is in good agreement with our predicted size based on the cDNA clone and provides further evidence that the cDNA isolated is the full-length *BARX1* transcript. A smaller band of unknown significance was also observed in pancreas. Additional expression data based on the results of *BARX1* PCR on 8 cDNA libraries demonstrates *BARX1* expression in fetal craniofacial tissue and human adult iris but not in lymphocytes, fibroblasts, choroid retina, retinal pigment epithelium, kidney or fetal liver (data not shown). *Barx1* expression in both mouse (Tissier-Seta et al. 1995) and chick (Barlow et al. 1999) was predominantly in the facial primordia, developing stomach and proximal limbs. Our observation of human *BARX1* in fetal craniofacial tissue is consistent with the results in mouse and chick.

**iii) Chromosomal Localization of *BARX1***

Murine *Barx1* is mapped to mouse chromosome 13 at 21 cM. Previously, a 16 cM interval on mouse chromosome 13 from 12 cM to 28 cM had uninterrupted synteny to the distal portion of the short arm of human chromosome 6 from 6p22-ter. To test the

location of human *BARX1* I first used gene specific primers to PCR amplify a series of contiguous BACs and YACs from human chromosome 6p. These results were negative indicating that the human *BARX1* gene is not located on the distal portion of human chromosome 6p (data not shown). Radiation hybrid mapping results indicated that *BARX1* maps to chromosome 9q12. To confirm this result primers were used to amplify DNA isolated from a human chromosome 9q cell line. A positive result was observed (data not shown). The mapping of *BARX1* to human chromosome 9q12 defines a new syntenic group on the mouse chromosome 13. This is the first evidence of a marker within this region of mouse chromosome 13 that is not located at human chromosome 6p.

**iiii) Mutational Analysis of *BARX1***

The mapping of *BARX1* to 9q12 precludes it from being the gene mutated in families A, B, E, and F. However, *BARX1* is a strong candidate gene for AR malformations based on its strong expression in human craniofacial tissue, human iris and in the neural crest derived craniofacial mesenchyme of the developing mouse, including in the developing tooth buds (Tissier-Seta et al. 1995). Patients with AR malformation have iris hypoplasia and other eye malformations of the eye involving tissues of neural crest origin.

Additionally, AR malformations can also be associated with craniofacial malformations and dental anomalies. There is a strong similarity between the tissues expressing *BARX1* and the tissues affected in AR malformations.

Mutational screening of the complete *BARX1* coding region, including intron/exon boundaries, did not result in the identification of any disease-causing mutations. However, six sequence alterations were observed (Figure 4-1 and Table 4-3). Four of the alterations were variants in untranslated regions. The first alteration is a T to C transition 40 bp 3' of the intron 2 splice donor. The second alteration is a C to T transition 30 bp 3' of the intron 3 splice donor. The third alteration is a C to G transversion 50 bp 3' of the intron 3 splice donor. The fourth alteration is a G to T transversion in the 3' untranslated region 17 nucleotides after the stop codon. Of the two coding sequence alterations, only one changed an amino acid. The first coding sequence alteration is an A to G transition at nucleotide 55 that causes the amino acid change T19A. This transition changes a threonine residue to an alanine residue within the polyalanine stretch described previously. This polymorphism was observed in 12 of the 55 patients screened and in 7 of 14 non-affected, control individuals (allele frequency of 14%). The facts that this alteration changes a threonine to an

alanine in a polyalanine stretch, and the appearance of this sequence change in unaffected control individuals, are evidence that the alteration is a polymorphism and not a disease-causing mutation. The second coding polymorphism is a G to C transversion at nucleotide 633. This is a silent change that does not affect the proline translated by this codon. Sixteen of the 55 patients screened were heterozygous and two of the patients were homozygous for the G633C allele (allele frequency of 18%).

None of the observed changes are likely to be etiological. The only coding nucleotide alteration that causes an amino acid change was also observed in unaffected controls. Of the four non-coding nucleotide alterations only the C/T in intron 3 was observed in unaffected controls. We conclude that the intronic T/C and C/G *BARX1* alterations are rare variants that did not appear in normal controls. Due to the location of these alterations within introns, and that they do not make cryptic splice sites, they are not likely etiological although this has not been ruled out. The G/T in the 3' UTR appeared in four affected individuals. This alteration is also non-coding and does not make a cryptic splice site and therefore is not likely to be etiological. Because it is highly unlikely that this alteration is etiological, this alteration was not tested in unaffected controls.

In this chapter, I report the cloning of the human *BARX1* gene and determination of its genomic structure. *BARX1* was localized to 9q12 by radiation mapping and identifies a new region of conserved synteny on mouse chromosome 13. Northern analysis indicates *BARX1* expression in testes, skeletal muscle, and heart and PCR amplification of cDNA libraries shows expression in iris and craniofacial tissues. The failure to identify *BARX1* disease-causing mutations in 55 patients with anterior segment ocular malformations suggests that *BARX1* may not be involved in these disorders. The only human disease mapped to 9q12 to date is hypomagnesemia with secondary hypocalcemia and *BARX1* is not an obvious candidate for this disease. *BARX1*, however, remains a strong candidate for unmapped disorders involving tooth and jaw development. Further identification of Bar class homeobox genes will increase our understanding of these developmental pathways and possibly elucidate the role of *BARX1*.

**E) REFERENCES**

1) Barlow AJ, Bogardi JP, Ladher R, Francis-West PH (1999) Expression of chick Barx-1 and its differential regulation by FGF-8 and BMP signaling in the maxillary primordia. Dev Dyn 214:291-302.

2) Boulikas T (1994) Putative nuclear localization signals (NLS) in protein transcription factors. J Cell Biochem 55:32-58.

3) Church GM, Gilbert W (1984) Genomic sequencing. Proc Natl Acad Sci U S A 81:1991-5.

4) Glaser T, Jepeal L, Edwards JG, Young SR, Favor J, Maas RL (1994) PAX6 gene dosage effect in a family with congenital cataracts, aniridia, anophthalmia and central nervous system defects. Nat Genet 7:463-71.

5) Gould DB, Walter MA (2000) Cloning, characterization, localization, and mutational screening of the human BARX1 gene. Genomics 68:336-42.

6) Hanna-Rose W, Hansen U (1996) Active repression mechanisms of eukaryotic transcription repressors. Trends Genet 12:229-34.

7) Higashijima S, Kojima T, Michiue T, Ishimaru S, Emori Y, Saigo K (1992) Dual Bar homeo box genes of Drosophila required in two photoreceptor cells, R1 and R6, and primary pigment cells for normal eye development. Genes Dev 6:50-60.

8) Hjalt TA, Murray JC (1999) The human BARX2 gene: genomic structure, chromosomal localization, and single nucleotide polymorphisms. Genomics 62:456-9.

9) Jones FS, Kioussi C, Copertino DW, Kallunki P, Holst BD, Edelman GM (1997) Barx2, a new homeobox gene of the Bar class, is expressed in neural and craniofacial structures during development. Proc Natl Acad Sci U S A 94:2632-7.

10) Kojima T, Ishimaru S, Higashijima S, Takayama E, Akimaru H, Sone M, Emori Y, et al (1991) Identification of a different-type homeobox gene, BarH1, possibly causing Bar (B) and Om(1D) mutations in Drosophila. Proc Natl Acad Sci U S A 88:4343-7.

11) Kojima T, Sone M, Michiue T, Saigo K (1993) Mechanism of induction of Bar-like eye malformation by transient overexpression of Bar homeobox genes in Drosophila melanogaster. Genetica 88:85-91.

12) Papalopulu N, Kintner C (1996) A Xenopus gene, Xbr-1, defines a novel class of homeobox genes and is expressed in the dorsal ciliary margin of the eye. Dev Biol 174:104-14.

13) Patterson KD, Cleaver O, Gerber WV, White FG, Krieg PA (2000) Distinct expression patterns for two Xenopus Bar homeobox genes. Dev Genes Evol 210:140-144.

14) Saito T, Sawamoto K, Okano H, Anderson DJ, Mikoshiba K (1998) Mammalian BarH homologue is a potential regulator of neural bHLH genes. Dev Biol 199:216-25.

15) Sato M, Kojima T, Michiue T, Saigo K (1999) Bar homeobox genes are latitudinal prepattern genes in the developing Drosophila notum whose expression is regulated by the concerted functions of decapentaplegic and wingless. Development 126:1457-66.

16) Senapathy P, Shapiro MB, Harris NL (1990) Splice junctions, branch point sites, and exons: sequence statistics, identification, and applications to genome project. Methods Enzymol 183:252-78.

17) Smith DM, Tabin CJ (1999) Chick Barx2b, a marker for myogenic cells also expressed in branchial arches and neural structures. Mech Dev 80:203-6.

18) Tissier-Seta JP, Mucchielli ML, Mark M, Mattei MG, Goridis C, Brunet JF (1995) Barx1, a new mouse homeodomain transcription factor expressed in cranio- facial ectomesenchyme and the stomach. Mech Dev 51:3-15.

# CHAPTER FIVE

# CHARACTERIZATION OF EIGHT PATIENTS WITH TERMINAL DELETIONS OF CHROMOSOME 6p25

The majority of this chapter has been taken from the manuscript:

Gould DB, Mirzayans F, Jaafar MS, Tetteyfio GA, Addison MK, Powell CM, MacDonald IM, Munier F, Ritch R, and Walter MA (2001). Characterization of eight patients with terminal deletions of chromosome 6p25 and identification of a possible locus for deafness. Human Genetics. Submitted.

Portions of this chapter have been previously published in:

Kume T, Deng KY, Winfrey V, Gould DB, Walter MA, and Hogan BL (1998). The forkhead/winged helix gene Mf1 is disrupted in the pleiotropic mouse mutation congenital hydrocephalus. Cell 93(6):985-96.

## A) INTRODUCTION

Analysis of patients with deletions of the terminal portion of the short arm of chromosome 6 is the third method I employed to identify genes at 6p25 involved in AR malformations. The goal is to characterize, at a molecular level, the extent of the deletion in each patient. By comparing the extent of the deletion in each patient to the clinical features present in each patient one hopes to be able to draw phenotype/genotype correlations. If correlations exist, it is possible to infer the location of the genes responsible for the clinical features with which the patients present.

Ocular malformations are just one of the possible phenotypic consequences of having a deletion of 6p25. As a result, the molecular characterization of the deletions in these patients is really the characterization of a contiguous gene syndrome rather than the simple mapping of an ocular malformation locus. The growing number of patients with deletions of 6p25 is useful to both describe the 6p25 deletion syndrome, and to map with greater accuracy the loci in this region that, when deleted, have phenotypic consequences. To date, thirty-three patients have been described with deletions of the short arm of chromosome 6, excluding ring

chromosomes or products of unbalanced translocations. Twenty six of these patients have terminal deletions (Alashari et al. 1995; D'Alessandro et al. 1992; Davies et al. 1999a; Davies et al. 1999b; Davies et al. 1995; Guillen-Navarro et al. 1997; Jalal et al. 1989; Kormann-Bortolotto et al. 1990; Kume et al. 1998; Law et al. 1998; Ouchi and Kasai 1982; Palmer et al. 1991; Plaja et al. 1994; Reid et al. 1983; Sachs et al. 1983; Walsh et al. 1997; Zurcher et al. 1990). Seven of the thirty-three patients have interstitial deletions (Davies et al. 1999a; Davies et al. 1996; Moriarty and Kerr-Muir 1992; van Swaay et al. 1988). Generally, these patients present with ocular malformations, craniofacial malformations, hearing loss, skeletal malformations, hydrocephally, cardiac malformations, and renal malformations. In this chapter, I present the complete clinical reports and deletion molecular characterizations of four patients with terminal deletions of chromosome 6 (Patients 1, 2, 3, and 4), and four patients with terminal deletions of chromosome 6 as the result of unbalanced translocations (Patients 5, 6, 7, and 8). I compare these cases to other 6p-deletion patients in the literature and discuss the possible roles that genes in the deleted regions may play in the observed phenotype.

## B) MATERIALS AND METHODS

### i) Patient Reports

#### Patient 1

The first patient (Tepperberg et al. 1994) was female with a very mild phenotype and a karyotype of 46XX, del (6) (p25.1-ter). She had prominent eyes with shallow orbits, mild hyperopia, and astigmatism. There were no slanted fissures, epicanthal folds, sclerocornea, nystagmus or strabismus and Schwalbe's line was not prominent. An echocardiogram was normal. Brain imaging was not performed. Facial dysmorphism included wide mouth, dysmorphic ears, hypoplastic midface, and dental malocclusion. There was no cleft palate, or micrognathia. The patient was reported to have scoliosis, proximally placed thumbs and chronic eczema. Bone imaging was not done. The patient had enuresis that was treated by a urologist with a collagen implant. There was no hearing loss, or nipple, fingernail, or toenail abnormalities.

#### Patient 2

A cell line, and clinical details of a second patient were obtained from Coriell Institute For Medical Research Cell Repository (#GMO6222). The patient's karyotype was 46XX, del (6) (p24-ter).

Phenotypic remarks were Dandy-Walker cyst, hydrocephalus, Peters' anomaly, hypertelorism, ear tags, low set ears, and normal Hageman factor level in blood.

**Patient 3**

The third patient was born breech at 38 weeks gestation following a pregnancy marked with oligohydramnios and an abnormal prenatal ultrasound. He suffered a fractured clavicle at birth and a left pneumothorax. Prenatal testing had shown a 46XY, del (6) (p24-ter) karyotype. He had bilateral microphthalmia, corneal opacities, with interstitial keratitis. The left eye had Peters' anomaly and vision was severely compromised. He was later noted to have nystagmus.

This patient also had extensive non-ocular features. Cardiac findings included a grade II/VI to grade III/VI murmur, a PDA (patent ductus arteriosus), a PFO (patent foramen ovale), right ventricular hypertrophy and left axis deviation. There was no VSD (ventricular septal defect) and the PFO closed with time. Hydrocephalus was noted at birth and a brain MRI revealed findings consistent with a diagnosis of Dandy-Walker variant. Among other findings the corpus callosum was observed to be thin and upwardly bowed and the middle and inferior portions of the cerebellar vermis were

absent. Although a MRI of the back revealed no anatomic abnormality of the spinal cord itself, the patient has severe, progressive, congenital scoliosis. The scoliosis required a number of surgeries and a brace.

Hydronephrosis was observed, more severe on the left side. A urogenital exam revealed the hydronephrosis to be secondary to left ureteropelvic junction obstruction. Additionally, the patient was noted to have a micropenis. Facial dysmorphism included microcephaly, hypertelorism, low set, posteriorly angulated ears, and a high arched palate. The patient had severe to profound hearing loss. Profound bilateral clubfoot was also observed to be more severe on the left foot than the right foot.

The patient has a history of chronic oliguria, chronic leukopenia and chronic neutropenia. An examination of the chest revealed widely spaced nipples however the x-ray of the chest was unremarkable. Liver and renal function tests were reported as normal. The patient has a notable allergy to Phenergen which resulted in the patient entering a catatonic state for several hours.

**Patient 4**

Patient four was a male with a *de novo* 46XY, del (6) (p24-ter) karyotype. He was born at term by C-section and was noted to have

dysmorphic features. At three years of age, a thorough ophthalmologic report noted slanted fissures, shallow orbits, bilateral hyperopia (+10.50), hypoplastic irides with marked decreased architecture, mild megalocornea and sclerocornea, and bilateral crescentic hyperpigmentation of the retina infero-temporal to the macula. A recent report diagnosed Rieger malformation and indicated that the retinal hyperpigmentation had faded away. Nystagmus, and strabismus were not noted. The lenses were clear and the IOPs were normal. The disk, macula and vessels were present and appeared to be normal. At birth the child had a PFO, a VSD, and tricuspid valve regurgitation, however, all three resolved by the age of one year without intervention. Other non-ocular features included Dandy Walker variant, agenesis of corpus callosum and brainstem, seizures and profound bilateral deafness. Hypertelorism, brachycephaly, flat mid-face, low-set ears, small nose, broad nasal bridge, frontal bossing, mild micrognathia, short neck, scoliosis, proximately flexed thumbs, club feet, mild clinodactyly of $5^{th}$ fingers were observed. The patient's nipples were widely spaced and there were five superior, supernumerary nipples. The patient's knees were normal and hips were stable in all ranges of motion. Delayed ossification was noted of the femoral heads and

humeral heads. Bone age was consistent with a one-year-old child when the patient was two years of age. Fingernails and toenails were noted as being soft and patient has eczema. Genitalia were normal. A renal exam was not been carried out. Liver and spleen were normal. Similar to patient 3, this patient shared an allergy to Phenergen that resulted in the patient entering a catatonic state for several hours.

**Patient 5**

Patient five has an unbalanced translocation of chromosomes 6 and 4 resulting in a deletion of a portion of the short arm of chromosome 6. The resulting karyotype is 46XY der(6) t(4;6) (p14;p25). The patient presented with congenital glaucoma and Rieger malformation including posterior embryotoxon, iris adhesions and a diffuse corneal opacity on the right eye. Bilateral elevated IOP was controlled on the left side with a trabeculotomy however the right eye did not respond to either of a trabeculotomy or trabeculectomy. The patient was also reported to have nystagmus and strabismus.

The phenotype of this patient was very mild. Clinical reports indicated no cardiac murmur, no facial dysmorphism, no neurological abnormalities, and no remarkable abnormalities of the

chest, hands and feet or kidneys. No formal hearing test was performed.

**Patient 6**

The sixth patient had an unbalanced translocation between chromosomes 6 and 8 that resulted in partial monosomy of the short arm of chromosome 6 and trisomy for a portion of the long arm of chromosome 8. The karyotype is 46XY der(6) t(6;8) (p25;q24.1). At birth the infant was hypotonic and had little spontaneous movement. Phenotypically, the patient presented with a malformation of the iridocorneal angle, and bilateral, congenital glaucoma. He had deep anterior chambers, dilated pupils, ectropian uvea and peripheral anterior synechia over 360°. The optic nerve head was found to be normal. There was moderate dilation of the occipital horns and cerebral ventricles suggestive of hydrocephalus. The cerebellum appeared normal and an EEG was unremarkable. An ASD (atrial septal defect) was noted in addition to PDA and PFO. Facial dysmorphism included turricephaly, hypertelorism, sparse eyebrows and lashes, and low set, anteriorly displaced ears. The patient had kyphoscoliosis, hemivertibrae (T5-T6), and absent ribs. Shoulders and pelvis were unremarkable, as was an abdominal ultrasound. Nail hypoplasia was noted.

**Patient 7**

The seventh patient has an unbalanced translocation resulting in a monosomy of 6p24-ter and a trisomy of 2q32-ter. Her karyotype is 46XX t(2;6) (q32;p24). A thorough and complete clinical report appears elsewhere (MacDonald et al. 1984). Briefly, as an infant the patient had apneic spells and cyanosis and brachycardia while feeding. Ocular examination revealed bilateral corneal opacifications and associated vascularization. There was bilateral aniridia. The left eye was slightly smaller than the right and the right eye has extensive retinal pigment epithelial washout and thinning of the retina. IOP was normal in each eye at a more recent examination.

Craniofacial malformations included microdolichocephaly, telecanthus, hypertelorism, flat, low-set ears, broad, flat, nasal bridge, cleft soft palate and high arched hard palate, micrognathia long philtrum, prominent premaxilla and a short neck.

The hands and feet had malformations. The hands had ulnar drift with flexion at the wrists and adducted thumbs. There is camptodactyly of the right $5^{th}$ and left $4^{th}$ and $5^{th}$ fingers. There was a valgus deformity of the left foot. The patient also had limited flexion and extension of elbows, knees, and hips and had

asymmetrical hypoplasia of vertebrae T12. Right hydronephrosis and a bilateral cystoureteral reflux were also noted.

The patient has progressive hearing loss and was fitted for a hearing aid at the age of 7 months. A CT scan of the head was normal, the cardiovascular system, chest, and abdomen were unremarkable, and the genitalia were normal.

**Patient 8**

This patient has an unbalanced translocation resulting in a deletion chromosome of 6p25 and a trisomy of the terminal portion of chromosome 10p. She presented with hypotonia, mild developmental delay and Rieger anomaly. Craniofacial malformations included hypertelorism, a flat nasal bridge, small, low set ears, micrognathia, prognathia and a small mouth with protruding tongue. The patient has scoliosis, a short neck, widespread nipples and malformation of both hands. There was no heart murmur. No neurological malformations or hearing loss were reported.

**ii) Microsatellite Analysis**

Blood samples or cell lines of each patient were collected and DNA was extracted using standard procedures. Informed consent

was obtained for all patients. To determine copy number for polymorphic loci, $^{35}$S-dATP was directly incorporated into PCR products. The PCR products were then separated on 6% polyacrylamide gels. Patients were scored as being heterozygous for a polymorphic locus when two alleles were observed, or as being homozygous/hemizygous for a polymorphic locus if only one allele was observed. Heterozygosities of all commercial markers are in excess of 85% with the exception of D6S942, which has a heterozygosity of approximately 50%. Farideh Mirzayans developed the FM1 marker in our lab from the DNA sequence of bacterial artificial chromosome J856G1. The primer sequence is 5'-GGCGAGCTTCAGTCCTTCT-3' for the forward primer and 5'-TTGCAGTGAGCCGATATCAC-3' for the reverse primer. The annealing temperature is 57°C and the product is 297 bp. The heterozygosity for FM1 is 78%.

## C) RESULTS

### i) Patients With Simple Deletions

Patients 1-4 have only deletions of chromosome 6p25 without other chromosomal rearrangements. A DNA sample was available

from the mother of Patient 4. DNA samples were unfortunately not available from the other parents of the four patients with simple deletions. Microsatellite analysis indicated that the deletion in Patient 4 was not of maternal origin. As a result of not having DNA from the parent from whom the deletions were inherited, it was possible to only define the maximum possible extensions of the deletions in Patients 1-4. The maximum possible terminal deletion is that part of the chromosome distal to the most telomeric heterozygous marker.

A deletion for Patient 1 could not be detected using our most distal marker although an extremely small deletion was detected cytogenetically (Tepperberg et al. 1994). This patient was heterozygous for markers D6S942, FM1, D6S1617, and D6S1006 suggesting that the deletion is not interstitial. The maximum deletions for the other three deletion patients are approximately, 13.9 cM (distal to D6S277) for Patients 2 and 3, and 27.2 cM (from D6S1006) for Patient 4 (Figure 5-1).

**Figure 5-1. Schematic of the distal tip of human chromosome 6p.**

The black boxes indicate regions where the patients are not deleted. White boxes indicate the minimum extent of the deletion. Grey boxes indicate the maximum extent of the deletion. Markers used are listed to the left of the patients' chromosomes under locus. Genes in this region are listed in bold print. The genetic distance, in cM (centiMorgans), from the telomere, of some markers are also indicated. "ND" indicates no data was available for that marker in a particular patient.

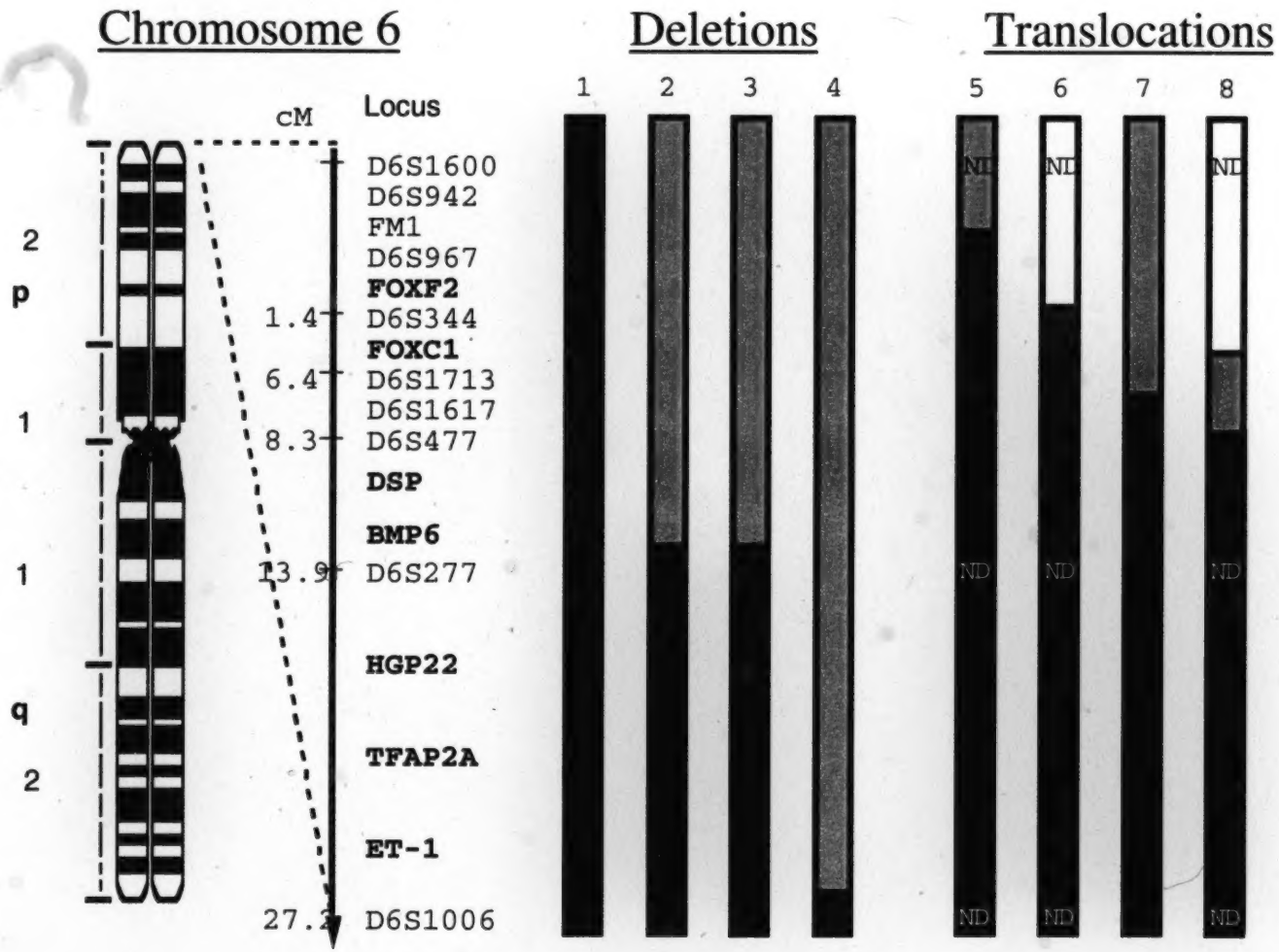
Chromosome 6
Deletions
Translocations
cM
Locus
D6S1600
D6S942
FM1
D6S967
FOXF2
1.4
D6S344
FOXC1
6.4
D6S1713
D6S1617
8.3
D6S477
DSP
BMP6
13.9
D6S277
HGP22
TFAP2A
ET-1
27.2
D6S1006
2
p
1
1
q
2
1
2
3
4
5
6
7
8
ND

### ii) Patients With Unbalanced Translocations

For the four patients with deletions of 6p25 as a result of unbalanced translocations, DNA from the parents was available in two of the cases (Patients 6 and 8). The extent the deletion for Patient 6 can be accurately determined because the markers at the breakpoint were informative. The deletion for Patient 6 was a deletion of paternal origin of 6.4 cM (distal to D6S1713) (Figure 5-1). For Patient 8 the deletion was inherited from her mother and the maximum extent of the deletion was 8.3 cM (distal to D6S477) (Figure 5-1). The minimum extent of the deletion was 6.4 cM (distal to D6S1713). Marker D6S1617 was uninformative.

DNA samples for the parents of Patients 5 and 7 were not available. Therefore only the maximum extent of the deletions could be defined as 1.4 cM (distal to D6S967) for Patient 5 and 6.4 cM (distal to D6S1617) for Patient 7 (Figure 5-1).

## D) DISCUSSION

### i) Genes Deleted In The 6p25 Region

A broad range of clinical features occurs frequently in patients with terminal deletions of the distal tip of human chromosome

6p25. In general groups, these features are: ocular malformations, craniofacial malformations, hearing loss, skeletal malformations, hydrocephally, cardiac malformations, and renal malformations. A number of genes have been mapped to the terminal portion of the short arm of chromosome 6. Many of these genes can be implicated as playing a role in the deletion phenotype based on observations in both animal models and humans.

*FOXC1 (Forkhead box C1)*

One of these important genes is *FOXC1* (*f*orkhead b*ox* C1). Patients 2, 3, 4, 6, 7, and 8 all have maximum deletions that include *FOXC1*. Mutations in the *FOXC1* gene at 6p25, cause eye anterior segment malformations in both humans (Mears et al. 1998; Mirzayans et al. 2000; Nishimura et al. 2001; Nishimura et al. 1998) and mice (Kume et al. 1998; Smith et al. 2000). Mice that are homozygous for a null allele of *Foxc1* also have congenital hydrocephalus (Kume et al. 1998; Smith et al. 2000).

Mutations of the *FOXC1* gene have also been implicated in congenital heart disease (Mears et al. 1998; Nishimura et al. 1998). Kume and co-workers demonstrated *Foxc1* expression in the endothelium of the developing heart and blood vessels (Kume et al. 1998) while Swiderski and co-workers implicate the role of the

mouse gene in formation of valves and atrial septum (Swiderski et al. 1999). This latter evidence suggests that deletion of *FOXC1* may be responsible, at least in part, for heart malformations observed in some of these patients (Table 5-1). There is a similar argument for the role of *FOXC1* in renal malformations as *Foxc1* has been shown to be expressed in mesonephric tubules and surrounding mesenchyme (Kume et al. 1998) and *Foxc1* homozygous mutants cause hydronephrosis in some mouse backgrounds (Kume et al. 2000).

Deletion of *FOXC1* may also contribute to skeletal malformations observed in deletion patients. *Foxc1* homozygous null mice have thin ribs and most of the ossification centers of the sternum are absent and the xiphoid process is misshapen (Hong et al. 1999; Kume et al. 1998). Taken together, these facts indicate that deletion of *FOXC1* might be at least partially responsible for the ocular, cardiac, renal, and skeletal abnormalities (Table 5-1) found in Patients 2, 3, 4, 6, 7, and 8 with terminal deletions of 6p25 encompassing *FOXC1*.

Table 5-1. Clinical features of deletion patients in this study and from a survey of the literature.

| Abnormality | Patient | | | | | | | | # Lit | References |
|---|---|---|---|---|---|---|---|---|---|---|
| | 1 | 2 | 3 | 4 | 5 | 6 | 7 | 8 | | |
| **Craniofacial** | | | | | | | | | | |
| Hypertelorism | | + | + | + | - | + | + | + | 13 | 1, 3, 4, 5, 8, 14, 21, 29, 32, 33, 36, 46 |
| Low/rotated ears | | + | + | + | - | + | + | + | 23 | 1, 3, 4, 5, 6, 8, 13, 14, 16, 21, 27, 31, 32, 33, 35, 36, 38, 44, 46, 49 |
| Nasal bridge | + | | | + | - | | + | + | 13 | 1, 5, 8, 13, 32, 33, 35, 39, 44, 49 |
| Arched/cleft palate | - | | + | | - | | + | | 15 | 1, 3, 6, 8, 16, 21, 29, 31, 32, 33, 38, 46, 49 |
| Micrognathia | - | | | + | - | | + | + | 11 | 4, 6, 8, 31, 32, 33, 36, 49 |
| Short neck | | | | + | - | | + | + | 13 | 1, 5, 6, 8, 21, 31, 32, 38, 49 |
| **Ocular** | | | | | | | | | | |
| Anterior Segment | - | + | + | + | + | + | + | + | 12 | 1, 3, 4, 5, 8, 14, 21, 27, 29, 36, 46, |
| Microphthalmia | | | + | - | - | | - | | 3 | 4, 16, 38 |
| Nystagmus | - | | + | - | + | | | | 3 | 5, 38, 14 |
| **Skeletal** | | | | | | | | | | |
| Chest | | | - | | - | + | - | | 8 | 4, 5, 16, 31, 32, 44 |
| Spine | + | | + | + | - | + | + | + | 3 | 16, 29, 39 |
| Hands | + | | | + | - | | + | + | 21 | 1, 4, 5, 6, 8, 13, 14, 16, 21, 27, 32, 33, 35, 39, 44, 49 |
| Feet | | | + | + | - | | + | | 16 | 1, 4, 5, 6, 14, 16, 21, 32, 33, 38, 39, 44, 49 |
| Joints | | | | - | | - | + | | 6 | 8, 16, 33, 39, 44, 49 |
| **Cardiac** | | | | | | | | | | |
| VSD | - | | - | + | - | | - | - | 6 | 4, 32, 35, 38, 44, 46 |
| PDA | - | | + | | - | + | - | - | 9 | 6, 14, 27, 32, 35, 36, 44, 46 |
| PFO | - | | + | + | - | + | - | - | | |
| ASD | - | | | | - | + | - | - | 5 | 3, 4, 14, 32 |
| Other | | | + | + | | | | | 10 | 1, 4, 5, 16, 21, 29, 31, 32, 33, 44 |
| **Hydrocephaly** | | + | + | + | - | + | - | - | 10 | 1, 3, 6, 8, 14, 16, 32, 33, 36, 49 |
| **Renal** | | | + | | - | | + | | 6 | 5, 6, 16, 27, 32, 38 |
| **Hearing loss** | - | | + | + | - | | + | - | 8 | 5, 14, 21, 33, 39, 49 |
| **Nipples** | - | | + | + | - | | | + | 10 | 1, 5, 8, 27, 32, 39, 49 |
| **Genitalia** | | | + | - | - | | - | | 12 | 1, 5, 13, 14, 21, 27, 31, 32, 39, 44, 46 |
| **Seizures** | | | | + | - | | | | 1 | 39 |
| **Fingernails/ toenails** | - | | | + | - | + | | | 8 | 3, 5, 6, 13, 32, 33, 38 |
| **Eczema** | + | | | + | - | | | | 1 | 21 |

"# Lit" refers to the number of 6p25 deletion patients described in the literature with the feature.

*TFAP2A (Transcription factor AP2 alpha)*

A second major gene at 6p25 is *TFAP2A* (transcription factor AP2 alpha). Patient 4 has a deletion that includes *TFAP2A*. *TFAP2A* deletions may be involved in many aspects of the 6p deletion syndrome. Some mice chimeric for null alleles of *tfap2A* develop without externally visible eyes (Nottoli et al. 1998; West-Mays et al. 1999) suggesting *tfap2A* may be involved in early ocular development. *Tfap2A* is expressed in pericardial tissue and aorta, and in the mesonephric region and urogenital mesoderm in embryonic nephric tissue (Mitchell et al. 1991) implicating involvement in cardiac, renal and genital malformations. Mice chimeric for null alleles of *tfap2A* also develop with severe craniofacial malformations including cleft lip with or without cleft palate and mandibular and maxillary dysmorphology (Nottoli et al. 1998). Mice heterozygous for the null allele showed abnormal curvature of the upper snout with reduced penetrance (Nottoli et al. 1998). These results indicate *TFAP2A* is involved in craniofacial development. In the chimeric mice mentioned above, 20% also had limb defects that included polydactyly and syndactyly (Nottoli et al. 1998). Independent experiments indicated that *tfap2A* null mice had thoracic abnormalities including missing clavicles, a rib cage that was not fused to the sternum, and scoliosis (Zhang et al. 1996).

Finally, *tfap2A* null homozygous mice were observed to lack middle ear bones and the tympanic ring (Zhang et al. 1996) suggesting that the deafness observed in some patients with deletions may be at least partially attributable to *TFAP2A* haploinsufficiency. These findings implicate deletion of *TFAP2A* in some of the ocular, skeletal, cardiac, renal, and hearing abnormalities in patients with deletions of chromosome 6. Patient 4 has anterior segment malformations, scoliosis, heart malformations and bilateral deafness (Table 5-1) and is deleted for *TFAP2A*.

*ET-1 (Endothelin 1)*

The third gene whose haploinsufficiency may contribute significantly to the 6p25 phenotype is *ET-1* (endothelin-1). Patient 4 is the only patient in our study with a deletion that includes *ET-1*. Murine *et-1* is expressed in the epithelium and mesenchyme of embryonic pharyngeal arches and in endothelium of large arteries (Maemura et al. 1996). Mice with homozygous null alleles of *et-1* have malformations of craniofacial tissues, including poorly developed mandible and cleft palate as well as absent auditory ossicles and tympanic ring (Kurihara et al. 1994). These mice also have aortic arch malformations and VSD with reduced penetrance (Kurihara et al. 1995). A second group demonstrated that mice

expressing a transgenic copy of human *ET-1* develop renal cysts, interstitial fibrosis, glomerulosclerosis and fatal kidney disease (Hocher et al. 1997). These results suggest that deletions of *ET-1* may be at least partially responsible for the observations of cardiac, renal and craniofacial malformations and hearing loss in Patient 4.

*BMP6 (Bone morphogenetic protein 6)*

The *BMP6* (bone morphogenetic protein 6) gene is also located at 6p25. Patients 2, 3, and 4 have maximum deletions encompassing *BMP6*. *BMP6* is very close to a heterozygous marker in patients 2 and 3 and since the deleted interval is only a maximum, regions near the maximum breakpoint are very possibly still present in two copies. Mice homozygous for a null allele of *bmp6* have delayed ossification of the sternum (Solloway et al. 1998). *BMP6* could thus be implicated in delayed ossification observed in Patient 4.

*OFC1(Orofacial clefting 1)*

A locus for orofacial clefting (OFC 1) has been localized to 6p25 (Davies et al. 1995). Two candidate genes, *HGP22* and *TFAPA*, have been suggested as *OFC1* candidate genes. Patient 4 is deleted for the region containing these genes. Disruptions in the murine *hgp22* gene with the insertion of a human transgene caused a short

snout and twisted jaw secondary to a developmental defect in the first branchial arch (Wakasugi et al. 1988). Therefore it is possible that *HGP22* haploinsufficiency could be involved in the craniofacial malformations in Patient 4.

A number of other genes at 6p25 are likely to have more restricted phenotypic consequences when deleted. Desmoplakin (*DSP*), elastase inhibitor/protease inhibitor 2 (*ELANH2*), and forkhead box F2 (*FOXF2*) are three of these.

*DSP (Desmoplakin)*

Desmoplakin is a constituent component and the most abundant protein in desmosomes. Desmosomes are important intercellular adhesive junctions in tissues experiencing mechanical stress and are particularly prominent in the epidermis. It has recently been demonstrated that a single null allele of desmoplakin is responsible for an autosomal dominant form of striate palmoplantar keratoderma (Armstrong et al. 1999). Based on these observations, DSP may play a role in the eczema observed in Patient 4 with a deletion that includes the *DSP* gene.

*ELANH2 (Elastase inhibitor)*

The *ELANH2* gene is a member of the SERPIN family of serine (or cysteine) protease inhibitors. ELANH2 is a monocyte/neutrophil derived elastase inhibitor that is not expressed in lymphoblastoid cells (Remold-O'Donnell et al. 1992). Patient 3 in this study is described as having chronic leukopenia approaching absolute neutropenia. Neutropenia is a decrease in the number of neutrophilic granular leukocytes in the blood. The deletion of *ELANH2* may be attributed to this condition, however, other patients with deletions that include *ELANH2* (Patients 2, 4, 6, 7, and 8; Figure 5-1) did not share this clinical feature.

*FOXF2 (Forkhead box F2)*

The *FOXF2* gene at 6p25 is from the same family of forkhead transcription factors as *FOXC1*. Murine *Foxf2* is expressed primarily in placenta and adult and fetal lung (Pierrou et al. 1994). Although the function of FOXF2 is unknown, binding sequences for the protein have been identified in the promoters of several lung specific genes (Hellqvist et al. 1996) and *in vitro* experiments suggest a role in recruitment of general transcription factors (Hellqvist et al. 1998). None of the patients in this study with deletions that include *FOXF2* (Patients 2, 3, 4, 6, 7, and 8), or in the literature, have been reported to have any congenital lung malformations.

### *ii) Genotype/Phenotype Correlation*

Attempts to characterize deletion syndromes are difficult. This may be due to the patients' clinical reports being incomplete or perhaps methods for determining the genotypes differ from study to study. Even considering these potential sources of error there exists a wide phenotypic variation from patient to patient. These differences may be explained in a number of ways.

First, patients with the exact same deletion may present with very different phenotypes depending on the genotype of the patient for the genes left in a hemizygous state. A deletion may uncover a number of recessive mutant alleles in one patient and not a second and thereby leaving the first patient with a much more severe phenotype. Similarly, the genotype of each patient throughout the entire genome may determine how well the patients are able to tolerate the deletion of each particular gene.

Secondly, there may be environmental factors contributing to the phenotype. For example *TFAP2A* is retinoic acid responsive, and therefore, *in utero* retinoic acid concentrations that vary from patient to patient may be a source of variation between two patients both deleted for the *TFAP2A* gene.

Third, the exact location of the breakpoints in similar cases may be different. This difference in location of the breakpoint may

be the difference between breaking within a gene versus just outside a gene. The function of some genes may not be compromised in a hemizygous state, however, a disruption in the middle of the coding region may have physiological consequences in rare situations of the creation of a dominant negative effect.

Fourth, the position effect of deleting part of a chromosome and/or juxtaposing new fragments of a chromosome can vary from individual to individual. Position effects may be observed as a result of the deletion of a regulatory element, silencer or enhancer for a particular gene or by altered control of remaining genes by ectopic regulatory elements brought in close proximity by the deletion or translocation (Kleinjan and van Heyningen 1998). In addition, Patients 5, 6, 7, 8, and A, B, D (Figure 5-2 and Table 5-2) all have deletions as a result of an unbalanced translocation. As a result, these patients are also each duplicated for a different part of the genome. It is not possible to determine the influence the portion of the duplicated chromosome has on the clinical phenotype in each of these patients with unbalanced translocations.

Most of the developmental malformations observed in patients with deletions of 6p25 are manifest at birth. The hearing loss, however, was reported in Patient C (Law et al. 1998) as being

**Figure 5-2. Schematic of extent of deletions for 8 patients in the literature with deletions characterized at a molecular level.**

The black boxes indicate regions where the patients are not deleted. White boxes indicate the minimum extent of the deletion. Grey boxes indicate markers that may or may not be deleted. Genes in this region are listed in bold print. The genetic distance, in cM (centiMorgans), from the telomere, of some markers are also indicated. Patient A is from Nishimura et al 1998. Patient B is case 2 from Pierquin et al. 1991 and CA from Davies et al. 1999b. Patient C is from Law et al. 1998 and SG from Davies et al. 1999b. Patient D is case 1 from Pierquin et al. 1991 and BD from Davies et al. 1999b. Patient E is HH from Davies et al. 1999b. Patient F is JW from Davies et al. 1999b. Patient G is case 2 from Davies et al. 1995. Patient U is from Davies et al. 1999a. Clinical features of terminal deletion patients are in Table 5-2. Clinical features of Patient U (the only interstitial deletion shown here) are in Table 5-3.

## Chromosome 6

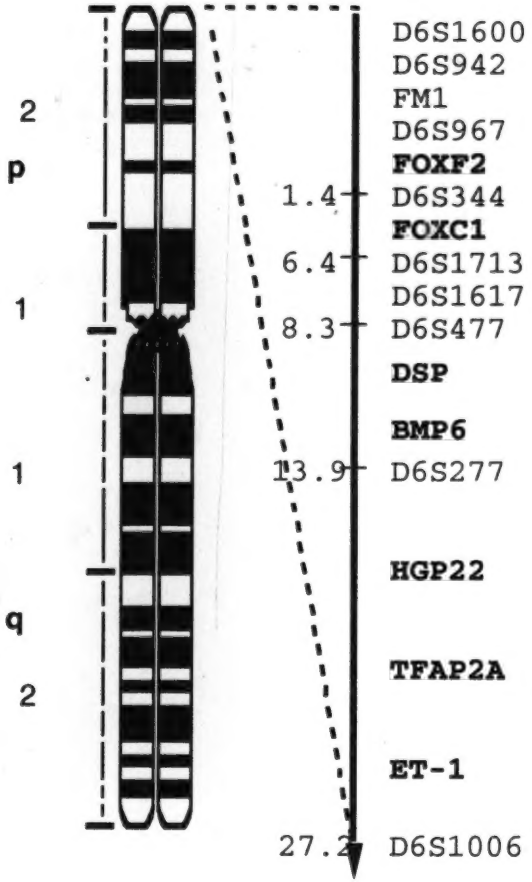


## Patients from the literature

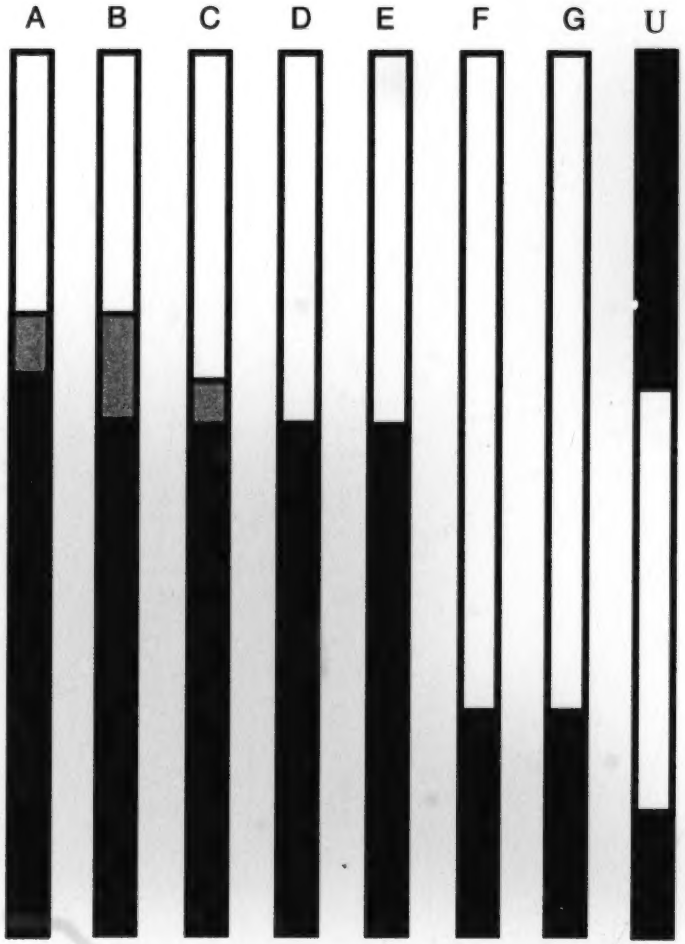

Table 5-2. Clinical features of patients with molecularly characterized terminal deletions.

| Clinical Features | Terminal Deletion Patients | | | | | | | | | | | | | | | Frequency observed/reported |
|---|---|---|---|---|---|---|---|---|---|---|---|---|---|---|---|---|
| | 1 | 2 | 3 | 4 | 5 | 6 | 7 | 8 | A | B | C | D | E | F | G | |
| **Terminal Deletion Classification** | | | | | | | | | | | | | | | | |
| Anterior segment | - | + | + | + | + | + | + | + | + | - | + | - | + | + | + | 12/15 |
| Hypertelorism | | + | + | + | - | + | + | + | | + | + | + | - | + | + | 11/13 |
| Hearing loss | - | | + | + | - | | + | - | | + | + | + | + | + | | 8/11 |
| | | | | | | | | | | | | | | | | |
| **Interstitial Deletion Classification** | | | | | | | | | | | | | | | | |
| Short neck | | | | + | - | | + | + | | - | + | - | - | - | | 4/9 |
| Clinodactyly/ Syndactyly | | | | + | - | | + | | | + | + | - | - | - | | 4/8 |
| Brain malformation | | + | + | + | - | + | - | - | + | + | - | + | - | - | + | 8/14 |
| Heart malformation | - | | + | + | - | + | - | - | + | + | + | - | - | + | + | 8/14 |
| Kidney malformation | | | + | | - | | + | | + | - | - | - | - | - | - | 3/10 |

Patients 1-8 this study. Patient A-G see figure legend 2 for references. Classifications proposed by Davies et al 1999b.

progressive. Any late or delayed onset phenotypes (perhaps scoliosis and eczema) may be missed by lack of follow up evaluations of the patients.

Reduced penetrance may also explain the absence of clinical features in some patients. Patients D and E do not appear to have any heart malformations even though all other patients deleted for *FOXC1* do have some heart malformation. This may be an example of reduced penetrance of the phenotype, or alternatively, the heart defect might have been minor and/or self-repaired by the time of examination. *Tfap2A* mice heterozygous for a null allele have reduced penetrance of craniofacial malformations (Nottoli et al. 1998) and mice homozygous for a null allele if *et-1* have VSDs with reduced penetrance (Kurihara et al. 1995).

Finally not all patients reported have complete clinical examinations reported or reliable chromosomal banding. Hopefully, as the number of patient reports increase, clinicians will have a better indication for what clinical features to look for in these patients. Of interest is the report of Patient 1 having a cytogenetically visable deletion however no deletion was observed using our PCR based detection method. It is possible that this patient has 6p25 translocated to some other portion of the genome

and therefore looks cytogenetically deleted while two copies are still able to be detected by PCR.

As a result of so many confounding variables the delineation of distinct syndromes for terminal deletions and interstitial deletions is very difficult. Davies and co-workers characterize the interstitial deletion syndrome as having kidney defects, short neck, structural eye malformations, and clinodactyly and terminal deletion syndrome as having eye anterior segment malformations, hearing defects, craniofacial abnormalities, low set ears and heart defects (Davies et al. 1999b). Including our study, there are 21 patients (8 reported here, and 13 from the literature) with deletions characterized at a molecular level. Of these 21 patients, 15 have terminal deletions (Table 5-2) and 6 have interstitial deletions (Table 5-3). Tables 5-2 and 5-3 summarize the frequency of observation of each clinical feature. From this I conclude that it is not clear that two distinct deletion syndromes exist. It is difficult to predict the extent of a deletion based on clinical features or conversely, predict clinical features based on knowledge of the extent of deletion.

The only features that stand out in this comparison are the presence of eye anterior segment malformations and hearing loss associated with deletions of 6p25.

Table 5-3. Clinical features of patients from other published reports with molecularly characterized interstitial deletions.

| **Clinical Features** | **Interstitial Deletion Patients** | | | | | | **Frequency** observed/reported |
|---|---|---|---|---|---|---|---|
| | U | V | W | X | Y | Z | |
| **Terminal Deletion Classification** | | | | | | | |
| Anterior segment | + | - | - | | - | | 1/4 |
| Hypertelorism | + | + | - | | - | - | 2/5 |
| Hearing loss | | - | - | | + | | 1/3 |
| | | | | | | | |
| **Interstitial Deletion Classification** | | | | | | | |
| Short neck | | + | - | + | + | | 3/4 |
| Clinodactyly/ Syndactyly | | + | - | + | + | + | 4/5 |
| Brain malformation | | + | - | + | + | | 3/4 |
| Heart malformation | + | - | - | + | + | | 3/5 |
| Kidney malformation | | - | + | + | - | | 2/4 |

Patient I from Davies et al. 1999a
Patients II, III and V are patients PF, 95-800 and 91-145 respectively from Davies et al. 1999b
Patient IV and VI are patients 2 and 1 respectively from Davies et al. 1996
Classifications proposed by Davies et al 1999b.

**iii) Evidence for Autosomal Dominant Deafness Locus**

Of six patients with interstitial deletions, the presence or absense of hearing loss was noted in 3 patients. Of these, only Patient Y had hearing difficulites (Table 5-3). Although hearing loss may be progressive and therefore missed due to later onset, it is not a feature that is likely to go unreported if observed. Therefore, it is likely that if hearing loss does exist in interstitial deletion patients it is rare. Of the 15 terminal deletion patients, the presence or absense of hearing loss was noted in 12 of which 9 had hearing loss. Patient 5 was deleted distal to marker D6S967 and did not have hearing loss suggesting that a deafness locus be located proximal to D6S967. Patient 6 was deleted distal to D6S1713 and had hearing loss suggesting that the deafness locus be located distal to D6S1713. Hearing loss in Patients 3, 4, 6, and 7, and no hearing loss in patients 1 and 5 are consistent with the hypothesis of a deafness locus between markers D6S1713 and D6S967. Patient 8, however, is at a minimum, deleted distal to D671713 and does not have hearing loss. This would suggest that the deafness locus be located proximal to D6S1713. One explaination for this would be that the autosomal dominant deafness locus has reduced penetrance. Additional clinical reports from patients with chromosome 6p25 deletions and linkage analyses with families with autosomal dominant hearing loss

are necessary to confirm this possible location of a hearing loss gene.

**iiii) Evidence for Eye Malformation Locus**

Twelve of the 15 patients with terminal deletions also have eye anterior segment malformations. Only four patients with interstitial deletions reported presence or absence of eye anterior segment malformations. Only one of these four patients (Patient U) had anterior segment malformations (Table 5-3). It is important to note that Patient U is the patient with the most distal-extending interstitial deletion (Figure 5-2). The distal points of the other 5 interstitial deletions lie proximal to the centromeric point of the deletion in Patient U. This suggests that it is not terminal versus interstitial that is important for clinical consequences, but the location of the deletion. The patients with terminal deletions and the patient with the most telomeric interstitial deletion seem most likely to have eye malformations. Of notable interest is Patient 5 who has congenital glaucoma and AR malformation including posterior embryotoxon, iris adhesions and corneal opacities. Patient 5 is not deleted for *FOXC1* (Figure 5-1). Mears and co-workers have suggested that a second eye anterior segment malformation locus exists distal to *FOXC1* (Mears et al. 1998). Therefore, this is further

evidence that there is another eye anterior segment malformation locus distal to *FOXC1* at 6p25, or, alternatively, the deletion in Patient 5 might include regulatory elements important for *FOXC1* expression.

**E) REFERENCES**

1) Alashari M, Chen E, Poskanzer L (1995) Partial deletion of chromosome 6p: autopsy findings in a premature infant and review of the literature. Pediatr Pathol Lab Med 15:941-7.

2) Armstrong DK, McKenna KE, Purkis PE, Green KJ, Eady RA, Leigh IM, Hughes AE (1999) Haploinsufficiency of desmoplakin causes a striate subtype of palmoplantar keratoderma. Hum Mol Genet 8:143-8.

3) D'Alessandro E, Santiemma V, Lo Re ML, Ligas C, Del Porto G (1992) 6p23 deletion mosaicism in a woman with recurrent abortions and idiopathic hypoprolactinemia. Am J Med Genet 44:220-2.

4) Davies AF, Mirza G, Flinter F, Ragoussis J (1999a) An interstitial deletion of 6p24-p25 proximal to the FKHL7 locus and including AP-2alpha that affects anterior eye chamber development. J Med Genet 36:708-10.

5) Davies AF, Mirza G, Sekhon G, Turnpenny P, Leroy F, Speleman F, Law C, et al (1999b) Delineation of two distinct 6p deletion syndromes. Hum Genet 104:64-72.

6) Davies AF, Olavesen MG, Stephens RJ, Davidson R, Delneste D, Van Regemorter N, Vamos E, et al (1996) A detailed investigation of two cases exhibiting characteristics of the 6p deletion syndrome. Hum Genet 98:454-9.

7) Davies AF, Stephens RJ, Olavesen MG, Heather L, Dixon MJ, Magee A, Flinter F, et al (1995) Evidence of a locus for orofacial clefting on human chromosome 6p24 and STS content map of the region. Hum Mol Genet 4:121-8.

8) Guillen-Navarro E, Chan W, Ragousssis J, Davies A, Ostrer H, Perle M (1997) A rare de novo microdeletion of distal chromosome 6p: clinical phenotype and molecular cytogenetic characterization. American Journal of Human Genetics 61.

9) Hellqvist M, Mahlapuu M, Blixt A, Enerback S, Carlsson P (1998) The human forkhead protein FREAC-2 contains two functionally

redundant activation domains and interacts with TBP and TFIIB. J Biol Chem 273:23335-43.

10) Hellqvist M, Mahlapuu M, Samuelsson L, Enerback S, Carlsson P (1996) Differential activation of lung-specific genes by two forkhead proteins, FREAC-1 and FREAC-2. J Biol Chem 271:4482-90.

11) Hocher B, Thone-Reineke C, Rohmeiss P, Schmager F, Slowinski T, Burst V, Siegmund F, et al (1997) Endothelin-1 transgenic mice develop glomerulosclerosis, interstitial fibrosis, and renal cysts but not hypertension. J Clin Invest 99:1380-9.

12) Hong HK, Lass JH, Chakravarti A (1999) Pleiotropic skeletal and ocular phenotypes of the mouse mutation congenital hydrocephalus (ch/Mf1) arise from a winged helix/forkhead transcriptionfactor gene. Hum Mol Genet 8:625-37.

13) Jalal SM, Macias VR, Roop H, Morgan F, King P (1989) Two rare cases of 6p partial deletion. Clin Genet 36:196-9.

14) Kleinjan DJ, van Heyningen V (1998) Position effect in human genetic disease. Hum Mol Genet 7:1611-8.

15) Kormann-Bortolotto MH, Farah LM, Soares D, Corbani M, Muller R, Adell AC (1990) Terminal deletion 6p23: a case report. Am J Med Genet 37:475-7.

16) Kume T, Deng K, Hogan BL (2000) Murine forkhead/winged helix genes Foxc1 (Mf1) and Foxc2 (Mfh1) are required for the early organogenesis of the kidney and urinary tract. Development 127:1387-95.

17) Kume T, Deng KY, Winfrey V, Gould DB, Walter MA, Hogan BL (1998) The forkhead/winged helix gene Mf1 is disrupted in the pleiotropic mouse mutation congenital hydrocephalus. Cell 93:985-96.

18) Kurihara Y, Kurihara H, Oda H, Maemura K, Nagai R, Ishikawa T, Yazaki Y (1995) Aortic arch malformations and ventricular septal defect in mice deficient in endothelin-1. J Clin Invest 96:293-300.

19) Kurihara Y, Kurihara H, Suzuki H, Kodama T, Maemura K, Nagai R, Oda H, et al (1994) Elevated blood pressure and craniofacial abnormalities in mice deficient in endothelin-1. Nature 368:703-10.

20) Law CJ, Fisher AM, Temple IK (1998) Distal 6p deletion syndrome: a report of a case with anterior chamber eye anomaly and review of published reports. J Med Genet 35:685-9.

21) MacDonald IM, Clarke WN, Clifford BG, Reid JC, Cox DM, Hunter AG (1984) Corneal pathology and aniridia associated with partial trisomy 2q, due to a maternal (2;6) translocation. Ophthalmic Paediatr Genet 4:75-80.

22) Maemura K, Kurihara H, Kurihara Y, Oda H, Ishikawa T, Copeland NG, Gilbert DJ, et al (1996) Sequence analysis, chromosomal location, and developmental expression of the mouse preproendothelin-1 gene. Genomics 31:177-84.

23) Mears AJ, Jordan T, Mirzayans F, Dubois S, Kume T, Parlee M, Ritch R, et al (1998) Mutations of the forkhead/winged-helix

gene, FKHL7, in patients with Axenfeld-Rieger anomaly. Am J Hum Genet 63:1316-28.

24) Mirzayans F, Gould DB, Heon E, Billingsley GD, Cheung JC, Mears AJ, Walter MA (2000) Axenfeld-Rieger syndrome resulting from mutation of the FKHL7 gene on chromosome 6p25. Eur J Hum Genet 8:71-4.

25) Mitchell PJ, Timmons PM, Hebert JM, Rigby PW, Tjian R (1991) Transcription factor AP-2 is expressed in neural crest cell lineages during mouse embryogenesis. Genes Dev 5:105-19.

26) Moriarty AP, Kerr-Muir MG (1992) Sclerocornea and interstitial deletion of the short arm of chromosome 6- -(46XY del[6] [p22 p24]). J Pediatr Ophthalmol Strabismus 29:177-9.

27) Nishimura DY, Searby CC, Alward WL, Walton D, Craig JE, Mackey DA, Kawase K, et al (2001) A Spectrum of FOXC1 Mutations Suggests Gene Dosage as a Mechanism for Developmental Defects of the Anterior Chamber of the Eye. Am J Hum Genet 68:364-372.

28) Nishimura DY, Swiderski RE, Alward WL, Searby CC, Patil SR, Bennet SR, Kanis AB, et al (1998) The forkhead transcription factor gene FKHL7 is responsible for glaucoma phenotypes which map to 6p25. Nat Genet 19:140-7.

29) Nottoli T, Hagopian-Donaldson S, Zhang J, Perkins A, Williams T (1998) AP-2-null cells disrupt morphogenesis of the eye, face, and limbs in chimeric mice. Proc Natl Acad Sci U S A 95:13714-9.

30) Ouchi K, Kasai R (1982) A case of partial monosomy 6p. Japanese Journal of Human Genetics 27:214.

31) Palmer CG, Bader P, Slovak ML, Comings DE, Pettenati MJ (1991) Partial deletion of chromosome 6p: delineation of the syndrome. Am J Med Genet 39:155-60.

32) Pierrou S, Hellqvist M, Samuelsson L, Enerback S, Carlsson P (1994) Cloning and characterization of seven human forkhead proteins: binding site specificity and DNA bending. EMBO J 13:5002-12.

33) Plaja A, Vidal R, Soriano D, Bou X, Vendrell T, Mediano C, Pueyo JM, et al (1994) Terminal deletion of 6p: report of a new case. Ann Genet 37:196-9.

34) Reid CS, Stamberg J, Phillips JA (1983) Monosomy for distal segment of Hageman factor. Pediatric Research 17:A217.

35) Remold-O'Donnell E, Chin J, Alberts M (1992) Sequence and molecular characterization of human monocyte/neutrophil elastase inhibitor. Proc Natl Acad Sci U S A 89:5635-9.

36) Sachs ES, Hoogeboom AJ, Niermeijer MF, Schreuder GM (1983) Clinical evidence for localisation of HLA proximal of chromosome 6p22. Lancet 1:659.

37) Smith RS, Zabaleta A, Kume T, Savinova OV, Kidson SH, Martin JE, Nishimura DY, et al (2000) Haploinsufficiency of the transcription factors FOXC1 and FOXC2 results in aberrant ocular development. Hum Mol Genet 9:1021-32.

38) Solloway MJ, Dudley AT, Bikoff EK, Lyons KM, Hogan BL, Robertson EJ (1998) Mice lacking Bmp6 function. Dev Genet 22:321-39.

39) Swiderski RE, Reiter RS, Nishimura DY, Alward WL, Kalenak JW, Searby CS, Stone EM, et al (1999) Expression of the Mf1 gene in developing mouse hearts: implication in the development of human congenital heart defects. Dev Dyn 216:16-27.

40) Tepperberg JH, Rao KW, Albright SG, Kaiser-Rogers K, Powell CM (1994) Deletion 6(p25.1) in a child with mild dysmorphic features and absence of major eye malformations: implications for the localization of genes involved in ocular development. American Journal of Human Genetics 55:A119.

41) van Swaay E, Beverstock GC, van de Kamp JJ (1988) A patient with an interstitial deletion of the short arm of chromosome 6. Clin Genet 33:95-101.

42) Wakasugi S, Iwanaga T, Inomoto T, Tengan T, Maeda S, Uehira M, Araki K, et al (1988) An autosomal dominant mutation of facial development in a transgenic mouse. Dev Genet 9:203-12.

43) Walsh LM, Lynch SA, Clarke MP (1997) Ocular abnormalities in a patient with partial deletion of chromosome 6p. A case report. Ophthalmic Genet 18:151-6.

44) West-Mays JA, Zhang J, Nottoli T, Hagopian-Donaldson S, Libby D, Strissel KJ, Williams T (1999) AP-2alpha transcription factor is required for early morphogenesis of the lens vesicle. Dev Biol 206:46-62.

45) Zhang J, Hagopian-Donaldson S, Serbedzija G, Elsemore J, Plehn-Dujowich D, McMahon AP, Flavell RA, et al (1996) Neural tube, skeletal and body wall defects in mice lacking transcription factor AP-2. Nature 381:238-41.

46) Zurcher VL, Golden WL, Zinn AB (1990) Distal deletion of the short arm of chromosome 6. Am J Med Genet 35:261-5.

# CHAPTER SIX

# DISCUSSION AND CONCLUSIONS

**LINKAGE ANALYSIS**

Large, well clinically described families are extremely powerful for mapping inherited disorders. Dr. Alan Mears and I used two families to map a novel locus for IGDA and secondary glaucoma (Mears et al. 1996). Heterogeneity for the two families was excluded and a combined maximum two-point LOD score of 12.33 was obtained with marker D6S967 at a recombination fraction of Theta=0.00 (Mears et al. 1996). This finding was significant because it was only the third locus identified for a secondary glaucoma.

Following the identification of an IGDA locus at 6p25, I demonstrated linkage to this locus in a family with a clinically distinct type of AR malformation, ARA (Gould et al. 1997). This is consistent with the locus at 4q25 being responsible for both ARS (Semina et al. 1996) and IGDS (Kulak et al. 1998).

Furthermore, I then found that a small family with ARS had suggestive linkage to 6p25. The mutation was subsequently identified in *FOXC1* (Mirzayans et al. 2000). This finding was the first evidence that mutations in a single gene can be responsible for AR malformations with and without the non-ocular, systemic features associated with the syndromic forms of the disorder. Evidence from our laboratory suggests that this observation is the

result of varying amounts of residual protien function. Mutant proteins with greater residual function have less severe phenotypes than those with less residual function. This may indicate a tissue dependant threshold for the amount of activity required for normal function. For example the eye seems to be more sensitive to decreased protein function that the teeth and therefore it requires a more severe mutation to cause dental abnormalities. The mutations in *FOXC1* identified to date, are all within the DNA binding domain (or upstream frameshifts) that disrupt DNA binding ability and create a haploinsufficiency at the cellular level.

Family E has a key recombinant individual that excludes *FOXC1* from the critical interval. There are three explanations for this. First, the families with malformations mapping to 6p25 may be heterogeneous. If this is true, a second gene exists distal to *FOXC1*. Secondly, the mutation in this family may be within a *FOXC1* regulatory element that is distal to the coding region. Finally, *FOXC1* may be causing the phenotype not via mutations in the gene but by its inclusion in a duplication event. Recently, two reports have been published of patients with AR malformations and duplications of this region (Lehmann et al. 2000; Nishimura et al. 2001). The presence of a duplication does not exlude the existence of a second eye development gene distal to *FOXC1*.

Continued research must be carried out to resolve this issue. The search for and mutational analysis of candidate genes in the critical interval is still underway (Farideh Mirzayans personal communication). Also, the presence of a duplication of 6p25 is also being explored. If results of mutational analysis of all coding sequence of genes within the critical interval are negative then the disease causing mutation may be within a promoter sequence or some other regulatory element. Promoter analysis is difficult to do and results are often ambiguous. One method to determine if a mutation of a *FOXC1* regulatory sequence is the cause of the disease would be to obtain a donor eye from an affected individual that is polymorphic for coding sequences within the gene. Quantification of the relative frequency of each allele in the transcripts may reveal one allele to be underrepresented. Obtaining the material for this line of work is extremely difficult.

**DELETION PATIENT ANALYSIS**

In parallel with the family linkage analysis, I conducted analysis of patients with deletions in the 6p25 region. The characterization of deletions at a molecular level is important to try to establish which genes are present and which are deleted. The

characteristic 6p25 deletion syndrome phenotype includes ocular, craniofacial, cardiac, skeletal, and renal malformations as well as hydrocephally and progressive hearing loss. A number of genes, including several developmentally regulated transcription factors, exist at 6p25 that may be implicated in various aspects of deletion phenotype. One patient of interest, Patient 5, was shown to have a deletion that is telomeric to *FOXC1*. Patient 5 has anterior segment eye malformations including posterior embryotoxon, iris adhesions and corneal opacities. This observation is consistent with either a second ocular development locus exists distal to *FOXC1* or an important *FOXC1* regulatory element is present in this region.

A second interesting finding from the molecular characterization of deletions is the preliminary identification of an autosomal deafness locus. Linkage analysis with families with autosomal dominant deafness that have not been mapped and characterization of further deletion patients will both help to support or refute this evidence. Future work with these patients should be to identify the exact location of each breakpoint at a nucleotide level and determine if individual genes are disrupted at these breakpoints.

## MUTATIONAL ANALYSIS OF CANDIDATE GENES

Previous secondary glaucoma loci identified were the Aniridia locus at 11p13 (Francke et al. 1979), and an Axenfeld-Rieger locus at 4q25 (Murray et al. 1992). Mutations in the *PAX6* gene at 11p13 (Hanson et al. 1993; Jordan et al. 1992) and the *PITX2* gene at 4q25 have subsequently been shown to cause the respective disorders. The *FOXC1* gene at 6p25 is mutated in some families mapping to this locus (Mears et al. 1998; Mirzayans et al. 2000; Nishimura et al. 1998). Also, the *LMX1B* gene at 9q34 has been identified as the gene responsible for Nail-Patella Syndrome which is also associated with glaucoma. All of these genes are developmentally regulated transcription factors that belong to different families based on their DNA binding domains.

Based on the identification of the above genes, it is reasonable to investigate transcription factors as candidate genes in those families mapping to 6p25 that do not have mutations in the *FOXC1* coding region, and also in sporadic AR malformation patients that do not have mutations of known genes. The *FOXF2* gene at 6p25 and *BARX1* gene at 9q12 are both developmentally regulated transcription factors. The *FOXF2* gene was sequenced in affected members of four families linked to 6p25 and no disease-causing mutations were identified. The *BARX1* gene was screened by SSCP

analysis for mutations in 55 patients with anterior segment malformations and no disease-causing malformations were identified.

The observation that no *FOXF2* disease-causing mutations were identified in the four families linked to 6p25 does not exclude it from being involved in sporadic or unmapped cases of AR malformations in sporadic cases. Perhaps a future experiment would be to screen *FOXF2* for mutations in AR malformations. The panel of 55 patients with anterior segment disorders that was screened for *BARX1* mutations would be a good cohort for such an analysis of *FOXF2* because there is a variety of phenotypes represented.

No *BARX1* mutations were identified in the panel of 55 patients with various anterior segment disorders. This is reasonable evidence that *BARX1* is not involved in anterior segment disorders. *BARX1* should be considered a candidate for future developmental disorders mapped to chromosome 9q12. Based on mouse expression data, disorders involving the stomach, eyes or teeth would be the most likely candidates. Recently, a family with autosomal recessive cataracts has been mapped near *BARX1* and is being screened for mutations (Heon et al. 2001).

## CONCLUSIONS

The recent sequencing of the human genome provides a unique and very valuable resource to researchers. Analysis of this sequence will indicate the sequence and location of many genes. The function of all of these genes is one of the main questions to be addressed in the post human genome project era. In the perspective of genetic research, familial linkage analysis and mapping loci will continue to be of importance. The continued localization of disease loci may be a rate-limiting step in the identification of new disease genes, again underscoring the importance of collection of patient resources. Once the chromosomal localization of a disorder is known, all genes in the region, their sequence and genomic structure will be readily available. In the previous cases of Aniridia, AR malformation at 4q25, and AR malformations at 6p25, the identification of the gene responsible followed the identification of the locus.

Currently, there are 6 known loci for primary open angle glaucoma (GLC1A, GLC1B, GLC1C, GLC1D, GLC1E, and GLC1F) (Table 1-2). Of these loci, only the gene for the GLC1A locus has been identified (Stone et al. 1997). Recently, a group of researchers used the analysis of sib pairs to identify further loci involved in POAG

(Wiggs et al. 2000). They demonstrated some level of linkage to three known loci, GLC1B, GLC1D, and GLC1E, while implicating new loci on chromosomes 2, 14, 17, and 19 (Wiggs et al. 2000). As the full human genomic sequence becomes available for each of the other loci, the genes should be more readily identified. The identification of even a few of these should shed some light on what types of genes may be involved in POAG and functional candidate genes can then be identified at remaining loci.

The goal to identify all genes underlying glaucoma is a first step. Characterization of the proteins and determination of proteins' functions is also important. The knowledge of how a mutant protein affects the cell or why too much or too little of a protein is pathogenic, will help us to understand the currently unknown etiology of glaucoma. This in turn will lead to better testing and treatment for those people who face losing their vision to glaucoma.

**REFERENCES**

1) Francke U, Holmes LB, Atkins L, Riccardi VM (1979) Aniridia-Wilms' tumor association: evidence for specific deletion of 11p13. Cytogenet Cell Genet 24:185-92.

2) Gould DB, Mears AJ, Pearce WG, Walter MA (1997) Autosomal dominant Axenfeld-Rieger anomaly maps to 6p25. Am J Hum Genet 61:765-8.

3) Hanson IM, Seawright A, Hardman K, Hodgson S, Zaletayev D, Fekete G, van Heyningen V (1993) PAX6 mutations in aniridia. Hum Mol Genet 2:915-20.

4) Heon E, Paterson A, Fraser M, Billingsley G, Priston M, Balmer A, Schorderet D, et al (2001) A progressive autosomal recessive cataract locus maps to chromosome 9q13-q22. Am J Hum Genet 68:772-7.

5) Jordan T, Hanson I, Zaletayev D, Hodgson S, Prosser J, Seawright A, Hastie N, et al (1992) The human PAX6 gene is mutated in two patients with aniridia. Nat Genet 1:328-32.

6) Kulak SC, Kozlowski K, Semina EV, Pearce WG, Walter MA (1998) Mutation in the RIEG1 gene in patients with iridogoniodysgenesis syndrome. Hum Mol Genet 7:1113-7.

7) Lehmann OJ, Ebenezer ND, Jordan T, Fox M, Ocaka L, Payne A, Leroy BP, et al (2000) Chromosomal duplication involving the forkhead transcription factor gene FOXC1 causes iris hypoplasia and glaucoma. Am J Hum Genet 67:1129-35.

8) Mears AJ, Jordan T, Mirzayans F, Dubois S, Kume T, Parlee M, Ritch R, et al (1998) Mutations of the forkhead/winged-helix gene, FKHL7, in patients with Axenfeld-Rieger anomaly. Am J Hum Genet 63:1316-28.

9) Mears AJ, Mirzayans F, Gould DB, Pearce WG, Walter MA (1996) Autosomal dominant iridogoniodysgenesis anomaly maps to 6p25. Am J Hum Genet 59:1321-7.

10) Mirzayans F, Gould DB, Heon E, Billingsley GD, Cheung JC, Mears AJ, Walter MA (2000) Axenfeld-Rieger syndrome resulting

from mutation of the FKHL7 gene on chromosome 6p25. Eur J Hum Genet 8:71-4.

11) Murray JC, Bennett SR, Kwitek AE, Small KW, Schinzel A, Alward WL, Weber JL, et al (1992) Linkage of Rieger syndrome to the region of the epidermal growth factor gene on chromosome 4. Nat Genet 2:46-9.

12) Nishimura DY, Searby CC, Alward WL, Walton D, Craig JE, Mackey DA, Kawase K, et al (2001) A Spectrum of FOXC1 Mutations Suggests Gene Dosage as a Mechanism for Developmental Defects of the Anterior Chamber of the Eye. Am J Hum Genet 68:364-372.

13) Nishimura DY, Swiderski RE, Alward WL, Searby CC, Patil SR, Bennet SR, Kanis AB, et al (1998) The forkhead transcription factor gene FKHL7 is responsible for glaucoma phenotypes which map to 6p25. Nat Genet 19:140-7.

14) Semina EV, Reiter R, Leysens NJ, Alward WL, Small KW, Datson NA, Siegel-Bartelt J, et al (1996) Cloning and characterization of

a novel bicoid-related homeobox transcription factor gene, RIEG, involved in Rieger syndrome. Nat Genet 14:392-9.

15) Stone EM, Fingert JH, Alward WL, Nguyen TD, Polansky JR, Sunden SL, Nishimura D, et al (1997) Identification of a gene that causes primary open angle glaucoma. Science 275:668-70.

16) Wiggs JL, Allingham RR, Hossain A, Kern J, Auguste J, DelBono EA, Broomer B, et al (2000) Genome-wide scan for adult onset primary open angle glaucoma. Hum Mol Genet 9:1109-17.

# APPENDIX 1

## Mutational Analysis of *BARHL1* and *BARX1* in Three New Patients With Joubert Syndrome

Douglas B. Gould and Michael A. Walter

Submitted to the American Journal of Medical Genetics.

**Abstract**

Joubert Syndrome (JS) is a rare but well-known disorder of the central nervous system. The major feature of JS is hypoplasia of the cerebellar vermis. Affected individuals are commonly the result of consanguinous marriages and multiple affected individuals are born to healthy parents suggesting an autosomal recessive mode of inheritance. Linkage studies have mapped a JS locus to 9q34 but have also shown evidence of genetic heterogeneity. A 2:1 male to female ratio is consistent with an X-linked locus. The partial cDNA of a human Bar class homeobox gene *BARHL1* has recently been mapped to 9q34. We have identified the full-length coding region of the human *BARHL1* gene and examined its expression by Northern analysis. We obtained clinical reports and collected DNA from three previously undescribed patients with JS and screened them by direct sequencing for mutations in the *BARHL1* gene. *BARX1*, a related homeobox gene on chromosome 9 was also screened for mutations. No disease causing mutations were identified in these two genes despite their expression profiles and map locations, suggesting that *BARHL1* and *BARX1* are not responsible for patients with JS.

## Introduction

Joubert Syndrome (OMIM # 213300) is a severe central nervous system disorder that primarily effects the cerebellum and brainstem. Diagnostic criteria include: cerebellar vermis hypoplasia, hypotonia, developmental delay, abnormal breathing and/or abnormal eye movements (Saraiva and Baraitser 1992), neuroradiologic evidence of the "molar tooth sign" (Maria *et al.* 1997), and typical facial features (Steinlin *et al.* 1997 and Maria *et al.* 1999). JS was first described in 1969 in a family with three affected males and one affected female with neonatal episodic hyperpnea alternating with apnea, abnormal eye movements, ataxia, hypotonia and mental retardation, associated with agenesis of the cerebellar vermis (Joubert *et al.* 1969). A second report describes a girl from a Swiss couple, distantly related to each other and two boys from an unrelated German couple. These patients also presented with neonatal episodic hyperpnea alternating with apnea, abnormal eye movements, hypotonia, mental retardation, and dysplasia of the cerebellar vermis (Boltshauser *et al.* 1977).

Many of the approximately 200 patients reported to date have additional clinical features associated with those of classical JS.

These additional clinical features include polydactyly (Joubert *et al.* 1969 and Egger *et al.* 1982), congenital retinal dystrophy (Kendall *et al.* 1990), renal cysts (Pellegrino *et al.* 1997) and fleshy tumors of the tongue (Egger *et al.* 1982). Many of the related clinical features of JS are general developmental malformations that are common in other syndromes (Saraiva and Baraitser 1992, Pellegrino *et al.* 1997, and Chance *et al.* 1999) resulting in diagnostic overlap. Therefore, it is not clear if JS is a distinct clinical and genetic entity or part of a spectrum of neurological disorders that present with cerebellar vermian hypoplasia. This overlap demonstrates the need for resolution of the molecular basis of these disorders.

JS is often diagnosed in cases of consanguinity or in families where there are multiple affected children of apparently healthy parents suggesting an autosomal recessive mode of inheritance. A JS locus has been identified at 9q34 (Saar et al. 1999) with at least one additional autosomal locus. The documented male/female ratio of 2:1 (Saraiva and Baraitser 1992 and Cantani et al. 1990) is consistent with an X linked locus as well.

The recessive mouse mutation *swaying* provided a potential animal model for JS. The homozygous mutant mice are characterized by ataxia, and hypotonia with malformations of the anterior region of the cerebellum. The *swaying* phenotype is due to

mutations in the *wnt-1* gene from the *Wnt* family of segment polarity genes represented in *Drosophila* by the *wingless* gene (Thomas *et al.* 1991). A subset of 16 patients that meet the criteria for JS were screened for mutations in the human *WNT-1* gene however no disease causing mutations were identified (Pellegrino *et al.* 1997).

A review of the neurogenetics of the developing cerebellum suggests important roles for early developmental genes including those containing homeoboxes (*engrailed-1* and *engrailed-2*) and paired boxes (*pax-2, pax-5* and *pax-8*) (Hatten *et al.* 1995, Yachnis and Rorke 1999, Millen *et al.* 1999). Recently, a homeobox gene *BARHL1* (Genbank accession # AF321618) of the Bar class of transcription factors, has been localized to human chromosome 9q34 (Bulfone *et al.* 2000) where a JS locus has been identified (Saar *et al.* 1999). In developing mice, *barhl1* is expressed in the early mesencephalon and rhombencephalon including the midbrain/isthmic boundary, cerebellar plates and rhombic lip (Bulfone *et al.* 2000) making *BARHL1* an attractive candidate gene for JS.

Here we report the clinical findings of three previously unreported patients with JS. We also identified the sequence of the full-length human *BARHL1* sequence and the intron/exon

boundaries. Direct sequence analysis of two of these patients did not reveal any disease-causing mutations in the *BARHL1* gene. We also screened these two patients for mutations in the related *BARX1* gene also located to the long arm of chromosome 9 (Gould et al. 2000).

## Materials and Methods

An *in silico* search using the partial *BARHL1* cDNA (GenBank accession no. AJ237816) was performed. We identified and obtained a cDNA (Research Genetics) (GenBank accession no. AI367090) that was sequenced using LICOR fluorescent sequencing as described previously (Gould et al. 2000).

Primers were generated for *BARHL1* and purchased from Gibco BRL. Mutational analysis of *BARHL1* and *BARX1* was conducted by direct sequence analysis as described previously (Gould et al. 2000). Sequence analysis was not performed on patient 1 because patients 1 and 2 are siblings and therefore presumed to have the same mutations.

The expression of human *BARHL1* was examined using human fetal and adult multi-tissue Northern blots purchased from Clonetech. The probe used was the 514bp product of primer pair

1F/2R (Table A-1 and Figure A-1). This product contains the whole coding region of exon 1 (466bp) and 48bp of 5'UTR (22bp) and intron 1 (26bp). Probe labeling, hybridization and post-hybridizaton washes were described previously (Gould et al. 2000).

**Case 1**

The first patient is a male born to non-consanguineous oriental/Pakistani parents with no prior family history. At birth he was noted to have bilateral postaxial polydactyly of the hands, hydrocephalus and respiratory distress. Later signs included global developmental delay, bilateral ptosis, bilateral horizontal nystagmus, hypotonia, ataxia, and tachypnea for the first six months. Hearing loss was noted in the left ear and at one year the patient began tongue thrusting. An abdominal ultrasound showed normal kidneys.

**Case 2**

The second patient is the brother of patient 1. This boy presented with polydactyly, congenital nystagmus, ptosis of the left eyelid, Dandy-Walker malformation, hypotonia, tachypnea and retarded development. His facial features included microcephaly

**Figure A-1. Schematic of the BARHL1 coding region.**

The hatched areas indicate coding sequence. The homeobox is indicated by a black box. Primer pairs are indicated under the schematic by arrows. The large bar under exon 1 indicates the 1F/2R PCR product used for Northern analysis. Introns are indicated by thin lines with the sizes indicated in base pairs.

1f/r
2f/r
4066bp
3f/r
1676bp
4f/r

**Table A-1 Primer Pairs Used to PCR Amplify BARHL1**

| Primer Set | Primer Oligonucleotide (5'-3') | | Product Size (bp) | Annealling Temperature (°C) |
|---|---|---|---|---|
| | Forward | Reverse | | |
| 1 | gaggacaggtcgcagctt | GTCCCCGTCTCCAAACAGT | 210 | 60 |
| 2 | CAGCAGCGACTGCTCTTC | caagttttcacctcctgctt | 361 | 60 |
| 3 | gccgaggttacacaaacg | ccctttctgcctctaccc | 347 | 60 |
| 4 | cgccatacgcgtttattt | acctgcgccctcagaaag | 399 | 60 |
| 1F/2R | gaggacaggtcgcagctt | caagttttcacctcctgctt | 514 | 60 |

Primers from non-coding regions are shown in lower case.
All reactions use 5% DMSO

with frontal bossing, a high arched palate and low set ears. The patient's fundus was normal upon examination. CT and MRI (Figure A-2a and A-2b) results indicated an enlarged foramen magnum, posterior fossa abnormalities, inferior and superior vermian cisterns were somewhat prominent and the fourth ventricle was mildly enlarged. The left cerebral peduncle and left upper pons were slightly larger than the right and there was mild vermian hypoplasia.

**Case 3**

The third patient is a female born to healthy nonconsanguinous parents with no prior family history. This girl presented with neonatal episodic hyperpnea and apnea, hypotonia, significant developmental delay, cerebellar vermis hypoplasia, multiple small renal cysts, jerky horizontal eye movements and retinal blindness indicated by absent ERG. An abdominal ultrasound indicated that the liver, pancreas, spleen, and gall bladder appeared normal, however, the kidneys appeared mildly enlarged with multiple cysts. A MRI (Figure A-2c and A-2d) confirmed that there was total posterior cerebellar aplasia and cerebellar vermian hypoplasia. There was a prominence and thickening of the posterior cerebellar peduncles. The fourth ventricle was dilated and the pons was slightly shortened.

**Figure A-2. Magnetic resonance imaging of patients 2 and 3.**

A) Sagital MRI of patient 2. B) Axial MRI of patient 2. C) Sagital MRI of patient 3. D) Axial MRI of patient 3. Arrows in frames A) and C) indicate regions of cerebellar vermian hypoplasia. Arrowheads in frames B) and D) indicate the molar tooth sign.

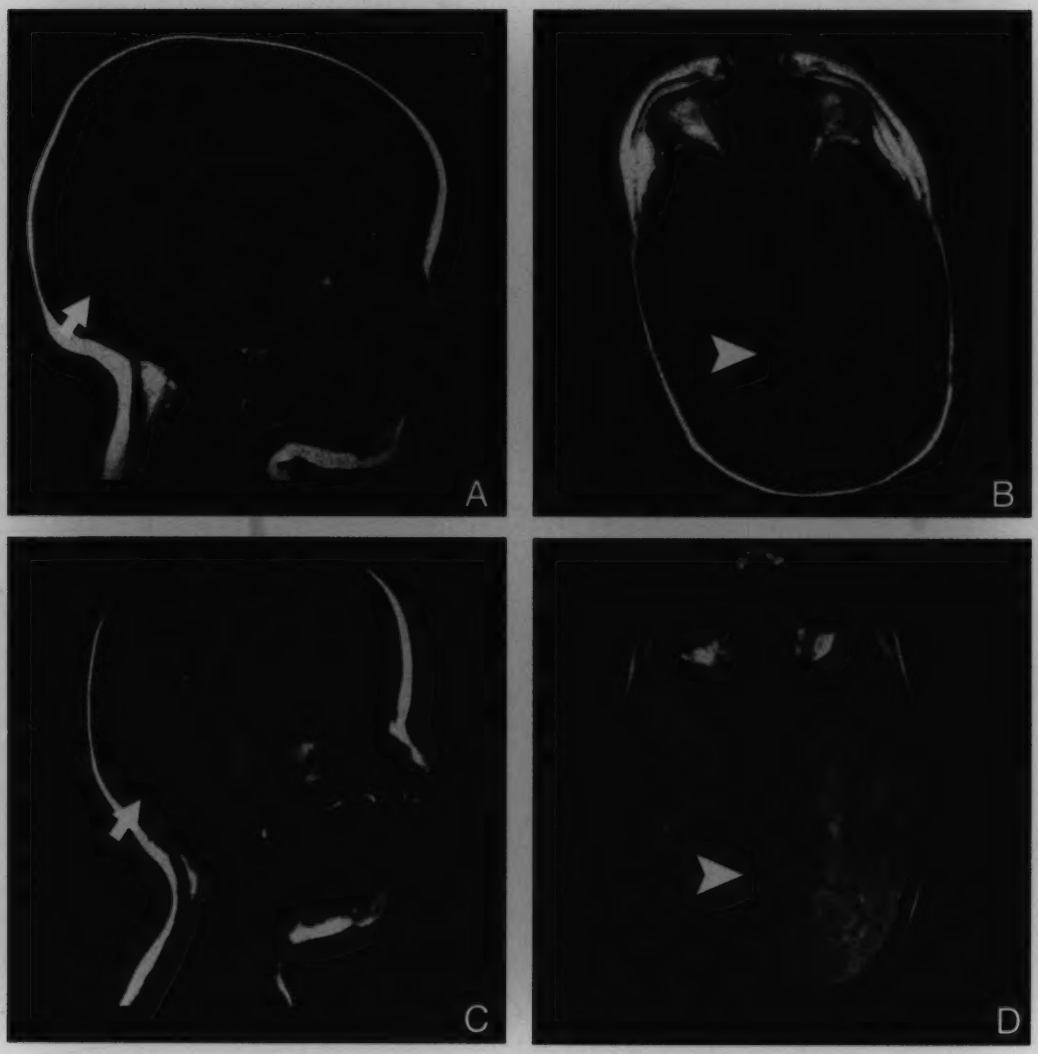
A
B
C
D

**Results**

The full length *BARHL1* coding sequence and intron/exon boundaries were discovered following two *in silico* searches using the human partial *BARHL1* sequence (GenBank accession no. AJ237816). The results of these searches were the identification of a 1289bp cDNA from 8-9 week human total fetus (GenBank accession no. AI367090) and discovery of the *BARHL1* genomic sequence in unfinished human chromosome 9 sequence (BAC RP11-143F18). The *BARHL1* cDNA clone was ordered and sequenced using LICOR fluorescent sequencing as previously described (Gould et al. 2000). The 1289bp cDNA clone was found to include nearly all of the three *BARHL1* coding exons, lacking only the first six nucleotides of exon 1. Intron exon boundaries (Table A-2) were identified by comparison between the *BARHL1* cDNA and the genomic sequence. Primers were generated to span the intron/exon boundaries and the entire *BARHL1* coding region (Figure A-1 and Table A-1).

The coding region of exon 1 (Figure A-1) was used to probe a commercially available multiple tissue Northern blot as described previously (Gould et al. 2000). This probe detected transcripts of approximately 2.5Kb in adult brain, 4.5Kb in fetal kidney, and 8.0Kb in adult liver (data not shown).

**Table A-2 Intron/Exon Boundaries for BARHL1**

| Splice Donors | Splice Acceptors |
|---|---|
| EXON 1.....CTGAGTATAAAGgtaagaaagcag.....Intron 1 | Intron 1.....ctgtgtccgcagTGAAGGAGGAGG.....EXON 2 |
| EXON 2.....CCAGAACCGCAGgtgaggcctggc.....Intron 2 | Intron 2.....ttcggcccccagGACTAAATGGAA.....EXON 3 |

Invarient bases are underlined.

DNA samples were collected from patients 2 and 3 above. DNA was not obtained from patient 1 because he is the sibling of patient 2. The patients' genomic DNA was amplified using the primers and conditions described in Table A-1. PCR products were sequenced as previously described (Gould et al. 2000). No sequence alterations were observed between these patients and the published *BARHL1* sequence.

Patient DNA samples were also amplified and sequenced for the *BARX1* gene using primers and conditions previously described (Gould et al. 2000). No sequence alterations were observed in *BARX1* in these two patients.

## Discussion

Here we describe three new cases of JS. Although JS is a well-known and severe disorder of the CNS, little is known about the genetic or molecular basis of the disorder. Previous efforts to identify candidate genes have relied strictly on the genes' expression patterns. The recent mapping of a locus for JS to 9q34 now allows potential candidate genes to be identified based on map position as well. Here we describe a mutational screen of a novel human gene *BARHL1*. *BARHL1* is a strong candidate based on its expression in

the developing CNS of mice and on its map position at 9q34 in humans.

Commercially available human fetal and adult Northern blots were used to determine the expression profile of human *BARHL1*. We detected transcripts of approximately 2.5Kb, 4.5Kb, and 8.0Kb in adult brain, fetal kidney and adult liver respectively (data not shown). The size of the transcript detected in adult brain is in agreement with the size of the transcript predicted from the coding sequence. The absence of a detectable transcript in fetal brain is notable, however, it is known that *BARHL1* is expressed very early in the brains of developing mice and therefore it is possible that the Northern blots we chose do not represent this time window. The transcripts detected in fetal kidney and adult liver could represent alternate *BARHL1* transcripts in different tissues or may be the results of cross hybridization to related genes.

No disease causing sequence alterations of *BARHL1* were identified in the two patients we sequenced. This is consistent with the suggestion that the *BARHL1* gene is not responsible for JS patients with mutations at the JS locus at 9q34. Never-the-less the existence of heterogeneity in JS however, means that *BARHL1* cannot be entirely out based on our results because these patients could have mutations of a non-chromosome 9 locus. While an X-linked

form of JS has been suggested (Saraiva and Baraitser 1992 and Cantani *et al.* 1990), Patient 3 is a female born to unaffected parents and therefore her condition is not likely to be due to a mutation at an X linked locus.

A second gene, *BARX1*, was also screened. Human *BARX1* has been located at chromosome 9q12 by radiation hybrid mapping and therefore may not be a strong candidate. However, both murine *Barx1* and *Barx2* were isolated based on their ability to bind regulatory elements of neural cell adhesion molecule, NCAM (Tissier-Seta *et al.* 1997 and Jones *et al.* 1997). NCAM is known to be involved in formation, proliferation and differentiation of the external granular layer of the cerebellum (Millen *et al.* 1999). No disease causing sequence alterations of *BARX1* were identified in the two patients we sequenced. This suggests that the *BARX1* gene is not responsible for JS in our patients.

No strong candidates for JS currently exist at 9q34. However gene identification using the available sequence of the human genome will assist investigations into identifying the gene(s)at 9q34 that cause JS.

**Acknowledgements**

The authors extend gratitude to the families who participated in this study. We thank Karen McElliggot and Dr. Stephen Bamforth for clinical information. We thank Dr. Robert Ashforth for assistance with MRIs. We thank Farideh Mirzayans, Jody Marshall, and Kerry McTaggart for technical assistance and Dr. Ian MacDonald and members of the Ocular Genetics lab for critical review of the manuscript. D.B.G. is supported by a Canadian Institute of Health Research (CIHR) doctoral fellowship, and M.A.W. is an Alberta Heritage Foundation for Medical Research (AHFMR) senior scholar and CIHR investigator.

**References**

Boltshauser E, Isler W. Joubert syndrome: episodic hyperpnea, abnormal eye movements, retardation and ataxia, associated with dysplasia of the cerebellar vermis. *Neuropädeatrie* 1977;**8**:57-66.

Bulfone A, Menguzzato E, Broccoli V, Marchitiello A, Gattuso C, Mariani M, Consalez GG, Martinez S, Ballabio A, Banfi S. *Barhl1*, a gene belonging to a new subfamily of mammalian homeobox genes, is expressed in migrating neurons of the CNS. *Hum Mol Genet* 2000;**9**:1443-1452.

Cantani A, Lucenti P, Ronzani GA, Santoro C. Joubert syndrome- A review of the fifty-three cases so far published. *Ann Génét* 1990;**33**:96-98.

Chance PF, Cavalier L, Satran D, Pellegrino JE, Koenig M, Dobyns WB. Clinical nosologic and genetic aspects of Joubert and related syndromes. *J Child Neurol* 1999;**14**:660-666.

Egger J, Bellman MH, Ross EM, Baraitser M. Joubert-Boltshauser syndrome with polydactyly in siblings. *J Neurol Neurosurg Psychiatry* 1982;**45**:737-739.

Gould DB, Water MA. Cloning, Characterization, Localization and Mutational Screening of the Human BARX1 Gene. *Genomics* 2000;**68**:336-342.

Hatten ME, Heintz N. Mechanisms of neural patterning and specification in the developing cerebellum. *Annu Rev Neurosci* 1995;**18**:385-408.

Jones FS, Kioussi C, Copertino DW, Kallunki P, Holst BD, Edelman GM. Barx2, a new homeobox gene of the Bar class, is expressed in neural and craniofacial structures during development. *PNAS* 1997;**94**:2632-2637.

Joubert M, Eisenring JJ, Robb JP, Andermann F. Familial agenesis of the cerebellar vermis. A syndrome of episodic haperpnea, abnormal eye movements, ataxia and retardation. *Neurology* 1969;**19**:813-825.

Kendall B, Kingsley D, Lanbert5 SR, Taylor D, Finn P. Joubert syndrome: A clinico-radiological study. *Neuroradiology* 1990;**31**:502-506.

Maria BL, Hoang KBN, Tusa RJ, Mancuso AA, Hamed LM, Quisling RG, Hove MT, Fennel EB, Booth-Jones M, Ringdahl DM, Yachnis AT, Creel G, Frerking B. "Joubert Syndrome" revisited: Key ocular motor signs with magnetic resonance imaging correlation. *J Child Neurol* 1997;**12**:423-430.

Maria BL, Boltshauser E, Palmer SC, Tran TX. Clinical features and revised diagnostic criteria in Joubert syndrome. *J Child Neurol* 1999;**14**:583-591.

Millen KJ, Millonig JH, Wingate RJT, Alder J, Hatten M. Neurogenetics of the cerebellar system. *J Child Neurol* 1999;**14**:574-582.

Pellegrino JE, Lensch MW, Muenke M, Chance PF. Clinical and molecular analysis in Joubert syndrome. *Am J Med Genet* 1997;**72**:59-62.

Saar K, Al-Gazali L, Sztriha L, Rueschendorf F, Nur-E-Kamal M, Reis A, Bayoumi R. Homozygosity mapping in families with Joubert syndrome identifies a locus on chromosome 9q34.3 and evidence for genetic heterogeneity. *Am J Hum Genet* 1999;**65**:1666-1671.

Saraiva JM, Baraitser M. Joubert syndrome: A review. *Am J Med Genet* 1992;**43**:726-731.

Steinlin M, Schmid M, Landau K, Boltshauser E. Follow-up in children with Joubert syndrome. *Neuropediatics* 1997;**28**:204-211.

Thomas KR, Musci TS, Neumann PE, Capecchi MR. *Swaying* is a mutant allele of the proto-oncogene Wnt-1. *Cell* 1991;**67**:969-976.

Tissier-Seta JP, Mucchielli ML, Mark M, Mattei MG, Goridis C, Brunet JF. Barx1, a new mouse homeodomain transcription factor expressed in cranio-facial ectomesenchyme and the stomach. *Mechanisms of Development* 1995;**51**:3-15.

Yachnis AT, Rorke LB. Neuropathology of Joubert syndrome. *J Child Neurol* 1999;**14**:656-659.